Post-transcriptional regulation of the transition from neural stem cells to early neuroblasts

Dissertation

submitted to the

Combined Faculty of Natural Sciences and Mathematics of the Ruperto Carola University Heidelberg, Germany

for the degree of

Doctor of Natural Sciences

Presented by

Yonglong Dang

Dissertation

submitted to the

Combined Faculty of Natural Sciences and Mathematics of the Ruperto Carola University Heidelberg, Germany

for the degree of

Doctor of Natural Sciences

Presented by

M. Sc. Yonglong Dang

born in Jinan, Shandong, China

Oral examination: July 25, 2019

Post-transcriptional regulation of the transition from neural stem cells to early neuroblasts

Referees: Prof. Dr. Ana Martin-Villalba

Prof. Dr. Aurelio Teleman

Abstract:

In mammals, the process of neurogenesis consists in the generation of various types of neuronal and glial cells from neural stem cells (NSCs). It begins intensively at the embryonic stage and continues through the whole adulthood. In adult rodents, neurogenesis is mainly located in two regions: the ventricular-subventricular zone (V-SVZ) of the lateral ventricles and the dentate gyrus of the hippo-campus. In the last two decades huge progress has been made to characterize the process in detail and to get further insights of its regulation. However, still some fundamental questions remain unanswered. Among those, whether post-transcriptional regulation plays a critical role in NSC activation and differentiation. In this project, I investigated protein synthesis and its modulation upon activation of NSCs using the mouse adult brain as an experimental model. The analysis of the nascent synthesized peptides in NSCs and early neuroblasts (ENBs) of the same lineage revealed that the level of global protein synthesis decreases upon the transition from NSCs to ENBs. The transcriptome and translatome analysis of NSCs and ENBs clearly showed an active involvement of post-transcriptional regulation in gene expression at the onset of NSC differentiation. In particular, translation of neuronal specification transcripts such as Sp8 and Dusp4 was enhanced. On the contrary, the translation of some mRNAs carrying the Terminal Oligo Pyrimidine (TOP) and the Pyrimidine Rich Motif (PRM) such as Sox2 and Rpl18 were selectively repressed. At this transition, we also observed a drop of mTOR activity upon cell cycle exit that was causally linked to repression of TOP- and PRM-transcripts. Altogether, our study underscored the role of protein synthesis and its regulation in NSC differentiation. It also demonstrated a causal link between cell cycle exit, TOR activity and exit of the stem cell state.

Zusammenfassung:

Bei Säugetieren besteht der Prozess der Neurogenese in der Erzeugung verschiedener Typen von Nerven- und Gliazellen aus neuralen Stammzellen (NSCs). Es beginnt intensiv im embryonalen Stadium und setzt sich durch das gesamte Erwachsenenalter fort. Bei adulten Nagetieren findet die Neurogenese hauptsächlich in zwei Regionen statt: der ventrikulär-subventrikulären Zone (V-SVZ) der lateralen Ventrikel und dem Gyrus dentatus des Hippocampus. In den letzten zwei Jahrzehnten wurden große Fortschritte gemacht, um den Prozess im Detail zu charakterisieren und in seine Regulierung einzugreifen. Trotzdem bleiben einige grundlegende Fragen offen. Dazu gehört die posttranskriptionelle Regulation, die eine wichtige Rolle bei der Aktivierung und Differenzierung von NSC spielt. In diesem Projekt wurde anhand des Mäusegehirns als Modellsystem die Proteinsynthese und ihre Modulation bei der Aktivierung der NSCs untersucht. Die Analyse der im Entstehungsprozess befindlichen Peptide während des Differenzierungsprozesses der NSCs zu frühen Neuroblasten (ENBs) zeigte, dass das Niveau der globalen Proteinsynthese bei diesem Prozess abnahm. Durch die Transkriptom- und Translatomanalyse der NSCs und ENBs wurde eine aktive Beteiligung der posttranskriptionellen Regulation an der Genexpression bei und kurz nach Beginn der NSC-Differenzierung sichtbar. Insbesondere wurde die Translation von neuronal-spezifischen Transkripten wie Sp8 und Dusp4 verstärkt. Im Gegensatz dazu wurde die Translation einiger mRNAs, wie beispielsweise Sox2 und Rpl18 selektiv unterdrückt. Dies hängt damit zusammen, dass diese mRNAs Träger des terminalen Oligo Pyrimidine (TOP) und des Pyrimidine Rich Motif (PRM) sind, deren Translation durch die Aktivierung von mTOR reguliert wird. Zu Beginn des Differenzierungsprozesse kommt es zum Austritt der Zelle aus dem Zellzyklus, was mit einer Abnahmen der mTOR-Aktivität einhergeht. Unsere Daten weisen darauf hin, dass die Rolle der Proteinsynthese und ihre Regulation in ursächlichem Zusammenhang zwischen dem Austritt der NSC aus dem Zellzyklus, bei der NSC-Differenzierung, und der posttranskriptionellen Modulation der Synthese einiger wichtiger Stammzellfaktoren steht.

Acknowledgement

I am very excited and grateful to realize that I am close to my doctoral degree! Looking backward, I am feeling so lucky to have so many nice people helping me and supporting me in the past years.

First of all, I would like to sincerely thank my supervisor Ana for the mentoring during my PhD studies in the lab. Your passion, your high standard in doing science really influenced and inspired me a lot. I am very grateful that you gave me the opportunity to do my PhD in your lab. The high quality and intensive training here will benefit my whole life. Thanks very much!

Thank you to Maxim. I learned lots of skills and tricks to do experiments from you. There are so many unforgettable days that we work together doing experiments. The recommended reviews from you were very fruitful.

Thanks to Suse for all the help and support. I enjoyed the days we worked together as a team intensively doing experiments. Your suggestions and guidance were very helpful. And also thanks for your patience correcting my PhD thesis.

Thanks to Avni, my first teacher when I newly joined the lab and knew little about mouse biology. I am grateful that you offered me your unfinished work as a PhD project so that I can challenge myself and learn lots of new staff. Thanks.

Thanks Georgios, a nice guy. Discussions with you and critical comments from you are always thought-provoking and rewarding. I am very impressed by your hard working spirit in doing science. Thanks also for the help of FACS.

And thank you to many more guys in the lab. Thanks for your help experimentally and in daily life. Gulce is a lady I always like to talk to and discuss science, very nice and easy-going. Thanks for your nice comments for my thesis. Sascha is guy with strong humor gene. Being with you is always fun and happy. Nikhil is a very nice friend. I like to enjoy food with you. And swimming is our shared hobby. And also thanks for the help with my experiments. Steffi has very high standard in working. Thanks for your cooperation and patience in teaching and sometimes pushing me to work to meet the high standard. You are very nice personally. And Irmgard, Manuel, Katrin, Oguzhan, Damian, Santiago… Thanks a lot for all the help you guys provided to me during my PhD.

Thank my TAC members, Prof. Aurelio Telemann and Prof. Georg Stoecklin. I am very grateful for your helpful comments and suggestions during my TAC meetings.

I would like to thank Steffen Scholpp from Exeter University, with whom I started my PhD in Germany. I learned and benefited a lot from your teaching and methodology for doing science. Though I had to change the lab due to your lab relocation, your support is always there! Thanks for all the help, making me feel that you are more like a friend. And also thank my former lab members Beni, Bernadett, Sabrina for their help during my stay in the Scholpp lab.

Thanks to my parents. Your unconditional love and support made me never give up my dream. I will continue to move forward for my goal. Thanks my brother Yongfeng for endless help and support. Thank you for spending much more time with our parents when I am away.

Finally, I want to thank my girlfriend, Dimeng. Thanks for your understand and support me with so much patience. I am so grateful for having you. You are unique and you are the best!

Content

List of Figures

List of Tables

Abbreviations

Atp2b1	Plasma membrane calcium-transporting ATPase 1
Birc6	Baculoviral IAP repeat-containing protein 6
DiCRY	Dcx-CreER-Rpl22.HA-eYFP
dTB	Double thymidine block
Dusp4	dual specificity protein phosphatase 4
4EBP1	4E binding protein 1
ENBs	Early neuroblasts
FACS	Fluorescence activated cell sorting
FUCCI	Fluorescent ubiquitination-based cell cycle indicator
HA	Hemagglutinin
ICC	Immunocytochemistry
IHC	Immunohistochemistry
LNBs	Late neuroblasts
mTOR	Mammalian target of rapamycin
NBM	Neural basal medium
NSCs	Neural stem cells
OB	Olfactory bulb
PIP3	Phosphatidylinositol (3,4,5)-trisphosphate
Plp1	Proteolipid protein 1
PRM	Pyrimidine rich motif
qPCR	Quantitative real time PCR
Rgs16	Regulator of G-protein signaling 16
Rheb	Ras homolog enriched in brain
RMS	Rostral migratory stream

Rps20	Ribosomal protein S20
SGZ	Subgranular zone
Sp8	Specificity protein 8
SVZ	Subventricular zone
TAM	Tamoxifen
TAPs	Transient amplifying progenitor cells
TiCRY	Tlx-CreER-Rpl22.HA-eYFP
Tlx	Tailless
Torin	Torin1
Vash2	Vasohibin-2
Vim	Vimentin

1 Introduction

In mammals, neurogenesis is the process of neural stem cells (NSCs) differentiation into neurons. This process involves many layers of regulations. Post-transcriptional regulation during the onset of NSC differentiation is incompletely understood.

1.1 Adult neurogenesis

In rodents, NSCs differentiate and give rise to functional neurons during development and in adulthood. Two neurogenic regions are present in the adult brain: the subventricular zone (SVZ) of the lateral ventricles and the subgranular zone (SGZ) of the dentate gyrus (DG) in the hippocampus (Bellusci et al., 1997; Clarke et al., 2000; Götz and Huttner, 2005; Ihrie and Alvarez-Buylla, 2011; Ming and Song, 2011).

In 1960s the group of Altman showed pioneering results in rats, with the first anatomical evidence of postnatal hippocampal neurogenesis (Altman and Das, 1965). Some years later, he published neurogenesis in the subependymal zone of the lateral ventricles. In his histological and auto radiographic studies, the cells in the subependymal layer of the lateral ventricles were shown to proliferate and migrate along the rostral migratory stream (RMS) towards the olfactory bulb (OB). This process was shown in both neonatal and adult rats (Altman, 1969). His work was ignored until 30 years later its reproduce by different groups (Kaplan and Hinds, 1977; Eriksson et al., 1998; Gould et al., 1999). Since then, adult neural stem cells were successively isolated by several groups (Reynolds and Weiss, 1992; Richards et al., 1992; Lois and Alvarez-Buylla, 1993). These findings support the possibility that a resident population of stem cells is the source to remedy neuronal loss throughout lifetime. NSCs in hippocampus were first characterized in 1997. Palmer and colleagues showed that the precursor cells isolated from the hippo-campus were capable of maintaining proliferative normal diploid progenitors *in vitro*, providing evidence for the existence of adult hippocampal NSCs (Palmer et al., 1997).

In the adult SVZ, NSCs give rise to neural precursor cells, which migrate along the RMS towards their final destination: the OB (Lois et al., 1996). This neurogenesis process is

under regulation of both intrinsic neurogenic transcription factors and extrinsic factors such as transmitters, hormones, and growth factors (Lledo et al., 2006). When reaching the core of the OB, the new born neurons migrate radially to invade the overlaying layers, where they become functional granule cells and periglomerular neurons, which are located in the deeper and the most superficial layer, respectively (Lledo et al., 2006).

Growing evidence showed that adult NSCs remained from an embryonic stage and were retained until adulthood (Fuentealba et al., 2015; Furutachi et al., 2015; Berg et al., 2019). During homeostasis, adult NSCs stay largely in a quiescent state in the brain (Morshead et al., 1994; Seri et al., 2001). These quiescent NSCs still retain fundamental epithelial properties. Their apical side extends to the lateral ventricle through the core of the pinwheel structure formed by ependymal cells and their basal side contacts the blood vessel (Mirzadeh et al., 2008). Once activated, these NSCs lose their ventricle contact and divide symmetrically to maintain the stem cell pool and support continuous neuron production (Obernier et al., 2018). It was estimated that in SVZ about 20-30% of NSCs self-renew and 70-80% of NSCs undergo differentiation (Obernier et al., 2018). NSC activation is associated with reduction in glycolytic metabolism, Notch and BMP signaling as well as increases in lineage-specific transcription factors and protein synthesis (Llorens-Bobadilla et al., 2015). The balance of NSC quiescence and activation is tightly controlled with the involvement of key signaling molecules such as BMPs (Mira et al., 2010). Recently Kalamakis and colleagues reported that with age NSCs in the SVZ tend to be more quiescent but once activated behave the same as NSCs in the young animal (Kalamakis et al., 2019). Apart from homeostatic activation, quiescent NSCs can also be activated upon multiple stimulatory signals such as injury or any other neurological diseases (Llorens-Bobadilla et al., 2015; Baser et al., 2017).

Prior to trigger their differentiation program, NSCs usually enter an intermediate state to become transit amplifying progenitor cells (Doetsch et al., 1999). Multiple lineages of such intermediate progenitor cells divide for a limited number of times and generate neurons and glial cells such as astrocytes and oligodendrocytes (Kriegstein and Alvarez-Buylla, 2009). NSC differentiation is a complicated process composing multiple layers of regulation, ranging from transcription to translation with numerous regulators involved. Basic helix-loop-helix (bHLH) transcription factors are such key regulators (Kageyama et al., 2005). The expression of activator type and repressor type of bHLH transcription

factors is well organized in NSCs during NSC maintenance and differentiation (Kageyama et al., 2005). Many more molecules were reported to affect the process of NSC differentiation at embryonic or adult stage either transcriptionally or through affecting the function of the intracellular organelle (Braccioli et al., 2017; Mendivil- Perez et al., 2017; Zhu et al., 2018). In addition, cell cycle also affects NSC differentiation. In the embryonic mouse, lengthened G1 phase induces neuroepithelial cell differentiation (Calegari and Huttner, 2003).

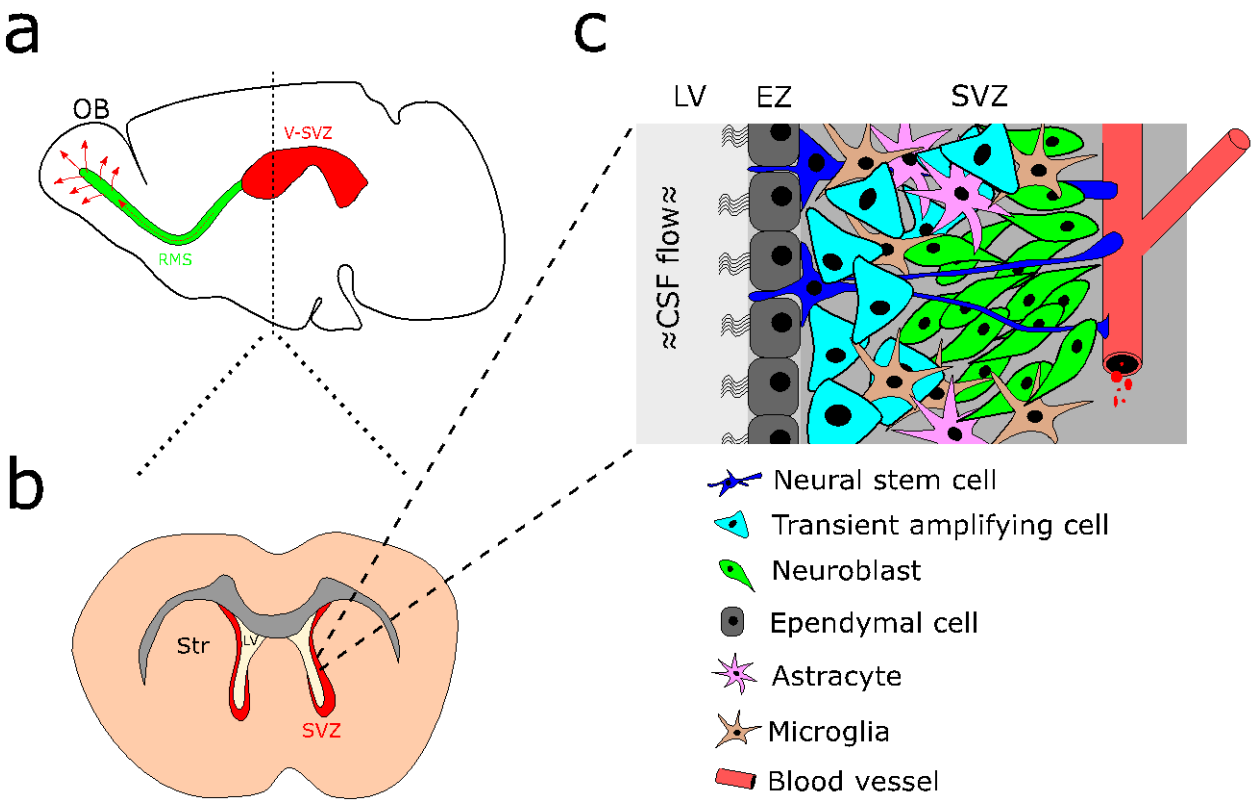

Figure 1. Neurogenesis in the V-SVZ of the adult mouse brain

(a) A schematic diagram of the adult mouse brain. The ventricle-subventricular zone (V-SVZ) continuously produces neuroblasts, which migrate along the rostral migratory stream (RMS) to reach the olfactory bulb (OB) and become local mature and functional intern neurons. (b) A cross-section view of the adult mouse brain. Str, striatum; LV, lateral ventricle. (c) A schematic diagram of the cellular components of the subventricular zone. Adult NSCs reside close to the ependymal zone (EZ) in the SVZ with extended redial processes contacting the lateral ventricles and blood vessels. CSF, cerebrospinal fluid. Figures were modified from (Franklin and Paxinos, 2008; Bond et al., 2015; Chaker et al., 2016).

1.2 Protein synthesis in eukaryotic cells

Protein synthesis, or translation, is a complex, multi-step, tight-regulated process. It occurs with the involvement of ribosomes, which are located in the cytoplasm or endoplasmic reticulum. The eukaryotic ribosomes are ribonucleoproteins composed of a 40S small subunit and an 80S large subunit. Each subunit comprises one or more ribosomal RNA(s) and a variety of ribosomal proteins. There are around 10^6 to 10^7 ribosomes in a eukaryotic cell. In some cases the number is even higher. For example, it was estimated that there are up to 10^{12} ribosomes in a single non-dividing cell during oogenesis in Xenopus (Rosbash and Ford, 1974). Recent reports showed that the composition of ribosomes is also in heterogeneity, being associated with translation of subpopulation of messenger RNAs (mRNAs) in the cell (Shi et al., 2017; Simsek et al., 2017).

Protein synthesis is the process of ribosomes translating mRNAs into proteins, which consists of translation initiation, elongation, and termination (Figure 2). Translation initiation is tightly controlled and is the rate-limiting step of the whole protein synthesis pathway. Translation initiation begins by the formation of 43S pre-initiation complex (PIC), which is composed of 40S ribosomal subunit, ternary complex eIF2-GTP-$tRNA^{Met}_i$ and some eukaryotic initiation factors (eIFs) such as eIF1, eIF1A, eIF2, eIF3 and eIF5 (Sonenberg and Hinnebusch, 2009; Aitken and Lorsch, 2012; Fraser, 2015; Hinnebusch, 2017). Binding of the PIC to the 5' UTR of mRNAs is recruited by eIF4F complex, comprising RNA helicase eIF4A, cap-binding protein eIF4E and scaffold protein eIF4G (Sonenberg and Hinnebusch, 2009). The PIC then scans downstream successive triplets for complementarity to the anticodon of $tRNA^{Met}_i$. Recognition of AUG leads to scanning arrest and hydrolysis of GTP in the eIF2-GTP-$tRNA^{Met}_i$ ternary complex. With release of eIF2-GDP and eIFs, 60S ribosomal subunit joins to form 80S initiation complex, an intact ribosome competent to enter elongation phase of protein synthesis (Pestova et al., 2007; Sonenberg and Hinnebusch, 2009). During elongation, new aa-tRNAs are selectively recruited to the ribosome through base-pairing between anticodon and the codon in the t-RNA and mRNA, respectively. Sequentially added amino acids are catalyzed to form polypeptides. When the ribosome reaches the stop codon, which

leads to ribosome disassemble and the release of polypeptides, protein synthesis is terminated (Hershey et al., 2018). For translation of most mRNAs, the formation of initiation complex is in a cap-dependent manner, which needs the aid of cap-binding proteins to recruit PIC to the 5' end of the mRNA to initiate translation. eIF4E is the most well-known cap-binding protein in mediating cap-dependent translation. Recent discoveries showed that eIF3d also works as a cap binding protein to mediate specialized translation, independent of eIF4E (Lee et al., 2016). However, mRNAs which have an internal ribosome entry site (IRES) element can directly recruit PIC without the involvement of the cap structure. Originally found in viral mRNAs, the existence of IRES element was later confirmed in cellular mRNAs, which are mainly involved in stress response (Jang et al., 1988; Pelletier and Sonenberg, 1988; Jang et al., 1989; Godet et al., 2019).

Protein synthesis in eukaryotic cells is a very complex process, involving numerous tightly controlled steps. Deeper knowledge on the regulatory mechanisms in protein synthesis would increase our understanding how neurogenesis is regulated.

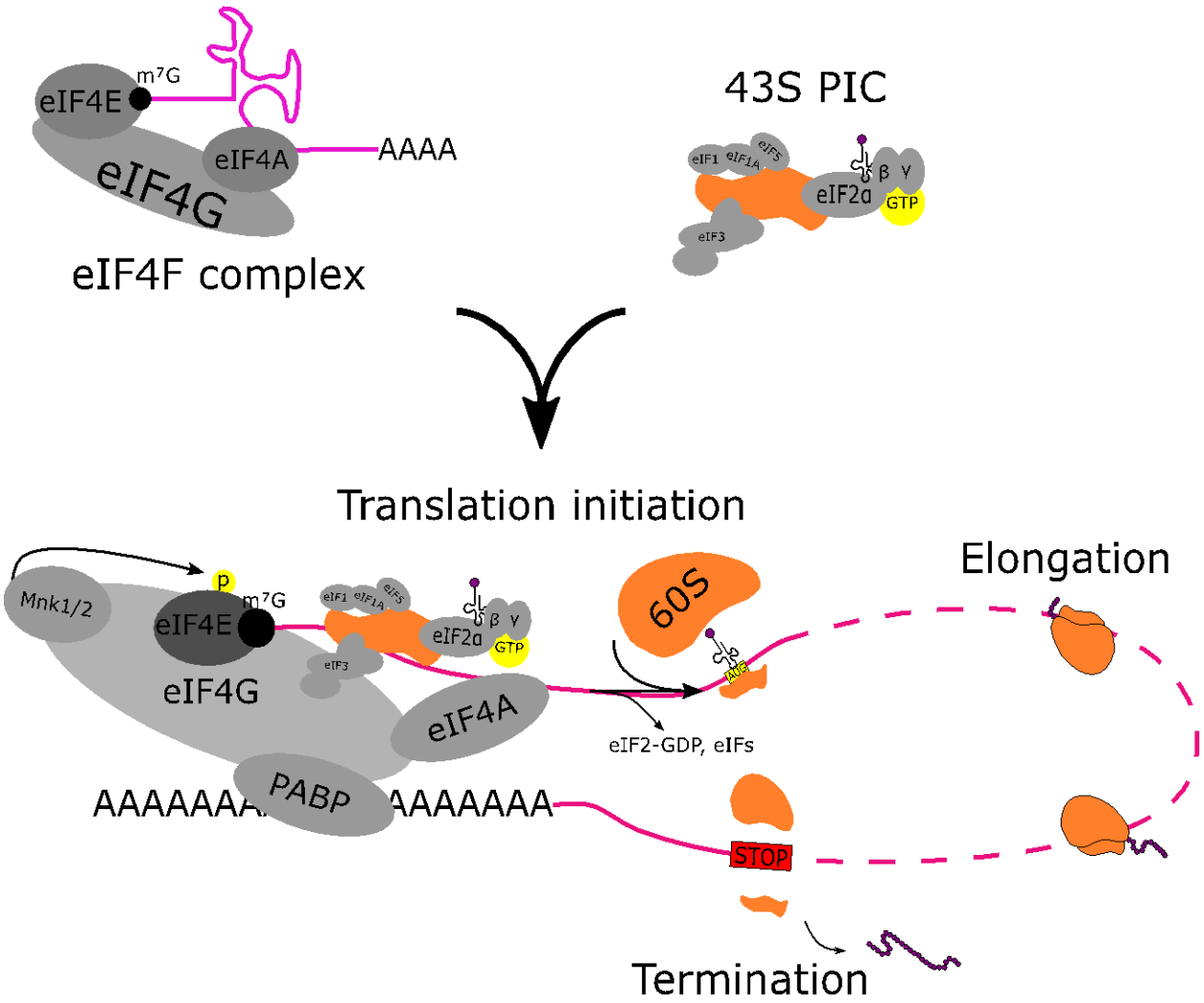

Figure 2. A brief overview of protein synthesis in eukaryotes

The eIF4F recruits 43S PIC to the 5'UTR region of the mRNA to initiate protein synthesis, which is the rate limiting step of protein synthesis, followed by elongation and termination. eIF4E in the eIF4F, is the cap binding protein. eIF4A is a helicase. eIF4G is a scaffold protein which also binds to poly(A)-binding protein (PABP), which connects the poly(A) tail of the mRNA to the eIF4F complex. Modified from (Robichaud et al., 2018).

1.3 mTOR signaling in translational control

Mammalian target of rapamycin (mTOR) is an atypical serine threonine kinase involving in many fundamental cellular activities such as cell growth, metabolism, and disease (Saxton and Sabatini, 2017). As the core component of two major complexes mTOR complex 1 (mTORC1) and mTOR complex 2 (mTORC2), mTOR is under the regulation of multiple pathways (Figure 3).

The most well-known role for mTOR is its involvement in translation, mainly mediated by mTORC1. Downstream targets of mTORC1 are p70S6 kinase 1 (S6K1) and 4E binding protein (4EBP) (Brown et al., 1995; Saxton and Sabatini, 2017). mTOR activity is crucial for translation initiation, e.g. when mTOR activity is low, S6K1 is dephosphorylated and 4EBP binds to the eukaryotic initiation factor 4E (eIF4E) to inhibit the assembly of the eIF4F complex and finally repress translation initiation (Graves et al., 1995; Lin et al., 1995; Gingras et al., 1998; Proud, 2002). On the other hand, activation of mTOR phosphorylates 4EBP, which causes the dissociation from eIF4E and thereby mediating translation initiation (Lin et al., 1994). 4EBP has a hierarchical phosphorylation mechanism for regulating eIF4E mediated cap dependent translation. The phosphorylation in Thr-37 and Thr-46 in 4EBP is not associated with the loss of eIF4E binding. However, phosphorylation at these sites is required for subsequent phosphorylation of several carboxy-terminal serum-sensitive sites (Gingras et al., 1999). In addtion, promotion of translation is mediated by the phosphorylation of S6K1 through mTOR. The phosphorylation levels of 4EBP and S6K1 are often used as indicators for mTOR activity.

mTOR activity tightly controls the translation of a subset of genes, those transcripts contain 5’ terminal oligopyrimidine (TOP) motif, which usually contains 4 to 14 “C” or “U” and locates at the 5’ end of the mRNA, following the cap structure (Levy et al., 1991; Meyuhas, 2000). First described in mammalian ribosomal protein mRNAs, TOP mRNAs were successively reported in multiple species (Levy et al., 1991; Avni et al., 1994; Meyuhas et al., 1996; Amaldi and Pierandrei-Amaldi, 1997; Carroll et al., 2004; Meyuhas and Dreazen, 2009). However, how TOP mRNAs are regulated by mTOR is still unclear. Damgaard and colleagues reported amino acid starvation-mediated mTOR inhibition

and activation of GCN2 kinase could induce binding of stress granule-associated TIA-1 and TIAR proteins to the 5' end of TOP mRNAs. This caused translational arrest of the 5' TOP mRNAs at the initiation step (Damgaard and Lykke-Andersen, 2011). Recent studies reported that LARP1 is a direct substrate of mTORC1, mediating TOP mRNA translation (Fonseca et al., 2015; Hong et al., 2017; Lahr et al., 2017; Philippe et al., 2018). When mTOR activity is too low to phosphorylate LARP1, LARP1 binds to both 5' and 3'UTRs of TOP mRNAs and inhibits their translation. mTOR activation phosphorylates LARP1, which then dissociates from the 5'UTR to relieve the inhibition of translation. Thoreen and colleagues suggested a unifying model that almost all the transcripts that are specifically regulated by mTORC1 have a TOP or TOP-like motif (Thoreen et al., 2012). The selective inhibition of those transcripts is caused by the decreased phosphorylation of 4EBP upon mTORC1 inhibition. However, this model needs to be further studied since there have been new TOP or TOP-like mRNAs successively detected.

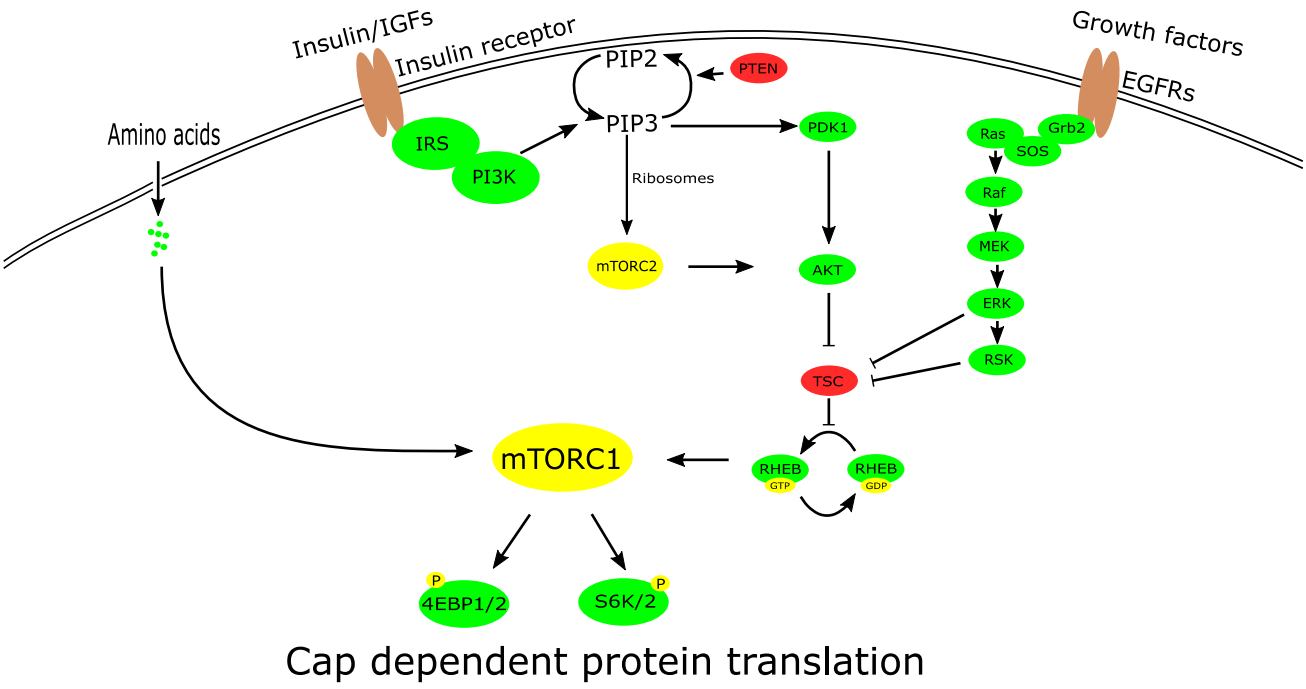

Figure 3. Regulatory network of mTOR signaling pathway

mTOR signaling pathway is regulated by multiple upstream regulators such as amino acids, insulin, growth factors. Modified according to (Silvera et al., 2010; Meng et al., 2018).

1.4 Post-transcriptional control during neurogenesis

Post-transcriptional regulation is an important process to control gene expression at the RNA level. In this process, RNAs are finely processed under multiple types of regulations like mRNA capping, alternative splicing, polyadenylation, mRNA nucleolar export, stabilization, translation. This process involves many types of regulators such as RNA binding proteins, microRNAs, long noncoding RNAs etc. RNA binding protein mediated regulation is most prevalent, the malfunction of which is often associated with severe diseases. The impaired function of the decapping enzyme DCPS, which functions in the last step of the 3′ end mRNA decay pathway, is linked to syndromic intellectual disability with neuromuscular defects (Ng et al., 2015). Mutations in core components of spliceosome were reported to cause impaired pre-mRNA splicing and retinitis pigmentosa (Cao et al., 2011; Tanackovic et al., 2011; Carey and Wickramasinghe, 2018). Lethal congenital contracture syndrome, a fetal motoneuron disease, is resulted from the mutation in mRNA export mediator GLE1 (Nousiainen et al., 2008). RNA binding proteins usually have zinc-finger RNA recognition motif, which allow them to recognize, bind and catalyze biochemical reactions (Colgan and Manley, 1997). Most of these RNA binding proteins are evolutionally conserved. Around 6% work in a tissue specific manner and the majority of them are ubiquitously expressed (Gerstberger et al., 2014).

In neurons, mRNAs are usually tightly controlled for local translation in response to rapid extracellular stimuli (Jung et al., 2012). Zappulo and colleagues reported that RNA localization is a key determinant of neurite-enriched proteome (Zappulo et al., 2017), suggesting the key role of post-transcriptional regulation in neuronal function. Notably, post-transcriptional regulation also plays a role in NSC fate control, including NSC differentiation. Numerous post-transcriptional regulation mechanisms involving mRNA splicing, mRNA decay and translation have been reported (Kim, 2016). RNA binding protein Musashi1 mediated translational repression of m-Numb activates Notch signaling for NSC maintenance (Imai et al., 2001; Kawahara et al., 2008). Meanwhile, Musashi1 inhibits translation of Doublecortin (DCX) to repress NSC differentiation (Horisawa et al., 2009). The mammalian Pumilio proteins Pumilio1 and Pumilio2, members of the PUF

family of sequence-specific RNA-binding proteins, bind thousands of targets, from which over 690 are involved in neurogenesis. They are involved in multiple processes such as stem cell fate and neurological functions by inhibiting translation, promoting mRNA decay or in certain contexts enhancing protein expression (Zhang et al., 2017; Goldstrohm et al., 2018). The neural-specific inactivation of Pumilio1 and Pumilio2 leads to a decrease in the number of NSCs in the dentate gyrus and impaired learning and memory (Zhang et al., 2017). However, studies of post-transcriptional control in translation during NSC differentiation are still in a low number. The role of post-transcriptional regulation in early onset of NSC differentiation remains to be elucidated.

1.5 Transcriptome and translatome analysis of NSCs and their progenies

Single cell RNA sequencing-based transcriptome analysis has advanced our knowledge in the process of dormant NSC activation (Llorens-Bobadilla et al., 2015). However, the transcriptome of a cell does not necessarily reflect its translatome. For the translation of an mRNA transcript, multiple layers of regulation may occur post-transcriptionally in response to multiple stimuli and result in dynamic levels of protein in the cell. Furthermore, transcriptome analysis normally requires cell isolation, which usually causes damage of cellular morphology and subsequently changed gene expression, introducing biases in the final sequencing data (Haimon et al., 2018). Therefore, it is very inaccurate to investigate protein information through analysis of the transcriptome. The development of translating ribosome affinity purification (TRAP) technique suggested a good solution for this problem (Doyle et al., 2008; Heiman et al., 2008). By labeling ribosomes with a tag protein to perform anti-tag immunoprecipitation, it is possible to isolate the ribosome-associated mRNAs in a cell, termed the translatome. Driven by a cell type specific promoter, it is also possible to isolate the translatome of a specific cell type in a complicated tissue or organ. Soon after the invention of this technique, Sanz and colleagues developed the Cre inducible Ribotag mouse line, which was a more robust system and had broader applicability (Sanz et al., 2009; Shigeoka et

al., 2016). The Exon 4 of the endogenous ribosomal protein 22 (Rpl22) in this mouse line is floxed by the lox P sites, followed by an identical Exon 4, which is tagged by hemagglutinin (HA). Multiple cell types can be targeted by crossing this line to a cell type specific Cre line.

In order to study the role of translation during neurogenesis, previous work in our lab established transgenic mouse models Tlx-CreER-Rpl22.HA-eYFP (TiCRY) and DCX-CreER-Rpl22.HA-eYFP (DiCRY) based on the Ribotag mouse line to analyze the transcriptome and translatome of NSCs and their progenies: early neuroblasts (ENBs) in the SVZ, late neuroblasts (LNBs) and neurons in the OB (Figure 4). HA tagging and parallel YFP expression were induced in the targeted cells by tamoxifen administration. Next generation RNA sequencing was performed to the fluorescence activated cell sorting (FACS) isolated YFP positive cells to acquire the transcriptome. Meanwhile, RNAs isolated through anti-HA immunoprecipitation were sequenced as the translatome. The transcriptome and translatome were acquired for NSCs, ENBs, LNBs, and neurons. In the following text, the term “RNA-seq” will be used to represent the sequenced transcriptome and the term “RiboIP-seq” to represent the sequencing data acquired from the translating ribosomes.

The combined analysis of transcriptome and translatome of the four types of cells identified numerous genes, which were selectively repressed or enhanced for translation upon the transition from NSCs to ENBs. De novo analysis of the regulatory region of these transcripts revealed that the translationally repressed gene transcripts featured a “CUCUU” Pyrimidine Rich Motif (PRM) in their 5’ UTR. This motif resembles the previous reported TOP or TOP like motif, suggesting its translational sensitivity to mTOR activity. However, the association of the PRM containing genes and mTOR activity as well as the molecular mechanism leading to repressed and enhanced gene translation during NSC differentiation remains to be investigated.

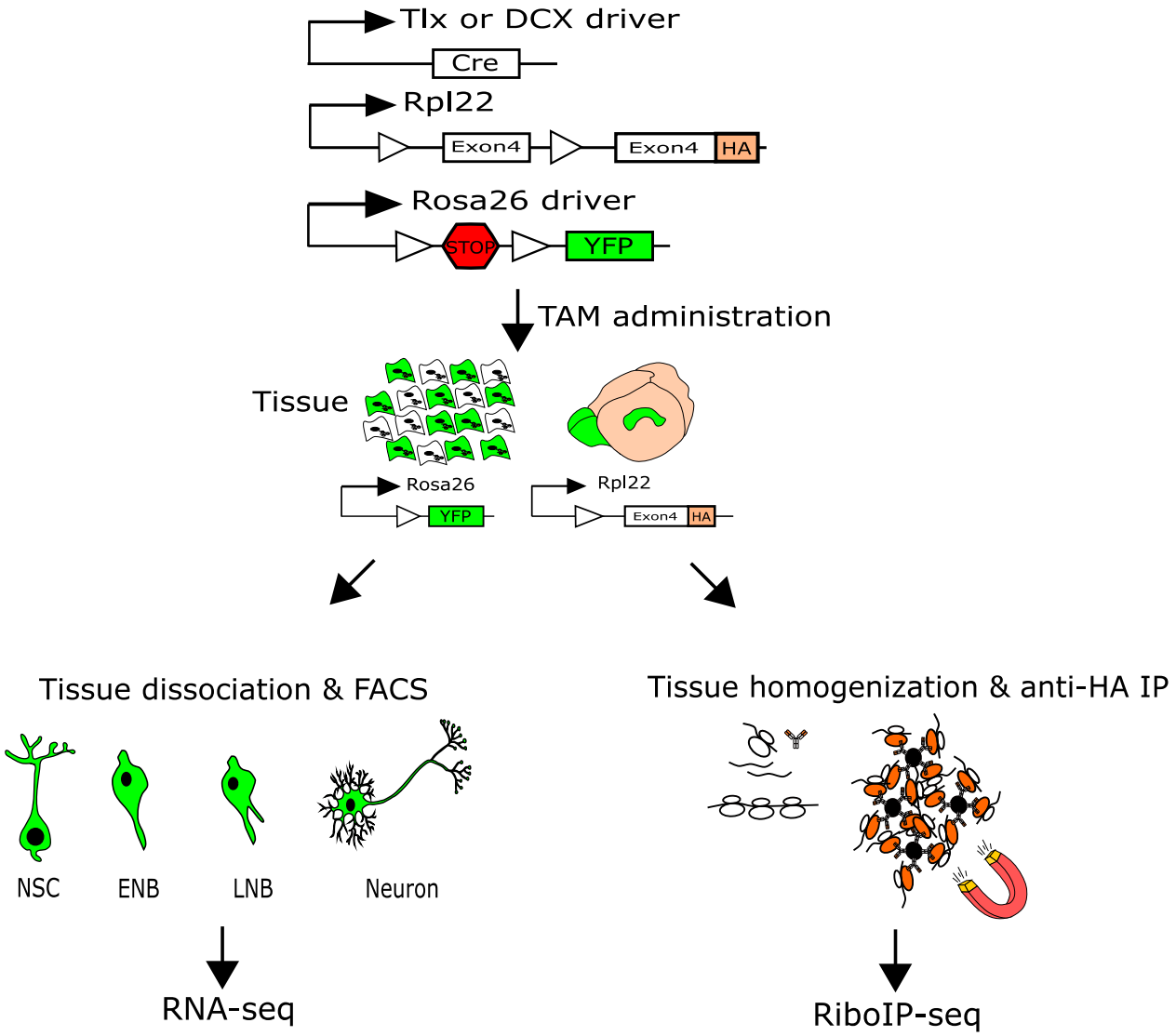

Figure 4. Ribo-tag mouse models allow parallel isolation of ribosome-bound mRNAs and total RNA of the same type of cells

Cell type specific Cre promoters drive gene recombination in NSCs and their progenies, introducing HA-tagged ribosomes and parallel YFP expression in the cells in a spatially and temporally controllable manner. Ribosome bound mRNAs and total RNAs of the same cells can be isolated by anti-HA immunoprecipitation (IP) and YFP based FACS followed by high throughput sequencing. Here NSCs, ENBs, LNBs and neurons were analyzed. Figures were modified from (Sanz et al., 2009; Baser, 2018).

1.6 Aim of the project

We attempt to investigate the molecular mechanism of early neural stem cell differentiation, and specifically focus on the role of mTOR during the post-transcriptional regulation of NSC differentiation. We would like to:

(1) Reveal the level of global protein synthesis along the NSC-to-ENB lineage;

(2) Investigate mTOR activity in NSCs and ENBs *in vivo*;

(3) Study how mTOR specifically regulates translation of PRM containing transcripts such as ribosomal protein Rpl18 and stem cell marker Sox2 during the process of early NSC differentiation.

2 Materials and methods

2.1 Materials

2.1.1 Instruments/software

Table 1, Instruments/software and their manufacturers/sources

Instruments	Manufacturer
Biophotometer	Eppendorf
CFX384 Touch™ Real-Time PCR Detection System	Bio-RAD
ChemiDoc Touch Imaging System	Bio-RAD
Density Gradient Fractionator	Teledyne Isco
FACS Analyser Fortessa	BD Biosciences
FACS Canto analyzer	BD Biosciences
FACS Canto sorter	BD Biosciences
FlowJo	FlowJo LLC
Gradient Makers Model SG 15	Thermo Fisher Scientific
Image Lab	Bio-RAD
ImageJ	NIH
Inkscape	Inkscape Project Software developer
Lab-Tek Chambers (8-well/16-well chamber slide)	Thermo Fisher Scientific
NanoDrop™ Spectrophotometer	Thermo Fisher Scientific
Qubit 2.0 Fluorometer	Life Technologies
SP5	Leica
Ultra-centrifuge Model L-90K	Beckman Coulter

2.1.2 Chemicals/Reagents/Kits

Table 2, Chemicals/Reagents/Kits and their source

Chemicals/Reagents/Kits	Source
Accutase	Sigma-Aldrich
Acid-Phenol: Chloroform (5:1), pH 4.5	Ambion
Agilent RNA 6000 RNA Pico Kit	Agilent
Amersham ECL Prime Western Blotting Detection Reagent	GE Healthcare
AZD2014	Biomol
Azide 488 or Azide 647	Thermo Fisher Scientific
β-mercaptoethanol	Sigma
BCA kit	Thermo Fisher Scientific
bFGF	Relia Tech
Boric Acid	Thermo Fisher Scientific
Bovine serum albumin (BSA)	Sigma
B27 Supplement	Life Technologies
Click-IT Cell Reaction Buffer Kit	Life Technologies
C Tubes	Miltenyi Biotec
Cycloheximide (CHX)	Sigma-Aldrich
C0mplete Protease Inhibitor Cocktail Tablets	Roche
D-(+)-Glucose	Sigma-Aldrich
Diethyl Pyrocarbonate (DEPC)	Sigma-Aldrich
Dimethyl Sulfoxide (DMSO)	Sigma-Aldrich
Dithiothreitol (DTT)	Sigma-Aldrich
dNTP Mix (10mM)	Fermentas
Epidermal Growth Factor (EGF)	Promocell
Ethanol	Riedel de Haen
Ethylenediaminetetraacetic Acid (EDTA)	Thermo Fisher Scientific

Fetal Bovine Serum (FBS)	Biochrom
Fluoromount-G	eBioscience
Fluoromount G with DAPI	Southern Biotech
Glutamine	Life Technologies
Glycerol	Sigma
Glycine	Sigma-Aldrich
Glycoblue	Ambion
Hank's Balanced Salts Solution (HBSS)	Life Technologies
Heparin Cell Culture Grade	Sigma-Aldrich
HEPES	Gibco
Hoechst 33342	Biotrend
Hydrochloric Acid (HCl)	VWR
Isoflurane	Baxter
Laemmli (4x Sample Buffer)	Bio-Rad
Laminin	Sigma-Aldrich
L-Glutamine (100x)	Invitrogen
LY294002	Cell signaling
Magnesium Sulfate ($MgSO_4$)	Sigma-Aldrich
Neural Tissue Dissociation Kit, Papain	Miltenyi Biotec
Neural Tissue Dissociation Kit, Trypsin	Miltenyi Biotec
Neurobasal Medium (NBM)	Thermo Fisher Scientific
Nonidet P-40 (NP-40)	Roche
Nuclease free water 10x 50 mL	Ambion
Oligonucleotide Primers	MWG
Omnican Insulin Syringes	Geyer
O-Propargyl-Puromycin (OP-Puro)	Jena Bioscience
Paraformaldehyde (PFA) Ampules (16%)	Thermo
Paraformaldehyde (PFA) (4%)	Roth
PBS (without Mg^{2+}/Ca^{2+})	PAA
Penicillin Streptomycin	Life Technologies

PicoPure RNA Isolation Kit	Arcturus
Pierce BCA Protein Assay Kit	Thermo Fisher Scientific
Pierce IP Lysis Buffer	Thermo Fisher Scientific
phosphatidylinositol-3,4,5-trisphosphate (PIP3)/AM(DOG)	Schultz Lab, EMBL
Pluronic F-127 (20% Solution in DMSO)	Invitrogen
Poly-D(L)-lysine hydrobromide (PDL or PLL)	Sigma-Aldrich
Potassium Chloride (KCl)	Applichem
Proteinase K	Peqlab
Potassium Phosphate Monobasic (KH_2PO_4)	Gerbu
Precision Plus Protein™ WesternC™ Blotting Standards	Bio-Rad
Puromycin	Life Technologies
QuantiTect Primer Assays	Qiagen
Qubit dsDNA High-Sensitivity (HS) Kit	Life Technologies
RNase-Free DNase Set	Qiagen
RNasin Plus RNase Inhibitor (RNAsin)	Promega
Sodium Acetate ($C_2H_3NaO_2$)	Ambion
Sodium Azide (NaN_3)	Merck
Sodium Chloride (NaCl)	Sigma
Sodium Chloride 0.9% Sterile (NaCl)	Braun
Sodium Dihydrogen Phosphate Monohydrate (NaH_2PO_4)	Roth
Sodium Dodecyl Sulfate (SDS)	Roth
Sodium Hydroxide (NaOH)	Sigma-Aldrich
Sodium Phosphate Dibasic Heptahydrate ($Na_2HPO_4 \cdot 7H_2O$)	Sigma-Aldrich
Sodium Tetraborate (Borax, $Na_2B_4O_7 \cdot 10H_2O$)	Merck
Sucrose	Sigma-Aldrich

Sunflower Oil	Sigma-Aldrich
SuperFrost Slides	Roth, Germany
SuperScript VILO cDNA Synthesis Kit	Life Technologies
SYBR Green PCR Master Mix	Applied-Biosystems
Tamoxifen	Sigma-Aldrich
Thymidine	Sigma
Torin 1 (simplified as Torin in the following text)	Biomol
Trans-Blot® Turbo™ RTA Midi Nitrocellulose Transfer Kit	Bio-Rad
Trichloroacetic Acid (Cl_3CCOOH)	Sigma-Aldrich
Tris Base ($C_4H_{11}NO_3$)	Sigma-Aldrich
Triton X-100	Sigma-Aldrich
Trypsin-EDTA (0.05%)	Life Technologies
Tween-20	Merck
Ultracentrifuge Tubes for SW41 rotor	Beckman Coulter
12% Criterion™ TGX Stain-Free™ Protein Gel, 18 well, 30 µl	Bio-Rad
10% Mini-PROTEAN® TGX Stain-Free™ Protein Gels, 10 well, 50 µl	Bio-Rad
40 µm strainer	BD Falcon

2.1.3 Solutions/media/buffers

Table 3, Solutions/media/buffers and their recipes

Experimental procedure	Buffer/Solution/Media	Recipe
Isolation of NSCs/ FACS	Tamoxifen solution	Tamoxifen, 10 mg/mL (final); $V_{sunflower\ oil}$: V_{EtOH}= 9:1.
	FACS buffer	10% FBS in PBS
	Dissection solution	50 mL 10x HBSS; 1.25 mL 1M HEPES; 3.25 g D- Glucose; 5 mL Pen/Strep; Adjust to 500 mL with ddH2O and filter (sterile).
Immunocytochemistry	Phosphate Buffered Saline (PBS), 1x	To prepare 20x PBS: 160g/L NaCl (final); 28.4g/L Na2HPO4 (final); 4g/L KCl (final); 4.8g/L KH2PO4 (final); pH 7.4 (final).
	0.1 M Phosphate buffer	77.4 mL of 1 M Na_2HPO_4; 22.6 mL of 1 M NaH_2PO_4; Dilute the combined 1 M stock solution up to 1 L with distilled H_2O; pH was finally adjusted to 7.4
	Tris-Buffered Saline (TBS), 10x	Tris base, 0.2 M (final); NaCl, 1.5 M (final); pH was finally adjusted to 7.2 - 7.4.
	Permeabilization buffer	0.25% Triton X-100, dissolved in PBS.
	Blocking solution	0.25% Triton-X 100 with 5% BSA in PBS (5g BSA and 0.25 mL Triton-X 100 per 100 mL PBS)
	Alkyne-Azide reaction buffer (1 mL) (The reaction buffer, additive and $CuSO_4$ were from Click-IT cell reaction buffer Kit)	876 µL 1x reaction buffer; 100 µL Addictive; 20 µL $CuSO_4$; 4 µL Azide 488 or Azide 647 (1:250 dilution).
Cell Culture	Neurobasal medium supplemented with growth factors (GFs)	500 mL Neurobasal Medium; 10 mL B27 supplement (50x); 5 mL L-Glutamine (200mM); 500 µL 2mg/mL Heparin (final: 2 µg/mL); 20 µL 0.5 µg/µL bFGF (final: 20 ng/mL); 20 µL 0.5 µg/µL EGF (final: 20 ng/mL).
	Borate buffer	1.24 g boric acid; 1.9 g sodium tetraborate (Borax); Adjust to 400mL with H_2O, adjust pH to

		8.5 and sterile filtered.
	PDL coating solution	1mg/mL Poly-D-Lysine, dissolve in borate buffer and sterile filtered.
	Laminin coating solution	50 µg/mL laminin, dilution in NBM.
	OP-Puro solution	Stock solution 20 mM (5% DMSO, 95% PBS); applied to cell cultures at 1:400 dilution (50µM final).
	Torin solution	Dissolve 10mg in 5.5mL DMSO to make 3mM stock (-80 °C); Dilute 1:30 in PBS to make 100µM working solution for use (-20 °C); Applied to cell cultures at 1:400 when use (final: 250nM).
Sucrose Gradient Fractionation	DEPC H_2O	Add 1 mL DEPC to 1 L H_2O. Leave in the hood overnight and autoclave.
	Gradient buffer (2x)	Tris-HCl pH 7.4 (40 mM); $MgCl_2$ (10 mM); NaCl (240 mM); Prepare in DEPC H_2O.
	Polysome Lysis Buffer supplemented with cycloheximide (PLB+)	3 mL Gradient buffer (2x); 2.56 mL DEPC H_2O; 240 µL Nonidet NP-40 (25%); 60 µL CHX (10mg/mL); 120 µL c0mplete protease inhibitor (50X); 6 µL b-mercaptoethanol; 15 µL RNAsin.
	Light sucrose gradient solution (17.5%)	7 g sucrose; 20 mL 2X Gradient buffer; 80 µL 1 M DTT (final: 2 mM) ; 0.4 mL 10 mg/mL CHX (final: 0.1 mg/mL); Adjust to 40mL with DEPC H2O.
	Heavy sucrose gradient solution (50%)	20 g sucrose; 20 mL 2X Gradient buffer; 80 µL 1 M DTT (final: 2 mM); 0.4 mL 10 mg/mL CHX (final: 0.1 mg/mL); Adjust to 40mL with DEPC H2O.
RNA isolation from sucrose gradient solution	Proteinase K solution	Per 1 mL of sucrose fraction: 37.5 µL 10% SDS; 7.5 µL 0.5 M EDTA; 1 µL Glycoblue; 4 µL 20 mg/mL Proteinase K
Western blot	PI (10x)	0.42 g NaF; 0.65 g NaN_3; 3.71 g p-nitrophenyl phosphate; 4.46 g Sodium pyrophosphate; 3.06 g

		beta-glycerolphosphate; Adjust to 100 mL
	C0mplete protease inhibitor	1 cocktail tablet, dissolve in 1 mL H_2O.
	Vanadate	Use sodium orthovanadate to prepare 100 mM solution, heat the solution up to boiling.
	Cell lysis buffer	Pierce IP Lysis Buffer supplemented with 1x protease inhibitors such as PI, c0mplete protease inhibitor and vanadate.
	Laemmli sample loading buffer	The Laemmli buffer was supplied with β-mercaptoethanol and diluted to 1x.
	Running buffer 10X	Dissolve 30.0 g of Tris base, 144.0 g of glycine, and 10.0 g of SDS in 1000 ml of H_2O. pH=8.3. Stored at room temperature and dilute to 1X before use.
	PBST/TBST	PBS or TBS supplemented with 0.1% Tween20
	Membrane transfer buffer	Prepare according to Trans-Blot® Turbo™ transfer kit (Bio-Rad).

2.1.4 Antibodies/reagents used for FACS

Table 4, Antibodies/reagents used for FACS

Antibodies/reagents	Conjugates	Manufacturer	Dilution	Isotype/Clone
Anti-O4 antibody	APC-vio770	Miltenyi Biotec	1:50	Mouse IgM/O4
Anti-Ter119 antibody	APC-Cy7	BioLegend	1:100	Rat IgG2b/ TER-119
Anti-CD45 antibody	APC-Cy7	BD Biosciences	1:200	Rat IgG2b/30-F11
Anti-CD133 antibody	APC	eBioscience	1:75	IgG1, kappa/13A4
Anti-GLAST antibody	PE	Miltenyi Biotec	1:20	Mouse IgG2a/ACSA-1
Anti-PSA-NCAM antibody	PE-Vio770	Miltenyi Biotec	1:75	Mouse IgM/2-2B
EGF (protein)	Alexa488	Life Technologies	1:200	-
EGF (protein)	Alexa647	Life Technologies	1:100	-
FcR Blocking Reagent	-	Miltenyi Biotec	1:20	-
Sytox Blue (1 mM)	-	Life Technologies	1:1000	-

2.1.5 Antibodies used for Western blot or immunofluorescence

Table 5, Antibodies used for Western Blot or ICC/IHC

Antibodies	Manufacturer	Clone	Molecular weight	Dilution	Host/Isotyoe
AKT	Cell signaling	Polyclonal	60 kDa	1:1000	Rabbit
Phospho-AKT (Ser473)	Cell signaling	Polyclonal	60 kDa	1:1000	Rabbit
DCX	Merck	Polyclonal	-	1:1000	Guinea Pig
Dusp4	Abcam	Polyclonal	44 kDa	1:500	Rabbit
4EBP1	Cell signaling	53H11	15 to 20 kDa	1:1000	Rabbit/IgG
Phospho-4EBP1 (Thr37/46)	Cell signaling	236B4	15 to 20 kDa	1:1000	Rabbit/IgG
GLAST	Frontier Institute	Polyclonal	-	1:1000	Guinea pig
Ki67	Novus Biologicals	SP6	-	1:100	Rabbit/IgG
Rgs16	OriGene	OTI3B4	25 kDa	1:2000	Mouse/ IgG1
PLP1	OriGene	Polyclonal	~ 26-29 kDa	1:400	Chicken
S6 Ribosomal Protein	Cell signaling	5G10	32 kDa	1:1000	Rabbit/IgG
Phospho-S6 (Ser240/244)	Cell signaling	Polyclonal	32 kDa	1:1000	Rabbit
S6 Kinase	Cell signaling	Polyclonal	70, 85 kDa	1:1000	Rabbit
Phospho-p70 S6 Kinase (Thr389)	Cell signaling	Polyclonal	70, 85 kDa	1:1000	Rabbit
Sox2	Abcam	EPR3131	34 kDa	1:1000	Rabbit/IgG
Tuberin/TSC2	Cell signaling	D93F12	200 kDa	1:1000	Rabbit
Phospho-TSC2 (Thr1387)	Cell signaling	Polyclonal	200 kDa	1:1000	Rabbit
Phospho-TSC2 (Thr1462)	Cell signaling	5B12	200 kDa	1:1000	Rabbit
Vash2	Abcam	Polyclonal	~ 41 kDa	1:500	Rabbit
Vinculin	Abcam	EPR8185	124 kDa	1:5000	Rabbit
YFP	Aves Labs	Polyclonal	-	1:1000	Chicken/IgY

2.1.6 Secondary antibody used for immunocytochemistry

Table 6, Secondary antibody used for ICC

Antibodies	Manufacturer	Conjugate	Dilution	Host
Anti-chicken	Dianova	DyLight488	1:500	Donkey
Anti-guinea pig	Life Technologies	Alexa546	1:500	Goat
Anti-rabbit	Life Technologies	Alexa555	1:500	Donkey

2.1.7 Primers used for quantitative PCR

Table 7, Primers used for quantitative PCR

Gene	Primer	Source	Cat. no.
Atp2b1	Mm_Atp2b1_1_SG QuantiTect Primer Assay	Qiagen	QT01072106
Birc6	Mm_Birc6_1_SG QuantiTect Primer Assay	Qiagen	QT00163863
Dusp4	Mm_Dusp4_1_SG QuantiTect Primer Assay	Qiagen	QT00140357
Plp1	Mm_Plp1_1_SG QuantiTect Primer Assay	Qiagen	QT00096096
Rgs16	Mm_Rgs16_1_SG QuantiTect Primer Assay	Qiagen	QT00137753
Rheb	Mm_Rheb_1_SG QuantiTect Primer Assay	Qiagen	QT00168133
Rps20	Mm_Rps20_1_SG QuantiTect Primer Assay	Qiagen	QT00251433
Sp8	Mm_Sp8_1_SG QuantiTect Primer Assay	Qiagen	QT01056930
Vash2	Mm_Vash2_1_SG QuantiTect Primer Assay	Qiagen	QT00114765
Vim	Mm_Vim_1_SG QuantiTect Primer Assay	Qiagen	QT00159670
Sox2	Mm_Sox2_1_SG QuantiTect Primer Assay	Qiagen	QT00249347

2.2 Methods

2.2.1 Animal models

All experimental mice (*Mus musculus*) were bred and housed under standard conditions in the animal facility of the German Cancer Research Center (DKFZ, Heidelberg, Germany). Legal requirements with regard to housing, space, temperature, humidity, enrichment, minimal stress and disease free etc. were ensured for the animals prior to experiments. The animals had access to food and water *ad libitum* and maintained in 12 hour dark/light cycles. All animal experiments were in accordance with the institutional guidelines and under animal permissions (DKFZ 288, DKFZ 352 and G-272/15) approved by the Regierungspräsidium Karlsruhe, Germany.

C57BL/6N mice (6-8 weeks old) hereafter referred to as wild type (WT). Two transgenic mouse lines were used. 1) TlxCreER-eYFP-Rpl22-HA (TiCRY) mice were generated by crossing Tlx-CreERT2 mice to R26-LSL-EYFP mice and Rpl22-HA mice. Tlx-CreERT2 mice were a nice gift from Prof. Hai-kun Liu. 2) Fluorescent ubiquitylation-based cell cycle indicator (Fucci2) mice were a kind gift from the Milsom lab in HI-STEM (Heidelberg, Germany). The official nomenclature of the above mentioned mice were listed in Table 8.

To induce recombination in the Cre/loxP-System, tamoxifen was injected intraperitoneally (i.p.) into 8 to 12-week-old mice at concentration of 40 mg/kg bodyweight. For cell cycle experiments, Fucci2 mice were sacrificed and NSCs were isolated and taken in culture. These NSCs were used for FACS analysis after synchronization.

Table 8, Official nomenclatures of transgenic mice

Short name	Official nomenclature
C57BL/6N	B6-Wlstm1.1 Arte Tg(CAG-Flpe)2Arte/Mbtr
Tlx-CreERT2	B6-Tg(Nr2e1-Cre/ERT2)1Gsc
R26-LSL-EYFP	B6.129X1-Gt(ROSA)26Sor-tm1(EYFP)Cos
Rpl22-HA	B6.129-Rpl22tm1.1.1Psam/Atp
TlxCreER-eYFP-Rpl22-HA	B6-Tg(Nr2e1-Cre/ERT2)1Gsc Gt(ROSA)26Sortm1(EYFP)Cos Fastm1Cgn Rpl22tm1.1Psam/Amv
R26p-Fucci2	B6-Tg(Gt(ROSA)26Sor-Fucci2)#Sia

2.2.2 Cell culture

a) Isolation and maintenance of primary neural stem cells

For NSCs isolation, 8-12 weeks old mice were sacrificed by cervical dislocation. SVZs were microdissected as a whole mount according to the previously described protocol (Mirzadeh et al., 2010). Cells were isolated by treating the tissue with trypsin and DNase supplied from the Neural Tissue Dissociation P kit in a Gentle MACS Dissociator (Miltenyi Biotec). After that, they were cultured in NBM in the presence of growth factors (20 ng/mL of bFGF and EGF).

b) Inhibitor treatments

To inhibit mTOR activity in NSCs, multiple compounds were used either individually or in combination. Torin was added to cells to reach a final concentration of 250 nM. The final concentration of LY294002 was 5 μM and the final concentration for puromycin was 0.5 μM.

c) Lab-Tek Chamber/glass slide coating

Lab-Tek Chamber/glass slides were firstly coated with 100 μg/mL PDL solution overnight at 37°C in a CO_2 incubator. After PDL removal by washing 2x 1h with sterile Milil-Q water, the slides were recoated with 50 μg/mL of laminin at 37°C for 2 h. Laminin was washed away with NBM, and cells were immediately plated for culture.

d) PIP3 treatment

PIP3/AM(DOG) was synthesized as described before (Dinkel et al., 2001) and was kindly supplied by the Schultz Lab (EMBL, Heidelberg, Germany). PIP3/AM, dissolved in DMSO, was stored at -80°C as a stock solution (50 mM). Cells were treated at final concentration of 10 µM. To facilitate penetration through the cell membrane, PIP3 was diluted in 20% pluronic F127/DMSO. After 10 min incubation at 37°C, PIP3 was washed away by centrifugation and the cells were replenished with fresh NBM. For double treatment with PIP3 and Torin, Torin was first added to the cells at a final concentration of 250 nM 5 min prior to PIP3 treatment, which was incubated for additional 10 min. PIP3 was washed out before Torin was re-added to the cells for 2 h incubation. Upon completion, Torin containing medium was replaced with fresh NBM.

e) Cell synchronization

NSCs at a low passage (passage 2) were synchronized by double thymidine block (dTB) to accumulate them at G1/S phase. Cells were incubated with a final concentration of 2 mM thymidine in normal NBM for 18 hours. Thereafter the cells were washed twice and fresh NBM was added to the cells for 9 hours to release the cell cycle block. The second round of thymidine treatment was performed for additional 16 hour to ensure a complete block of NSCs at G1/S phase.

f) Polysome profiling of NSCs *in vitro*

For each sample, 10^6 NSCs were seeded in a 150 cm^2 flask 3 to 4 days before cells lysis. Cells were used for polysome profiling at 70% confluency. 17.5% - 50% sucrose gradient was formed in polypropylene centrifugal tubes for SW41 rotor by mixing 5.5 ml of each freshly prepared sucrose solution in a SG15 gradient maker. The tubes were kept at 4°C until use to hold the sucrose solution pre-cooled.

To prevent ribosome dissociation from mRNAs during cells lysis and centrifugation, CHX was added to each flask and the cells were incubated at 37°C for 5 min to freeze preformed polysomes. Afterwards cells were collected by centrifugation. After two rounds of wash with 10 ml of ice-cold PBS containing CHX, pellets were re-suspended in 600 µL of polysome lysis buffer (PLB) and kept on ice for 10 min, followed by

centrifugation at 15000 g, 4°C for 10 min to remove cell debris including the nuclei. The supernatant containing the cytoplasmic lysate was transferred into a new reaction tube, lysate concentration was measured by absorption at 254 nm in Nanodrop and the same amount of each lysate was loaded onto sucrose gradient solution in the tubes. PLB was used to equilibrate the tubes before placing them into the centrifugal buckets of a SW41 rotor. Centrifugation was performed at 35000 rpm at 4°C for 2.5 hours using an L8M Beckman Ultracentrifuge. After centrifugation, the content of each tube was fractionated with a density gradient fractionator and 12 fractions of 1 mL volume were collected. During fractionation, the absorption of the fractionated solutions was measured at 254 nm to draw polysome profiles across the gradient. The obtained fractions were kept at -80°C until further processing.

To analyze RNA distribution across the polysome profiles, total RNAs from individual fractions were extracted and used for cDNA synthesis and qRT-PCR. (Data produced jointly with Dr. M. Skabkin, division of Molecular Neurobiology, DKFZ)

g) Differentiation assay

NSCs were seeded on a glass slide pre-coated with Poly-D Lysine and laminin in NBM supplied with growth factors as previously described. Following overnight incubation, growth factors were withdrawn and 4 hours later the cells were treated with PIP3, Torin or DMSO as described in figure legends. After 7 days of culturing under differentiation conditions (NBM without growth factors), cells were fixed with 2% PFA and immunohistochemically stained for Sox2 and DCX (Data produced jointly with Dr. S. Kleber, division of Molecular Neurobiology, DKFZ).

h) Neurosphere Assay

To perform a neurosphere assay upon treatment with PIP3, DMSO and PIP3/Torin like previously described for PIP3 treatment (d), early neuroblasts were FACS sorted and 500 cells were plated on PDL and laminin-coated 16-well Lab-Tek chambers (Thermo Fisher Scientific). 5 wells were quantified for each condition. The number of spheres was calculated after 7 days in culture (Data produced jointly with Dr. S. Kleber, division of Molecular Neurobiology, DKFZ).

2.2.3 Flow cytometry

a) Cell sorting

Mice were sacrificed by cervical dislocation. SVZs were microdissected from the brains. SVZs from up to 5 mice were pooled as one sample for sorting. Samples were dissociated using the Neural Tissue Dissociation kit and a Gentle MACS Dissociator (Miltenyi Biotec). Sytoxblue (Thermo Fisher Scientific, 1:500) was used to detect and exclude dead cells. NSCs or ENBs were sorted following the protocol described before (Llorens-Bobadilla et al., 2015). GLAST, Prominin and EGFR were used as markers for NSCs, PSA-NCAM was used to sort ENBs.

b) Cell cycle phase analysis

NSCs isolated from Fucci2 mice were used to detect cell cycle phases by FACS after synchronization.

During cell cycle progression of the Fucci2 NSCs, fluorescently labeled Cdt1 and Geminin accumulate, labeling the nuclei of the G1 phase cells in red and S/G2/M phase cells in green, respectively. Thus, this dual color imaging technique makes it possible to pinpoint cell cycle phases for alive cells by FACS. Wild type NSCs without any fluorescence were used as control to define the negative population and set up the proper gates. The distribution of FITC and mCherry was analyzed in those cells. All Fucci flow cytometry cell cycle data was acquired with a FACS Analyser Fortessa (BD Biosciences) and was further analyzed using FlowJo.

2.2.4 Confocal microscopy and image processing

Cell images for lineage tracing and PIP3 treatment were acquired with a Leica TCS SP5 confocal microscope (Leica, Germany). Sequential scanning was used during imaging for different fluorophores to reduce cross interference between channels. All images within compared groups were acquired with identical settings. ImageJ/Fiji was used for image processing.

For OP-Puro, SOX2 and pS6 quantifications, a custom-written macro was applied to ImageJ/Fiji software for unbiased segmentation and quantification of pixel intensity and cell size. The integrated pixel intensity, reflecting the amount of incorporated OP-Puro amount, was normalized to ENBs as control group within the same experiment. All cells in the image were quantified for OP-Puro intensity. Those cells which showed dim YFP expression were discarded, leaving bright YFP positive cells for comparison. Besides, cell type markers were also used to further trace NSCs and ENBs of the YFP lineage. In graphs, mean and SD values were shown. Inkscape was used for the figure assembly.

2.2.5 Biochemistry techniques/assays

a) OP-Puro assay

The sorted cells were seeded in a Lab-Tek Chamber filled with 200 µL NBM without growth factors for 2 hours. OP-Puro solution was added to the cells and incubated at 37°C for 1 hour. Fixation of the OP-Puro treated cells was performed with 200 µL 4% PFA directly (final PFA concentration: 2%). Afterwards fixed cells were washed twice with PBS to remove residual OP-Puro. Cells were permeabilized with 0.25% Triton-X 100 solution and used for immunostaining. OP-Puro “click” reaction solution supplemented with Alexa Fluor 647-coupled azide was added to the cells and incubated for 30 min at room temperature following two times wash with PBST and one more time with PB solution. Finally, cells were mounted with Fluoromount G with DAPI (Southern Biotech) and used for subsequent microscopy.

b) Immunocytochemistry

Chambers or coverslips were pre-coated with PDL solution and laminin. Cells were seeded and cultured in the chambers with 200 µL NBM (containing growth factors) for 2 hours to attach. The double coated surface of the chambers/cover slips improved cells attachment, thereby reducing cell loss due to several rounds of washing after fixation. 4% PFA was added to the chambers/coverslips with NBM to double the total volume so that cells were fixed in 2% PFA. 20 min later, cells were washed with PBS for two times

followed by incubation with 0.25% Triton-X 100/PBS for 10 min for permeabilization. Two-time PBS washing was performed before blocking in 5% BSA for 30 min at room temperature. Cells were incubated with primary antibodies at 4°C overnight followed by incubation with corresponding secondary antibodies at room temperature for 1 hour. At least two-time PBS wash was used for both primary and secondary antibody staining to reduce the background. Finally, cells were dried, and mounted in standard mounting media including DAPI. The glass slides were used for confocal microscopy after drying at room temperature overnight in dark place.

c) Western blot

To perform a Western blot using freshly isolated *in vivo* cells, 12 to 20 mice were sacrificed to prepare for FACS isolation. Around 10 000 cells for *in vivo* NSCs and ENBs were sorted in protein low bind Eppendorf tubes. 5 µL of Glycoblue was added to the cells for centrifugation at full speed for 5 min. FACS buffer was discarded and 50 µL of IP lysis buffer supplemented with protease inhibitors was added to the cell pellet before kept at -80°C overnight to promote cells lysis. Next day, BCA kit was used estimate the protein concentration, the rest proteins were used for Western blot. Due to a small amount of the input protein and a limited number of possible re-probing steps for WB membranes, several rounds of FACS and WB were performed. Vinculin was used as a loading control. For WB of the cells in culture, 10^6 cells were lysed in 150 µL of lysis buffer and kept at -80°C overnight.

Next day, samples were thawed on ice. Each sample was mixed with a 30 gauge syringe for several times to improve lysate homogenization. The lysate was centrifuged at 13,000 rpm for 10 min at 4°C and the supernatant was transferred into a new reaction tube without touching the pellet. Protein concentration of the lysate was measured with the BCA kit. 10 µg of total protein was prepared in 1x Laemmli buffer and was heated for 5 min at 95°C to denature. Samples were loaded onto a 10% precast gel and run for 40 min at 200 Volt in 1x running buffer. After electrophoresis, roteins were transferred from gel onto a nitrocellulose membrane in the Trans-blot turbo instrument (Bio-Rad). TBST with 5% BSA was used for membrane blocking and correspondent primary antibodies were added for overnight incubation at 4°C. After that, the membrane was washed in

PBST or TBST for 3 times, with 10 min for each, to remove unbound primary antibodies. Secondary antibodies were added and incubated at room temperature for 1 h, followed by 3 times washing. Amersham ECL Prime reagent was prepared and added to the membrane to detect antibody signal in ChemiDoc Touch Imaging System.

2.2.6 RNA extraction

a) RNA extraction from sorted cells

Total RNA was extracted from cells with a PicoPure RNA isolation kit following manufacturer's protocol. The kit is designed to recover RNA from less than 10 cells and can also be used to recover up to 100 µg RNA. DNase I was used as recommended by the kit to eliminate genomic DNA contamination, allowing for high quality RNA recovery. The extracted RNA was finally obtained in 11 µL water. RNA concentration was measured with a NanoDrop Spectrophotometer and RNA samples were stored at -80°C until further analysis.

b) RNA extraction from sucrose gradient fractions

RNA extraction from sucrose gradient fractions was performed according to the protocol described by Faye and colleagues (Faye et al., 2014) with minor modifications.
300 µL of each fraction was placed in a reaction tube to incubate with 16.7 µL Proteinase K solution at 50°C for 1 h. The equal volume of phenol: chloroform (5:1) was added upon incubation. Extra 200 µL of chloroform were added to fractions 7-12 to avoid phase inversion as a result of high sucrose concentration in these fractions. After vortexing for 30 seconds, fractions were centrifuged at full speed at room temperature for 5 min. The upper aqueous phase of each fraction was taken out and transferred into a new reaction tube. Equal volume of chloroform was added to the aqueous solution, mixed and centrifuged at full speed for 5 min. The upper aqueous solution was again taken out and transferred into a new reaction tube filled with 1/10 volume of 3 M sodium acetate (pH 5.2) and 2.5 volume of cold, absolute ethanol. After 15 sec of vortex, all samples were placed at -20°C overnight. On the next day, samples were centrifuged at

full speed for 30 min at 4°C. The liquid phase was discarded, leaving the pellet, which was once washed with 75% ethanol. Then, pellets were air dried for 7 min at RT and dissolved in nuclease free H_2O. Finally, all samples were quantified for RNA concentration using Qubit Fluorometer and stored at -80°C until further usage.

c) cDNA synthesis

RNAs were extracted from the freshly isolated NSCs and ENBs or sucrose gradient fractions. For qPCR analysis, the cDNAs were synthesized using SuperScript VILO cDNA Synthesis Kit.

2 µL of each RNA sample (but not more than 2.5 µg of total RNA) were used as input to synthesize cDNA in a 20 µL reaction using a SuperScript VILO cDNA synthesis kit (Table 9). Reactions were incubated at 25°C for 10 min followed by 42°C for 60 min and 85°C for 5 min. cDNA sample stocks were stored at -20°C until further analysis.

Table 9, cDNA synthesis reaction composition

Component	Quantity
5x VILO Reaction Mix	4 µL
10x SuperScript Enzyme Mix	2 µL
RNA (up to 2.5 µg)	2 µL
Nuclease free water	12 µL

2.2.7 Real-Time Quantitative PCR

Real-Time Quantitative PCR (qRT-PCR) was used to estimate relative transcriptional expression of candidate genes. qPCR reactions were performed using 384-well plates in a CFX384 Touch™ Real-Time PCR Detection System. Each well contained a 10 µL reaction, including 5 µL of SYBR Green master mix, 3 µL of H_2O, 1 µL of primers and 1 µL of corresponding cDNA. Primers from Qiagen were thawed and directly used without dilution. cDNAs were diluted according to their concentrations (e.g. 2-5 times for RNA from sorted NSCs and ENBs; up to 10 times for RNA from cultured cells). All reactions were performed with 3 technical replicates. Actb was used as an internal control to

compare different cells types (NSCs vs ENBs) or different treatments (DMSO vs Torin). Relative expression of genes was calculated using ΔΔCt method.

2.2.8 Computational analysis

Bioinformatic analysis for both the repressed and up-regulated genes was performed in collaboration with Manuel Göpferich (division of Molecular Neurobiology, DKFZ) and Dr. Bernd Fischer (division of Computational Genome Biology, DKFZ).

2.2.9 Statistical analysis

The used statistical tests varied with the type of input data and they were specified in the respective figure legends.

Data were presented as mean ± SD in GraphPad Prism 6. Statistical significance was determined using unpaired Student's t test, with $p < 0.05$ for appropriate significance and $p < 0.01$ for extremely high significance.

3 Results

In order to gain comprehensive understanding of neurogenesis, previous work in our lab using lineage tracing mice has been undertaken to acquire the transcriptome and translatome of NSCs and their progenies such as ENBs, LNBs and neurons. The analysis revealed unique gene expression landscapes of each type of cells and unveiled a strict lineage-dependent regulation in the expression of the genes involved in protein biosynthesis and its control, what could indicate a critical role of post-transcriptional regulation in the process of neurogenesis. The following calculation of translation efficiency based on the comparison of the transcriptome and translatome of each stage identified a number of candidate genes undergoing post-transcriptional regulation. A series of studies were conducted *in vivo*, ex vivo and *in vitro* in order to determine the mechanism guiding post-transcriptional regulation during NSC differentiation, which is described in the following text.

3.1 Validation of RNA-seq data for NSCs and ENBs

Here we performed qPCR to validate the lineage tracing based RNA-seq data upon the NSC-to-ENB transition (Figure 5).

NSCs and ENBs were FACS isolated and collected using dissected SVZs pooled from mice. Total RNA was extracted from each type of cells and converted into cDNA, which was used for qPCR to detect the relative changes in the abundance of mRNAs for previously found candidate genes.

The earlier performed RNA-seq analysis showed that a number of genes encoding important cell fate defining transcription factors like Sox2 and Pax6 exhibited no change upon the NSC-to-ENB transition. Transcripts like plasma membrane calcium-transporting ATPase 1 (Atp2b1), baculoviral IAP repeat-containing protein 6 (Birc6), regulator of G-protein signaling 16 (Rgs16), and vasohibin-2 (Vash2) also showed no significant change. However, we detected up-regulation for dual specificity protein phosphatase 4 (Dusp4) and specificity protein 8 (Sp8) upon the transition. The mRNA levels of ribosomal protein S20 (Rps20), intermediate filament gene vimentin (Vim), myelin proteolipid protein gene proteolipid protein 1 (Plp1) and mTOR activator Ras

homolog enriched in brain (Rheb) in ENBs dropped to 20% -50% of the level in NSCs, manifesting significantly repressed gene expression upon the transition (Figure 5, a). Interestingly, the expression changes observed by qPCR showed similar result (Figure 5. b). Correlation analysis performed for the fold changes acquired from qPCR and RNA-seq showed a high correlation (Cor = 0.94), indicative of high accuracy of previously performed RNA-seq (Figure 5. c).

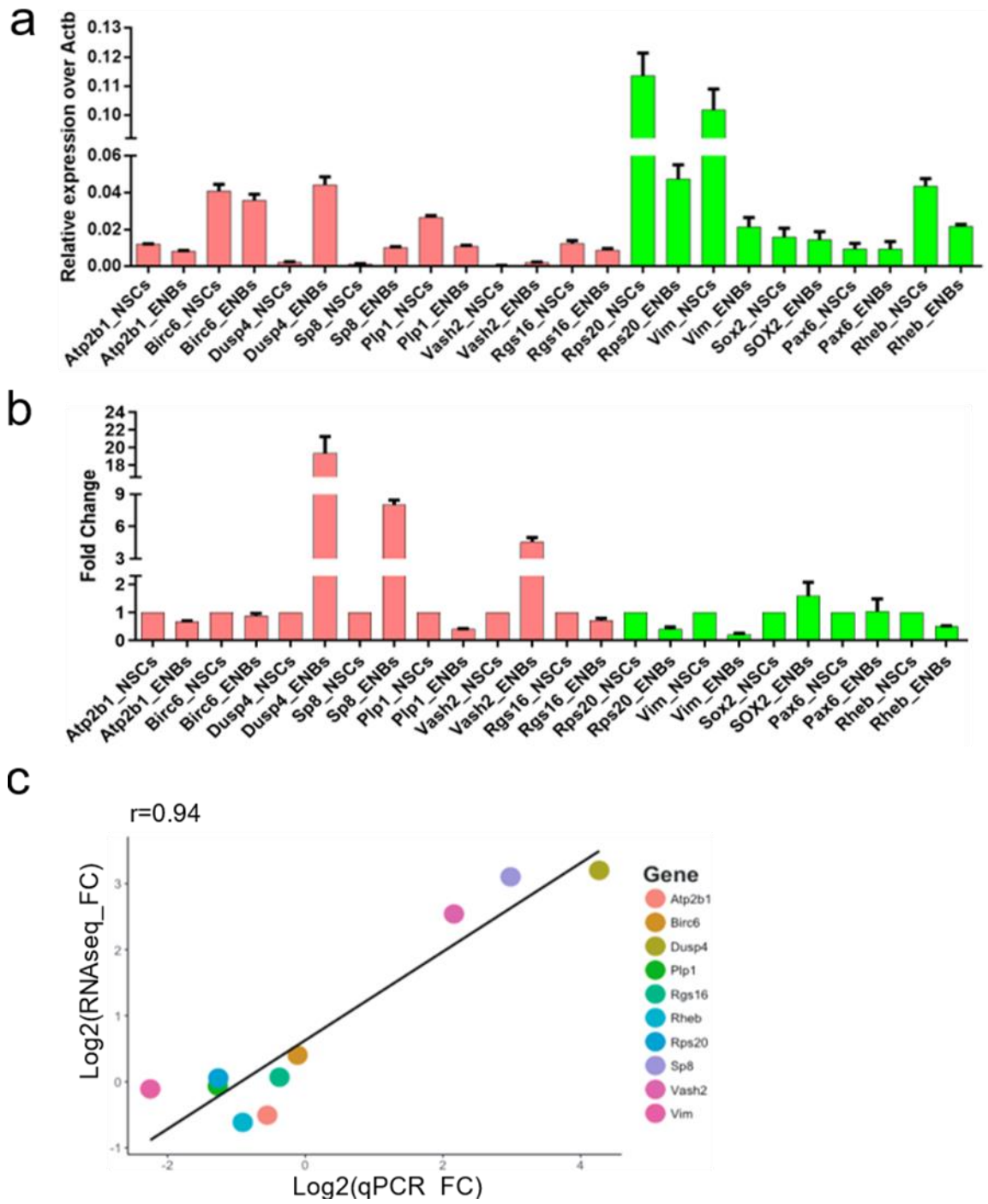

Figure 5. RNA-seq and qPCR data show strong correlation

(a) Relative qPCR quantification of mRNAs for the indicated genes in freshly isolated NSCs and ENBs. Actb was used as an internal control to normalize gene expression. (b) Fold change in mRNA abundance according to RNA-seq upon NSC-to-ENB transition. Fold changes were calculated for abundance of the analyzed mRNAs in ENBs over NSCs. (c) Pearson's correlation coefficient computed between the log2 mRNA read counts upon NSC-to-ENB transition and log2 fold change from qRT-PCR values.

3.2 Validation of translation efficiency derived from RiboIP-seq and RNA-seq

Previous work in our lab calculated the translation efficiency of genes in NSCs and ENBs by normalizing translatomes to their corresponding transcriptomes. Upon the NSC-to-ENB transition, genes such as Birc6, Dusp4, Sp8, Plp1, Vash2, Rgs16 exhibited increased translation and Rps20, Rpl18, Rps17, Sox2 and Pax6 etc. showed repressed translation.

To validate these data, we checked the protein levels of FACS isolated NSCs and ENBs based on the above mentioned genes (Figure 6). Vinculin, a membrane-cytoskeletal protein stably expressed across different cell types, served as a loading control. The absence of appropriate antibodies restricted the number of proteins we could test, especially operating with a very limited amount of cell lysate from the sorted cells. For example, we tried but failed to test PAX6, RPL18 and RPS17 proteins. After some pilot experiments, we chose SP8, DUSP4, PLP1, RPS20 and SOX2 for Western blot analysis. For the NSC-to-ENB transition, there was increased amount of SP8 and DUSP4. PLP1 exhibited the same protein level. On the contrary, the level of RPS20 dropped significantly. An even more significant drop was observed for SOX2. We quantified the intensity of the protein bands and normalized them to the loading control ACTB. The fold changes in the abundance for the candidate proteins were calculated as ENBs to NSCs. Intriguingly, the values were highly correlated to the previously determined translation efficiency for each protein, meaning the high throughput RiboIP-seq data was in good quality, giving high credibility to the post-transcriptional analysis for each candidate gene. Gene ontology analysis revealed that the translationally enhanced genes are involved in neuronal functions such as axon extension, synaptic plasticity and the repressed genes are enriched in ribosome biogenesis and translation, indicating the need for translational arrest and neuronal specific gene expression during the early onset of NSC differentiation (Figure 6. c).

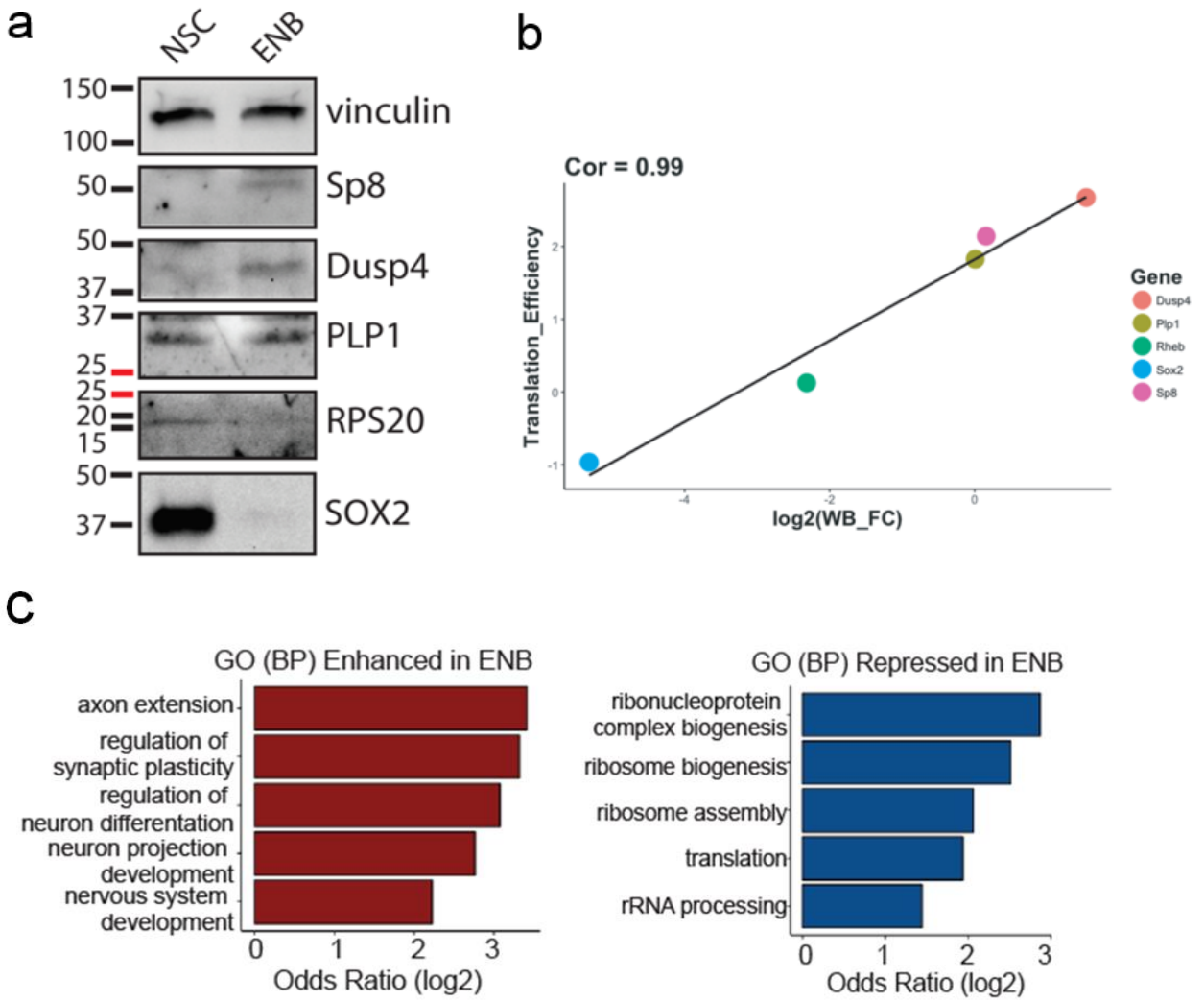

Figure 6. Validation of translation efficiency data through Western blot and GO analysis

(a) Western blot analysis of the protein level for the candidate genes showing considerable change upon NSC-to-ENB transition. (b) Pearson's correlation coefficient computed between the NSC-to-ENB log2 read counts from the high throughput sequencing-based translation efficiency and the log2 fold change according to intensities from western blots. (c) Gene ontology (GO) analysis of repressed and enhanced genes according to the translation efficiency list.

3.3 Onset of differentiation is accompanied with global drop in protein synthesis

Based on cell surface marker expression (Figure 7), quiescent and active NSCs as well as their progenies were isolated for OP-Puro assay to study the level of global protein synthesis (Baser, 2018). Very dynamic changes were observed among these neuronal populations and the level of global protein synthesis in ENBs was significantly lower than in NSCs. However, the level of global protein synthesis along the neuronal lineage remained unknown. Here we specifically focused on the variation of global protein synthesis upon the NSC-to-ENB transition. To study this, NSCs and ENBs from the lineage traced mice were isolated to perform OP-Puro assay (Figure 8).

TAM was administrated to the TiCRY mice to induce recombination at the Rosa26 locus, and to label the NSCs and their progenies with the expression of YFP. 5 days later, the amount of YFP labeled NSCs and ENBs reached the highest number. SVZs from these mice were micro-dissected and prepared for FACS (Figure 7). After proper gating for specific cellular markers, doublets and non-target cell exclusion, NSCs and ENBs were collected in high purity (Figure 7).

After ICC and OP-Puro assay, the well-mounted cells were analyzed by confocal microscopy. ENBs exhibited smaller size than NSCs (Figure 8, c). Cells expressing low intensity of YFP, GLAST or DCX were discarded due to the possibility of being false positive, leaving the bright ones for the following OP-Puro quantification. From 2752 NSCs and 2534 ENBs, we recovered 70 NSCs and 71 ENBs for microscopy due to subsequent washing steps after cells staining. After the exclusion of the false positive cells, 38 YFP positive NSCs and 52 YFP positive ENBs were used for OP-Puro quantification. An extremely significant drop of OP-Puro incorporation upon the NSC-to-ENB transition was detected, manifesting that this transition is accompanied by a dramatic down regulation of global protein synthesis (Figure 8. d).

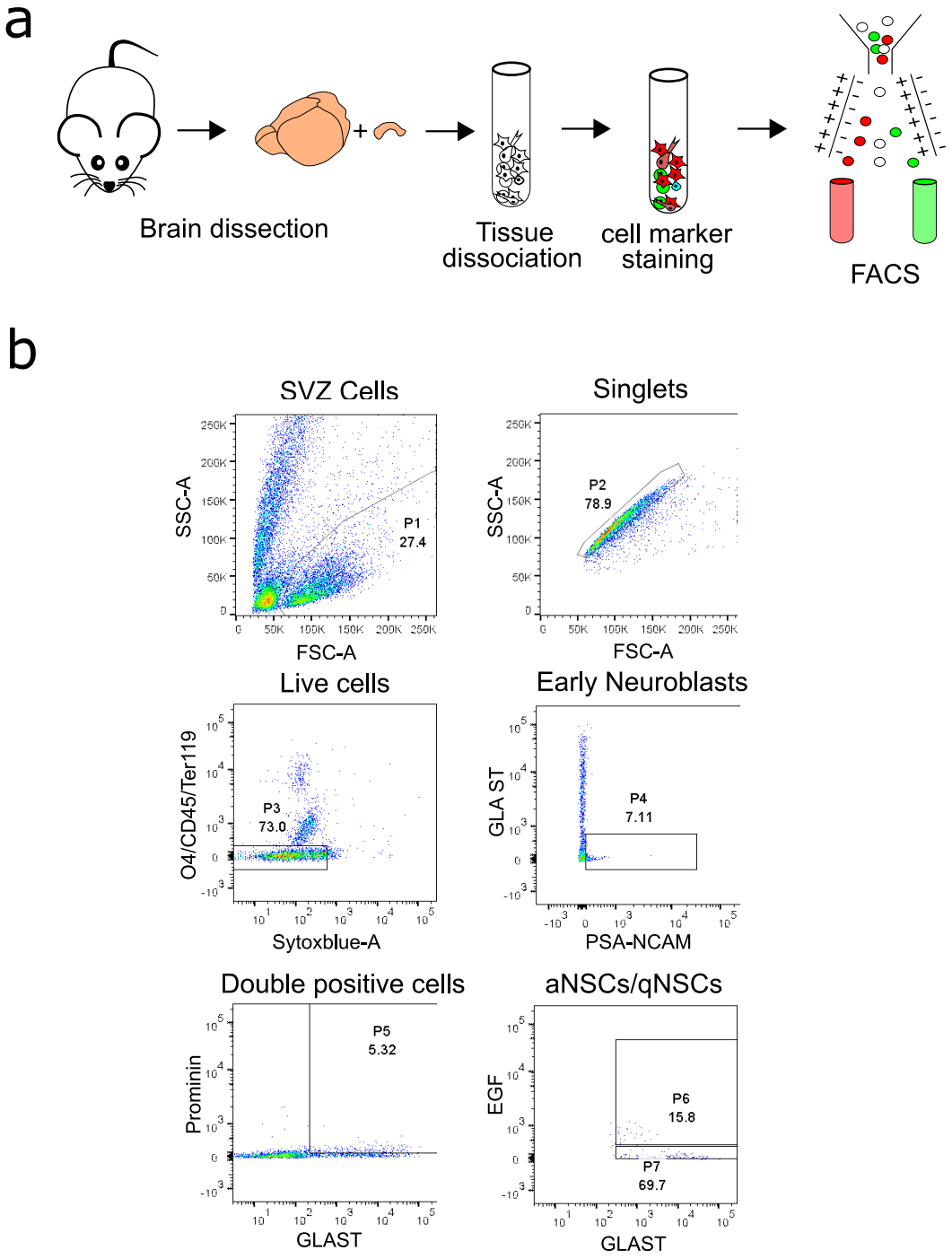

Figure 7. Strategy to sort NSCs and ENBs by flow cytometry

(a) Schematic view of FACS workflow. SVZ cells were immunostained for cell surface markers and were analyzed by flow cytometry. (b) FACS strategy to sort for aNSCs and ENBs. First SVZ cells were gated stringently; Second doublets were excluded; Third dead cells, O4+ cells like oligodendrocytes, CD45+ cells such as microglia, Ter119+ cells like erythroid cells were excluded. Fourth the GLAST-/PSA-NCAM+ ENBs were sorted. Fifth the GLAST+/Prominin+/EGF+ NSCs were sorted. The percentage of each population (P) is highlighted in the plots.

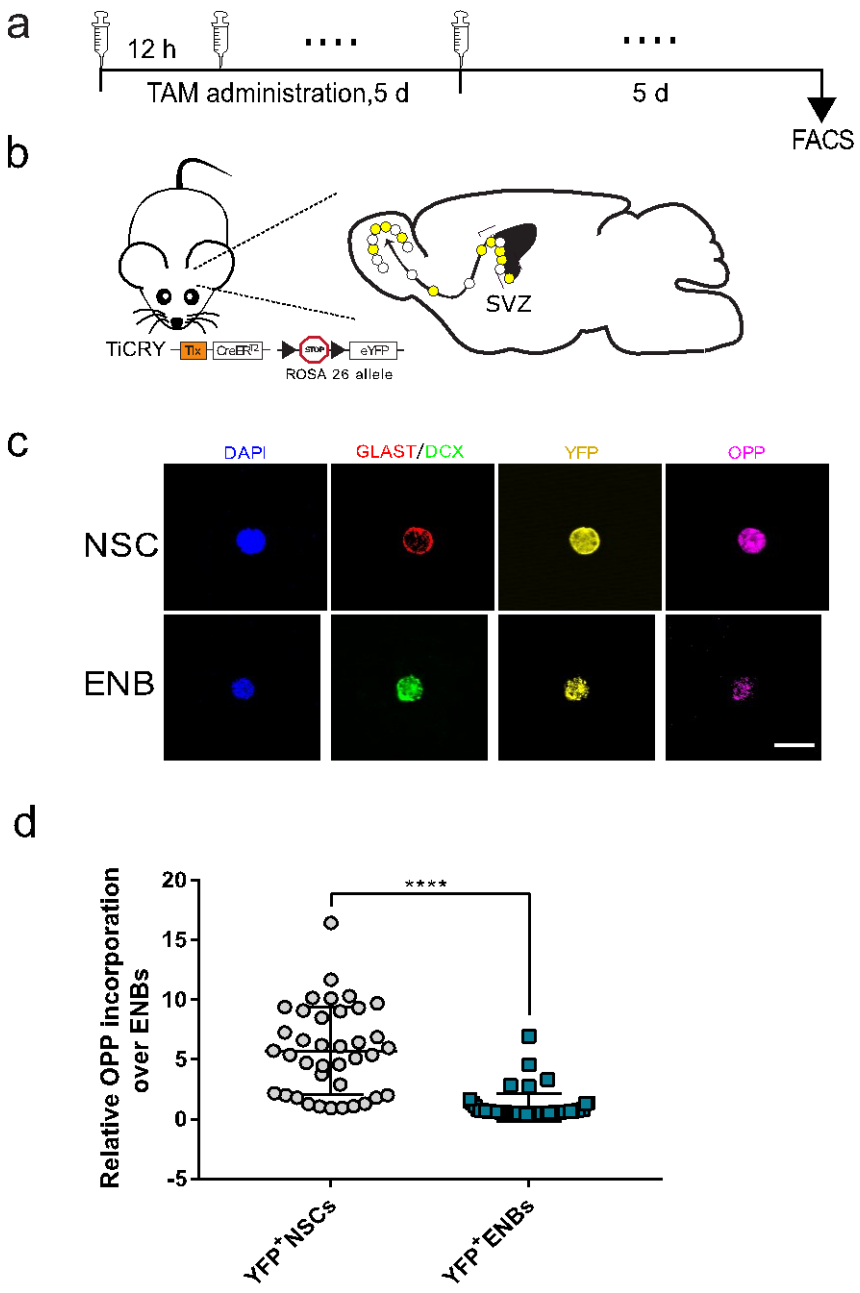

Figure 8. Level of global protein synthesis dropped during NSC lineage progression

(a) Scheme of tamoxifen administration. TAM was administrated intraperitoneally (i.p.) to the TiCRY mice (n=6) with one shot every 12 hours for 5 days, 10 mg tamoxifen in total for each mouse. 5 days post-injection the mice were used for SVZ dissection to isolate NSCs and ENBs by FACS. (b) Schematic description of TiCRY mice and the migrating path of YFP NSCs lineages from the SVZ to the OB. (c) Representative confocal images after immunostaining and OP-Puro assay. (d) Quantification of OP-Puro incorporation of NSCs (n=38) and ENBs (n=52) (relative to ENBs). Statistical significance was calculated by student's t-test; **** $p<0.001$. Scale bars: 10 µm.

3.4 The activity of mTOR is dropped upon the NSC-to-ENB transition

Upon the NSC-to-ENB transition, the level of global protein synthesis dropped. Specifically, Dusp4, Sp8 and more neuronal genes were translationally enhanced, what could be the drive of neuronal cell fate specification. Notably, a set of gene transcripts containing PRM in their 5' UTR was translationally repressed at ENBs stage. Among these transcripts, there were stem cell markers Sox2 and Pax6 as well as mRNAs encoding ribosomal proteins. These transcripts were exclusively repressed at ENBs stage, presumably due to the low activity of their common positive regulator mTOR.

To determine the molecular mechanism responsible for the transition of NSCs to ENBs *in vivo* and meanwhile inspired by the enriched mTOR-dependent mRNAs in the ENBs, we focused on the role of mTOR in the regulation of the above mentioned candidate genes and try to gain insights into the control mechanism of NSC differentiation.

Freshly FACS isolated NSCs and ENBs were used to analyze the abundance and modifications of mTOR signaling components by Western blot analysis (Figure 9). Comparing to NSCs, ENBs exhibited reduced expression of TSC2 the mTOR upstream inhibitor, and significantly lower level of RHEB, which is the direct upstream activator of mTOR. However, we could not detect any phospho Ser1378 or phospho Thr1462 in TSC2 (data not shown), maybe due to the limited input protein material. There was no change in the expression level of total p70 S6 kinase. However, the level of phospho p70 S6K, the direct catalytic product of mTOR, was considerably decreased in the ENBs. A well-described substrate of p70 S6 kinase ribosomal protein S6 exhibited a drop in its total level and a much more significant drop in its phospho level, indicating a very low mTOR activity in ENBs (Figure 9. a). Of note, the amount of Sox2 mRNA remained equal in NSCs and ENBs while the protein dropped dramatically upon the NSC-to-ENB transition (Figure 9. b), suggesting a strong post-transcriptional repression of Sox2 translation. This is likely to be associated with the decreased activity of mTOR since Sox2 mRNA has a PRM in its 5' UTR, which can confer mTOR dependence. The following studies were carried out focusing on the regulation of mTOR in Sox2 expression.

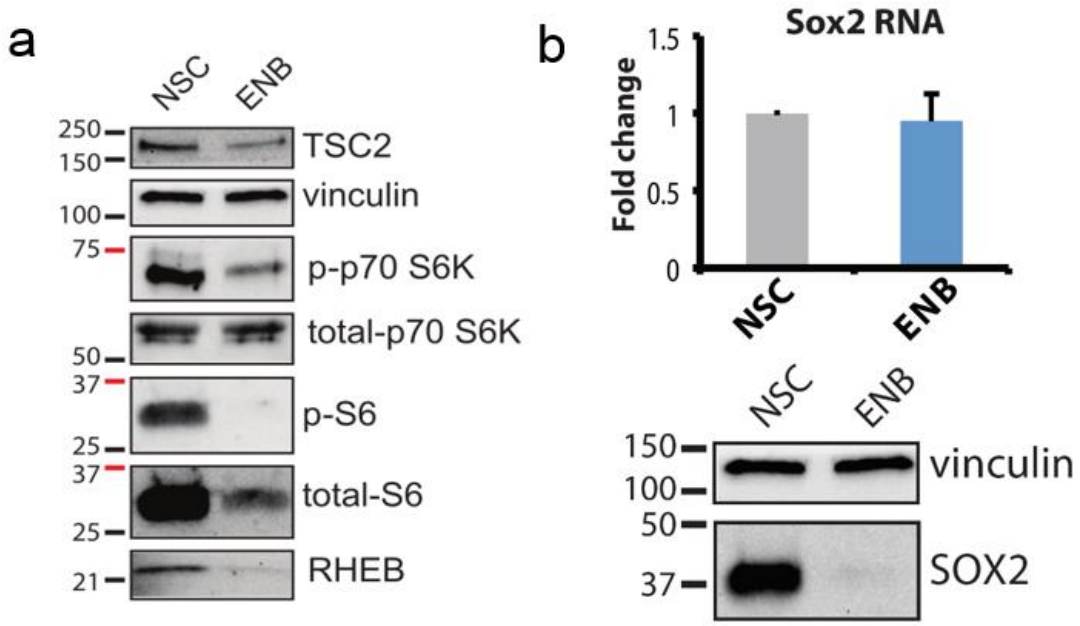

Figure 9. NSC-to-ENB transition is accompanied with reduced mTOR activity and post-transcriptional repression for Sox2 expression

(a) Western blot analysis of mTOR activity upon the NSC-to-ENB transition using cells collected by FACS. Vinculin served as a loading control. Vinculin was used as a loading control. (b) qPCR and Western blot analysis of Sox2 upon the NSC-to-ENB transition. Vinculin was used as a loading control for Western blot analysis.

3.5 Inhibition of mTOR has no effect on the level of SOX2

The *in vitro* NSC culture allows more detailed and convenient studies of molecular mechanisms, which is very complicated and barely possible to carry out *in vivo* because of very limited number of NSCs and their progeny in adult mammalian brain.

Torin, a chemical compound fully inhibiting mTORC1 and mTORC2, was used to treat NSCs to mimic the decreased level of mTOR activity in ENBs.

2 hours after treatment, although the mTOR upstream regulators TSC2 and RHEB did not show any change, the phospho level of two typical mTOR substrates p70-S6 kinase and 4EBP dropped significantly. The level of phospho ribosomal protein S6 exhibited a decrease after 2 hours vehicle treatment and a more significant decrease after 2 hours of Torin treatment. Of note, their total level remained unchanged, indicating significant decrease in mTOR activity. SOX2 did not show any significant changes upon mTOR inhibition (Figure 10). We also tried an alternative mTOR inhibitor, AZD2014 and again did not observe a significant change for the level of SOX2 (data not shown). This led us to consider alternative methods to investigate Sox2 translation.

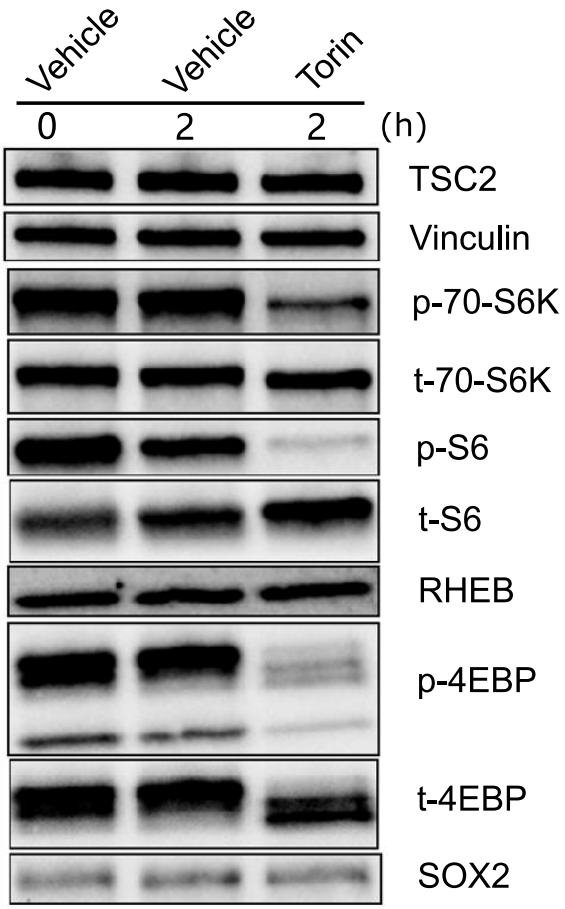

Figure 10. The level of SOX2 remained constant when mTOR activity is reduced *in vitro*

Torin treatment was incubated for 2 h. DMSO treatment served as a vehicle controls and was incubated for 0 h and 2 h. Vinculin served as a loading control.

3.6 Sox2 ribosome loading is not affected upon mTOR inhibition

We performed polysome profiling to investigate the distribution of mRNAs according to the number of bound ribosomes on them (Figure 11).

Upon Torin treatment, the overall RNA distribution displayed a shift to earlier fractions. Moreover, the increased amount of the material in the zone of monosome and ribosome subunits in the Torin treated group compared to the vehicle control group indicated efficient repression in the translation of corresponding mRNAs, indicating their dependence on mTOR.

We analyzed a number of candidate genes involved in the repressed and enhanced translation during NSC differentiation as well as mTOR insensitive transcripts like Actb and Sox9. As controls, the translation of which is mTOR insensitive, Actb and Sox9 mRNAs didn't exhibit any shifted distribution to lighter fractions, indicating tight association of their mRNA to the ribosomes.

We observed a significant shift of Rpl18 mRNAs away from polyribosomes to the mRNP/monosome fractions upon Torin treatment, demonstrating reduced accessibility to the translational machinery in contrast to the control vehicle treatment. The same shift was observed for Rps17, eIF3f, eEF1b2 mRNAs. Dusp4 demonstrated a slight shift to heavier polyribosomes, confirming increased translation efficiency upon mTOR inhibition. However, the Sox2 mRNA distribution did not show any shift (Figure 11), reflecting unchanged translation efficiency.

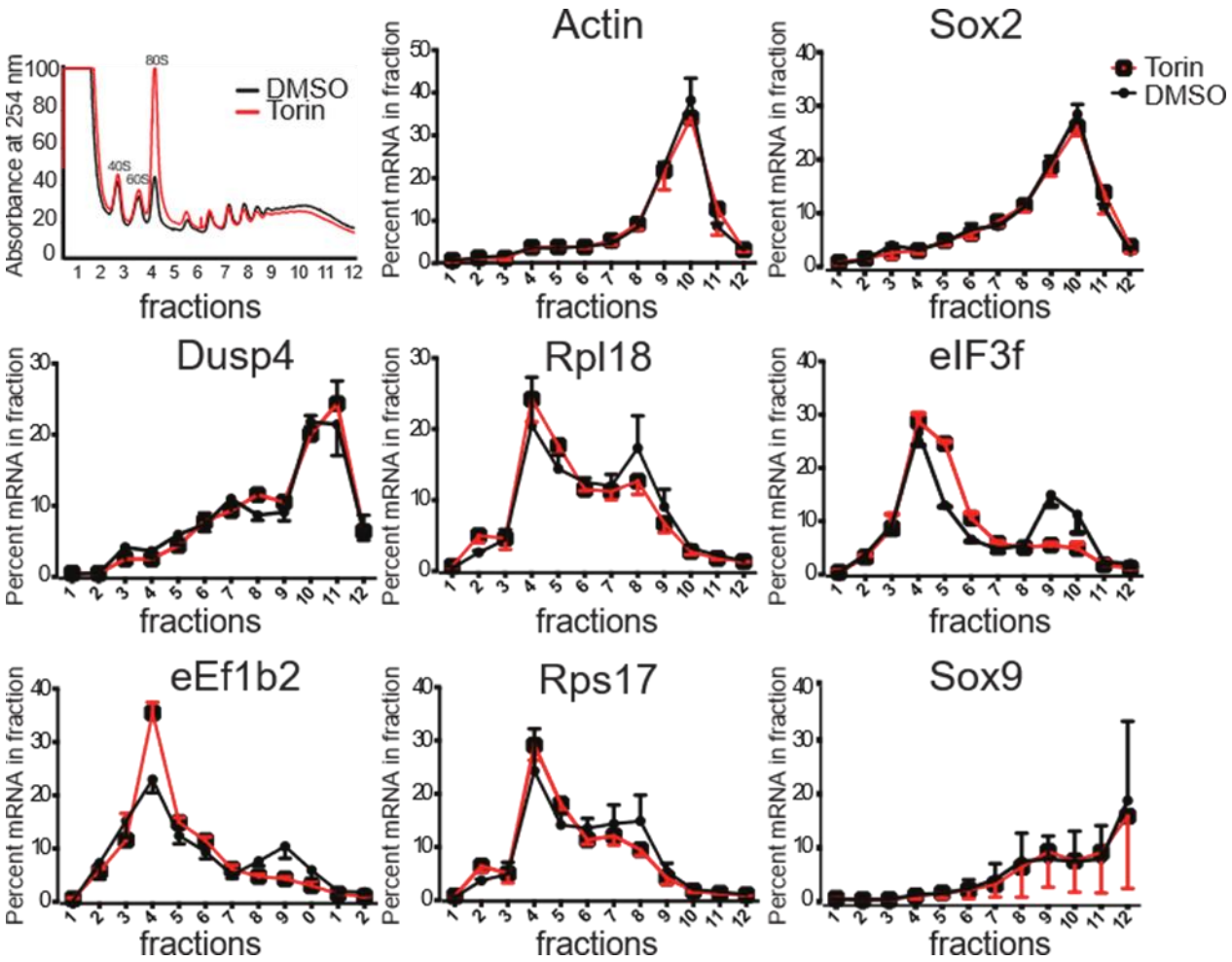

Figure 11. Polysome profiling of NSCs exhibits different profiles for the of candidate gene transcripts upon mTOR inhibition by Torin

The first plot shows the overall polysome profiles of the treatments. The rest plots show specific analysis of the following gene transcripts: Actb, Sox2, Dusp4, Rpl18, eEF3f, eEF1b2, Rps17 and Sox9. Torin treatment was incubated for 2 hours. DMSO treatment served as a vehicle control.

3.7 The level of SOX2 protein is not affected by modulation of mTOR upstream regulators

In vivo, mTOR activity is controlled by many factors such as the abundance of growth factors, the availability of amino acids, PI3K activity etc. Here we investigated the effect of growth factors and PI3K activity on Sox2 translation in NSCs (Figure 12).

NSCs were cultured in NBM with the presence or absence of growth factors and subsequently subjected to treatments such as LY294002, an inhibitor targeting upstream mTOR activator PI3K, as well as Torin or LY294002/Torin. When cultured in NBM with growth factors, the LY294002 treatment significantly decreased the level of p-4EBP, indicating LY294002 mediated reduction in mTOR activity. We did not observe a significant drop for the level of p-AKT and p-TSC2, whereas they dropped considerably upon Torin treatment. Growth factor withdrawal decreased mTOR activity as shown by diminished level of p-4EBP and p-AKT as well as their total proteins. However, Sox2 expression was not affected upon the growth factor withdrawal or LY294002 treatment, indicating that modulation of mTOR activity via its upstream regulators does not impact the level of SOX2 protein.

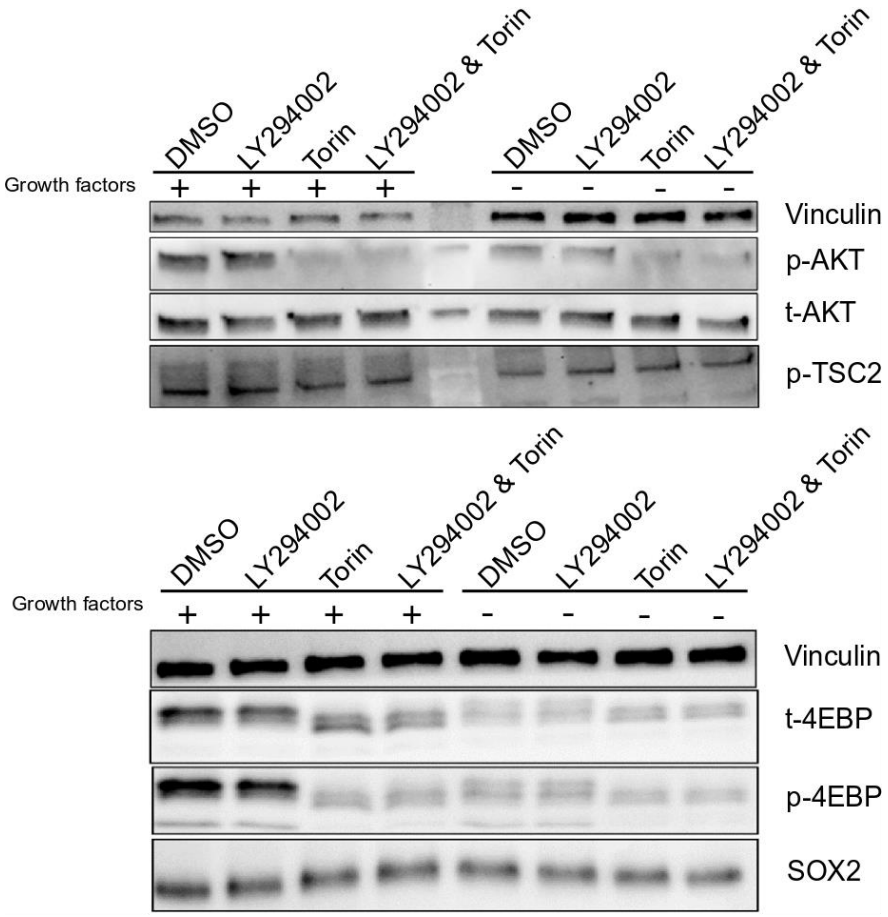

Figure 12. Upstream modulation of mTOR doesn't affect the abundance of SOX2 protein

NSCs were cultured in NBM with or without growth factors. Cells were incubated with DMSO, LY294002, Torin or LY294002/Torin for 2 hours. DMSO served as a vehicle control.

3.8 Translation of Sox2 mRNAs is not affected by modulation of mTOR activity via its upstream regulators

Next, we investigated the effect of PI3K inhibition on Sox2 mRNA translation (Figure 13). Actb and Rpl18 mRNAs were used as controls. Indeed, distribution of Actb mRNA did not show any shift to lighter fractions upon either Torin or LY294002 treatment. Also, LY294002/Torin combinatorial treatment showed a shift to heavier fractions for Actb but not for Rpl18. Rpl18 mRNA showed a typical binary distribution. One portion of the Rpl18 mRNA is actively in translation whereas the rest not and co-sedimentated with free ribosomal subunits and monosomes. Sox2 polysome profiles upon the treatments were almost identical to the control. Sox2 mRNA was mainly present in the polyribosome fractions, indicating its insensitivity to the PI3K inhibition.

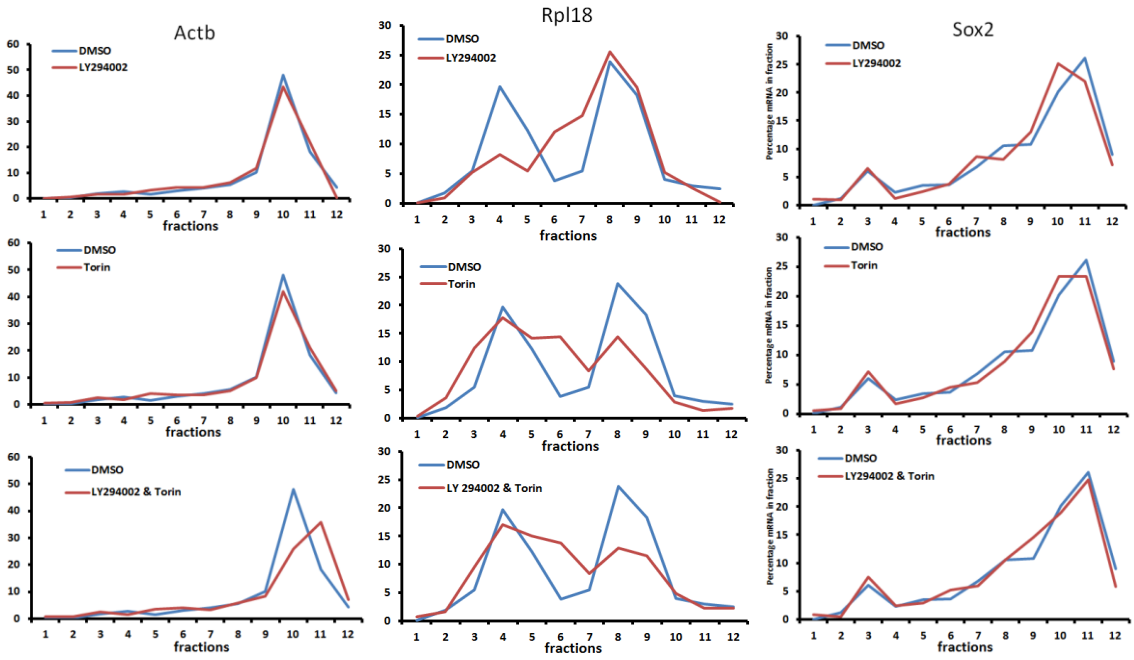

Figure 13. Sox2 mRNA translation is resistant to the repression of upstream mTOR regulators
NSCs cultured with growth factors were treated with LY294002, Torin, or LY294002/Torin for 2 hours. DMSO served as a negative control. Actb, Rpl18 and Sox2 were analyzed.

3.9 Active Sox2 translation is further confirmed

Puromycin treatment was introduced in the polysome profiling experiment to double check if Sox2 mRNA was under-going active translation upon Torin treatment (Figure 14). As structural analog of the aminoacyl-transfer RNA (aa-tRNA), puromycin is recognized by ribosomes as the acceptor end of aa-tRNAs, resulting in transfer of nascent polypeptide to puromycin followed by dissociation of the resulted complex and final release of the ribosomes from mRNAs (Starck and Roberts, 2002).

In contrast to the selective effect of Torin on the translation of mTOR sensitive transcripts, puromycin represses translation in a transcript unspecific manner. The RNA distribution of Actb was not changed upon Torin treatment but shifted to lighter fractions upon puromycin treatment, indicating strong block of translation by puromycin. Similar translational block was observed for Rpl18. The effect of Torin on Rpl18 translation is stronger than that of puromycin, indicating a very high sensitivity of Rpl18 mRNA to mTOR activity reduction. Sox2 exhibited a shift to lighter fractions upon puromycin treatment when compared to the controls, confirming that Sox2 mRNA is undergoing active translation upon Torin treatment and did not recapitulate the repression detected *in vivo* upon the NSC-to-ENB transition.

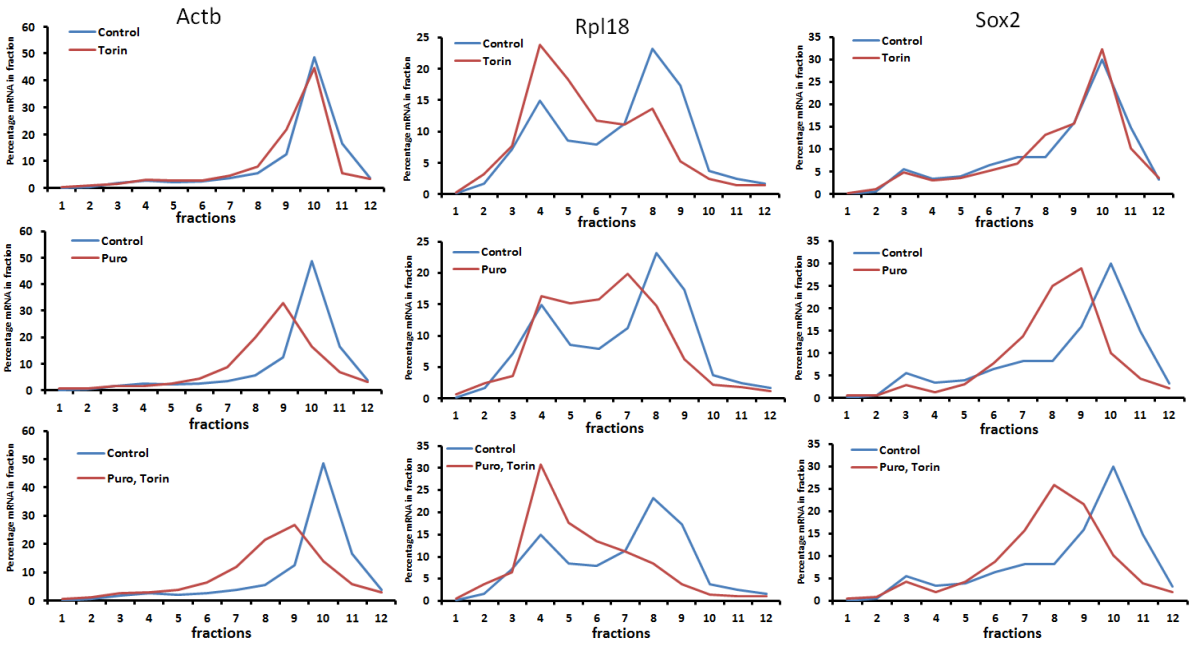

Figure 14. Active translation of Sox2 mRNA upon Torin treatment was further confirmed by polysome profiling

NSCs were treated with Torin, Puromycin or Torin/Puromycin. Torin treatment was incubated for 2 hours and puromycin for 20 min. Actb, Rpl18 and Sox2 were analyzed.

3.10 The activation of mTOR reverts ENBs to stemness state

To investigate the role of mTOR in Sox2 mRNA translation *in vivo*, we focused on sorted NSCs and ENBs due to their close physiological state to their counterparts *in vivo*. NSCs and ENBs were sorted and subjected to the modulation of mTOR activity to study the effect on Sox2 mRNA translation (Figure 15).

Sox2 is a stem cell marker. Therefore, NSCs served as a positive control and were directly PFA fixed after sorting. To demonstrate whether differentiation of ENBs is mTOR dependent, a membrane-permanent phosphatidylinositol-3,4,5-trisphosphate (PIP3) was introduced to modulate mTOR activity in the cells. ENBs were stimulated with either PIP3 or PIP3/Torin for the indicated time points. The expression levels of Sox2 and pS6 as mTOR activity indicator were analyzed. Upon PIP3 stimulation, a significant increase in Sox2 and pS6 expression levels were detected in ENBs, which was reduced when mTOR was additionally inhibited (Figure 15. b, c). In summary, the increase of mTOR activity could induce SOX2 expression in ENBs and presumably revert the differentiation process.

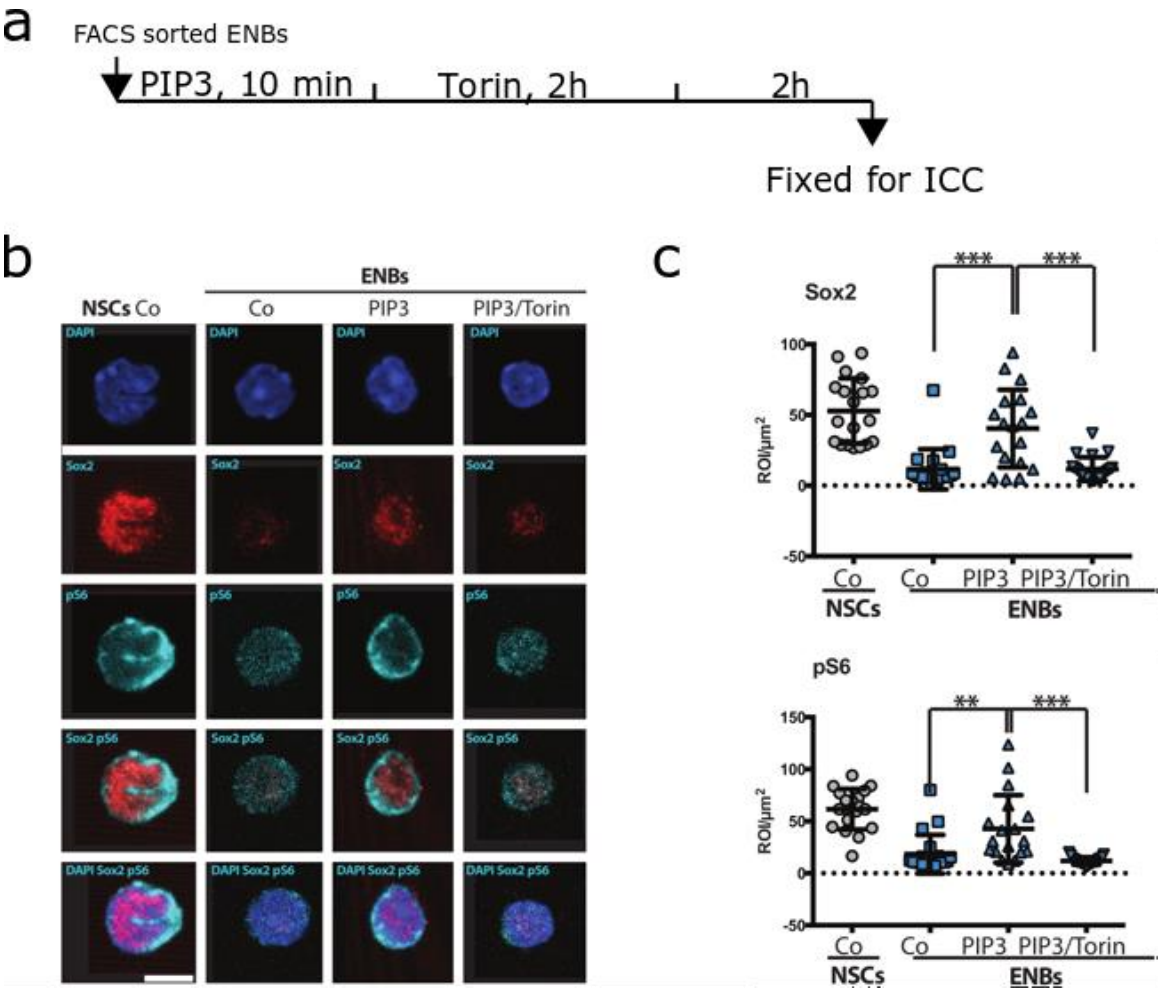

Figure 15. Activation of mTOR in ENBs promoted SOX2 expression

(a) Scheme of PIP3 or control treatment for ENBs. DMSO served as a vehicle treatment (b) Representative ICC image of SOX2 (red) and pS6 (turquoise) from microscopy. Co, vehicle control. Scale bar: 5 µm. (c) Quantification of the relative expression level of SOX2 and pS6. For each condition, 20 cells were analyzed and the intensity was normalized to the cell area. Statistical significance analysis was performed by student's t-test $p < 0.01$**, $p < 0.005$***.

3.11 ENBs regain stem cell features by activation of mTOR

Previous experiments showed that increased mTOR activity in ENBs leads to the re-expression of SOX2 in ENBs. We hypothesized that this could enable ENBs to regain stem-cell like behavior. To prove this hypothesis freshly isolated ENBs by FACS were used for neurosphere forming assay (Figure 16).

Cells were treated with PIP3 to activate mTOR activity. DMSO or PIP3/Torin treatments were used as controls. 7 days after the plating and treatments, formed spheres were counted (Figure 16. a, b). Intriguingly, in the PIP3 treated group, the ENBs formed on average 4 spheres per well, significantly more than the DMSO or Torin/PIP3 treated groups (Figure 16. b, c). These results showed that mTOR activation in ENBs hampered their differentiation program and reverted the cells to a stem cell-like phenotype.

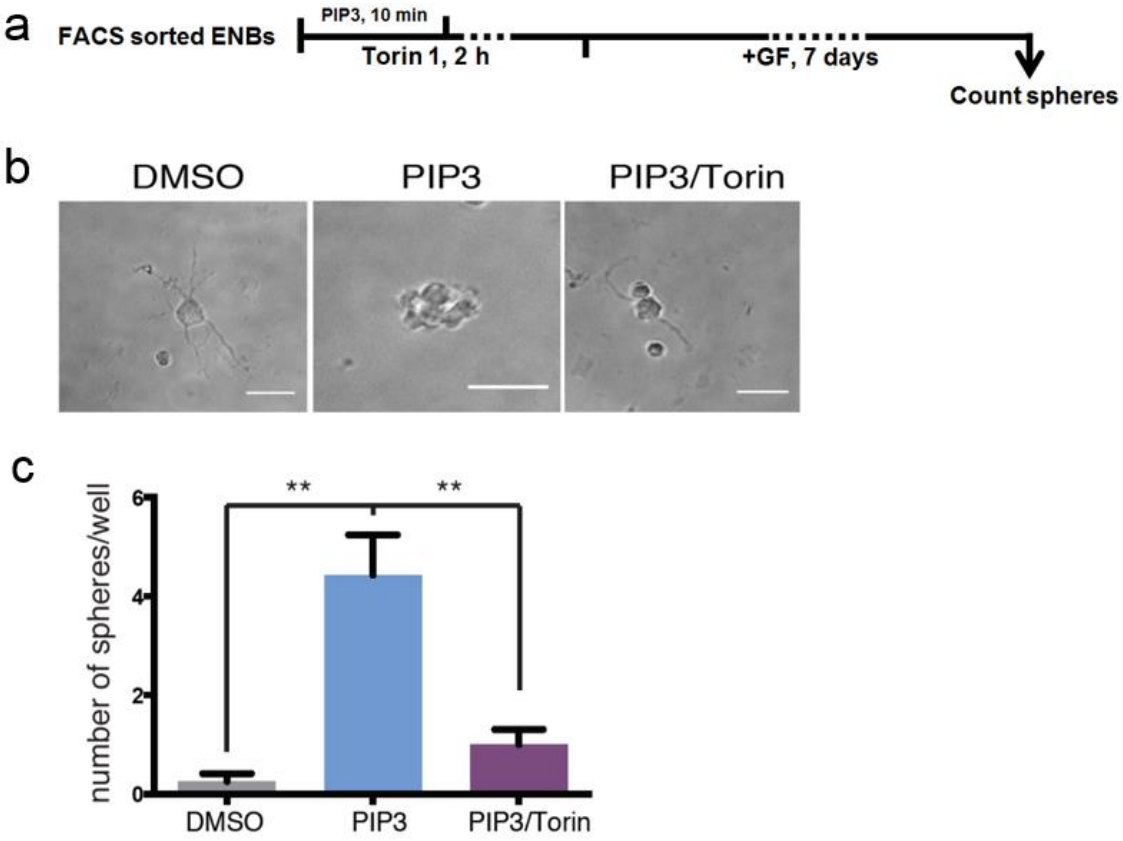

Figure 16. Activation of mTOR in ENBs forms neurospheres

(a) Scheme of the sphere assay for the FACS sorted ENBs after treatments. (b) Schematic pictures of neurospheres. (c) Quantification of neurospheres for each treatment. Statistical significance was calculated by student's t-test, $p < 0.01$**. Scale bar: 10 µm.

3.12 Activation of mTOR disrupts NSC differentiation *in vitro*

Next, we asked whether activating mTOR in NSCs which undergo differentiation would also affect Sox2 expression and also the process of differentiation. NSCs were cultured under differentiation conditions and in parallel treated with PIP3, PIP3/Torin or DMSO vehicle control for the indicated times points (Figure 17. a). During the process of differentiation, NSCs loose the expression of stemness marker SOX2 and start expressing neuronal markers such as DCX. Moreover, their morphology resembled more neurons, characterized by developing dendrites and axons. After 7 days under differentiation conditions, cells were fixed and stained for SOX2 and DCX.

Under control conditions around 70% of the cells were SOX2 positive and around 30% showed DCX expression. These cells showed already dendrites and axon-like processes, indicating the differentiation process. Similar observations were detectable in PIP3/Torin double treated cells. Whereas PIP3 treatment only inhibits NSCs differentiation since none of the analyzed cells showed DCX expression. This pointed out that the NSC differentiation process was blocked by mTOR activation (Figure 17. b, c).

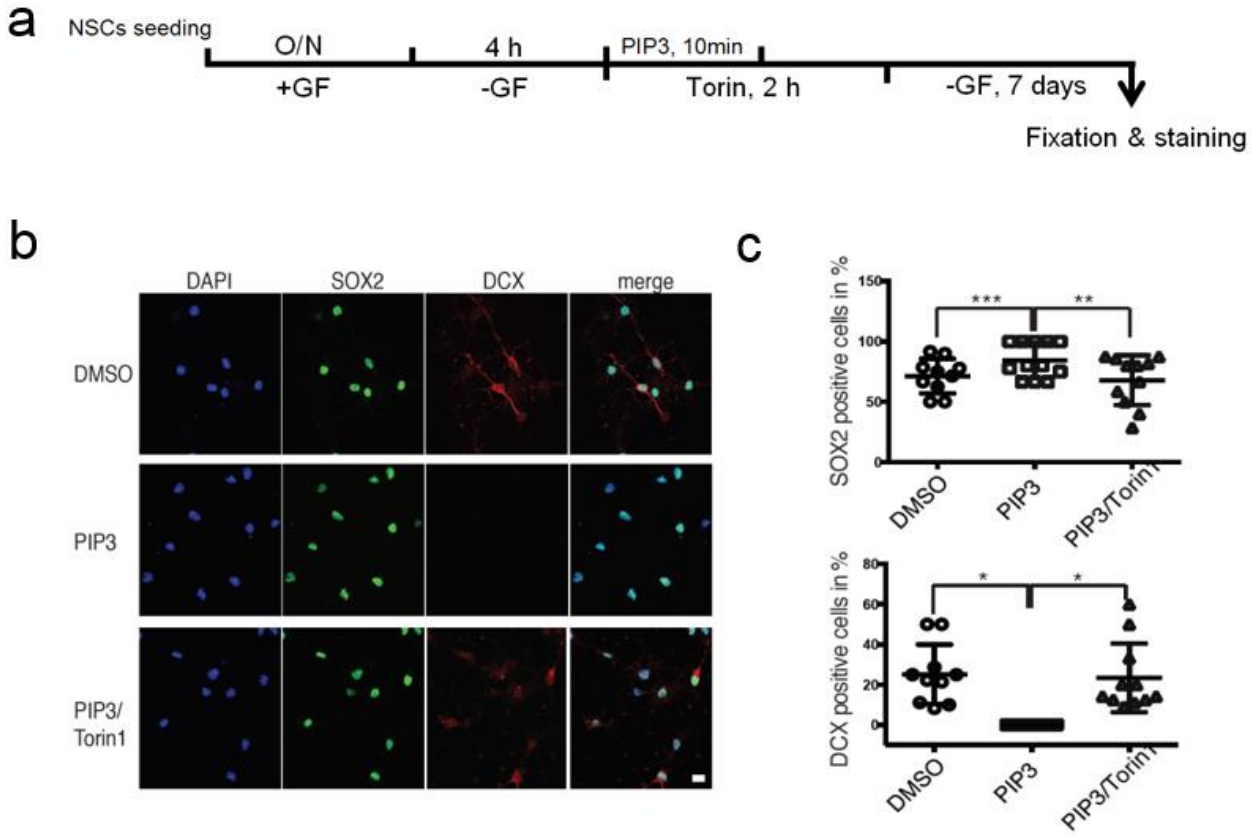

Figure 17. mTOR activation in NSCs blocks the undergoing differentiation

(a) Scheme of NSCs differentiation assay with treatment of PIP3, DMSO vehicle control, and PIP3/Torin for the indicated time points. (b) Representative confocal microscopy showing SOX2 (green) and DCX (red) expression in NSCs undergoing differentiation. Scale bar: 10 μm. (c) Quantification of SOX2 or DCX positive cells across treatments. Statistical significance was calculated by student's t-test $p < 0.05$*, $p < 0.01$**, $p < 0.005$***.

3.13 NSCs *in vitro* can be synchronized at late G1/early S phase

mTOR is highly involved in NSC maintenance *in vivo*, however during neurogenesis NSCs have to exit from the cell cycle before starting their differentiation program. Since we detected that mTOR activation has important effects on the expression of stem cell marker SOX2 ex vivo, we further wanted to investigate how Sox2 mRNA translation is regulated. Therefore, NSCs were synchronized by using double thymidine block (dTB). To estimate the efficiency of this method, we first synchronized cultured NSCs isolated from fluorescent ubiquitination-based cell cycle indicator 2 (Fucci2) mice, followed by subjecting the cells to FACS analysis. This technique allows the visualization of cell cycle progression in live cells, marking cells in G1 and S/G2/M phase with mCherry and GFP, respectively.

NSCs isolated from the Fucci2 mice were cultured up to passage 2, followed by cell cycle synchronization via dTB (Figure 18. a). Afterwards, NSCs were collected and analyzed by a flow cytometer (Figure 18. b). Without synchronization, 27.6% of the cells stayed in S/G2/M phase and 69.4% staying in G1 phase. While after cell synchronization, the ratio of cells in the S/G2/M phase went up to 37.8% and the ratio of cells in the G1 phase remained similar, being 68.5%. The unsynchronized cells were characterized by a mCherry gradient, indicating the increasingly accumulated Cdt1 during G1 phase progression (Figure 18. b).

Cells expressing low mCherry accounted for 31.3% of all cells after doublet exclusion and mCherry level went down to 6.3% after cell cycle synchronization, suggesting accumulation of cells in late G1/S phase (Figure 18 b). As a result of synchronization, an increase of FITC positive cells from 27.6% to 37.8% could be detected (Figure 18. b).

In addition, a time course experiment was performed to demonstrate how long the synchronization lasts after releasing the cells from synchronization (Figure 19). The percentage of mCherry positive cells decreased, accompanied by an increase of FITC positive cells, caused by the progression of NSCs from G1 to S phase. After that, the ratio of mCherry positive cells increased and the ratio of FITC positive cells decreased continually for 5 hours, indicating cells cycling into G1 phase. There is a drop for the percentage of both FITC and mCherry cells probably because the cells loose FITC

expression when entering early G1 phase and still hasn't expressed mCherry. Over time, the percentage of mCherry positive cells went up again, which indicates that more cells progress into G1 phase. Basically, cell cycle release for 10 hours illustrated that synchronized NSCs need approximately 10-12 hours to re-enter the early G1 phase. Overall, the Fucci2 NSCs were successfully synchronized by double thymidine treatment, resulting in over 90% of the NSCs staying in late G1/early S phase (Figure 19).

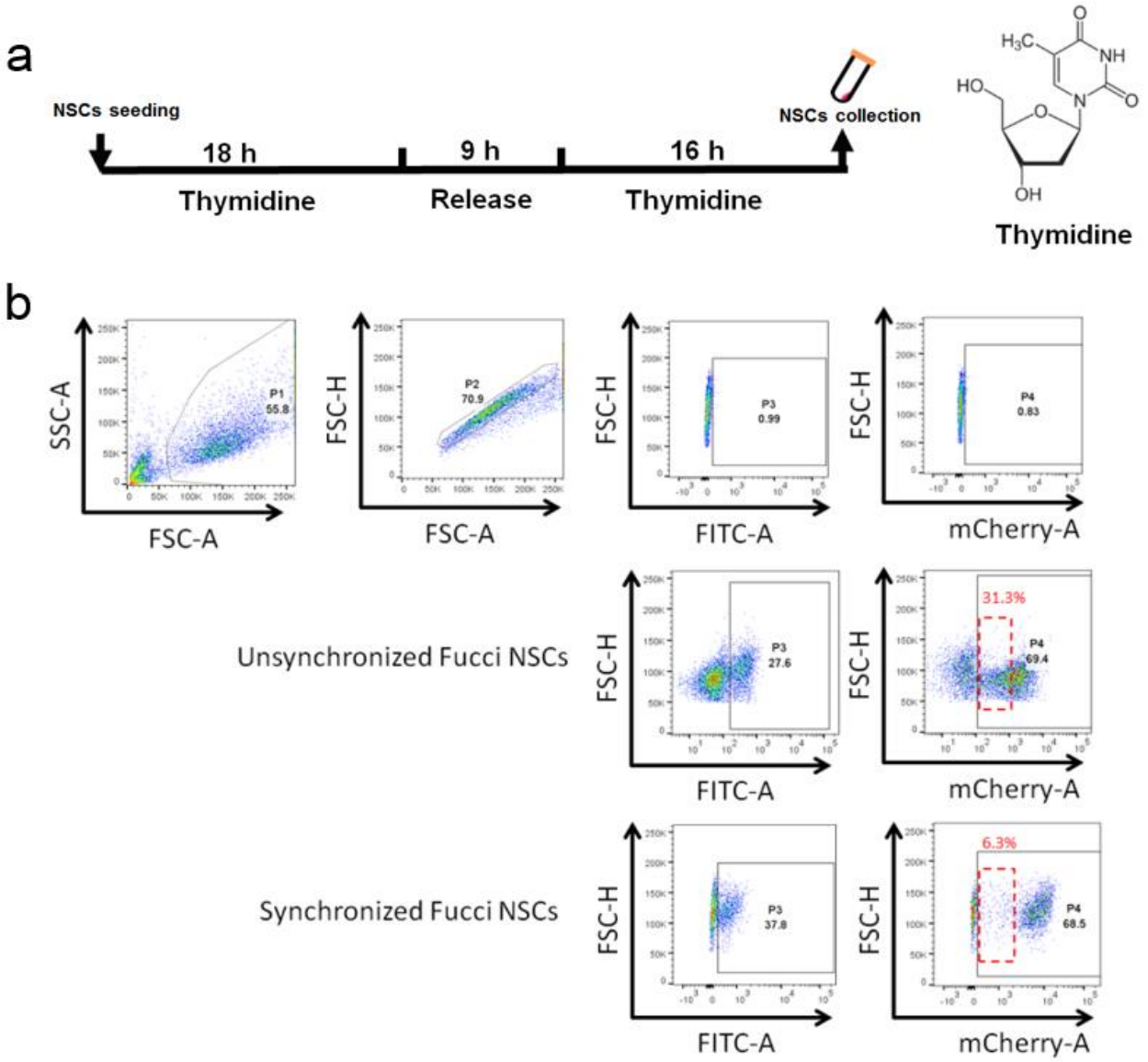

Figure 18. Double thymidine block and FACS analysis

(a) Scheme of double thymidine block for NSCs cell cycle synchronization *in vitro*. (b) Cell cycle phase analysis of dTB synchronized Fucci2 NSCs via flow cytometry. WT cells served as control.

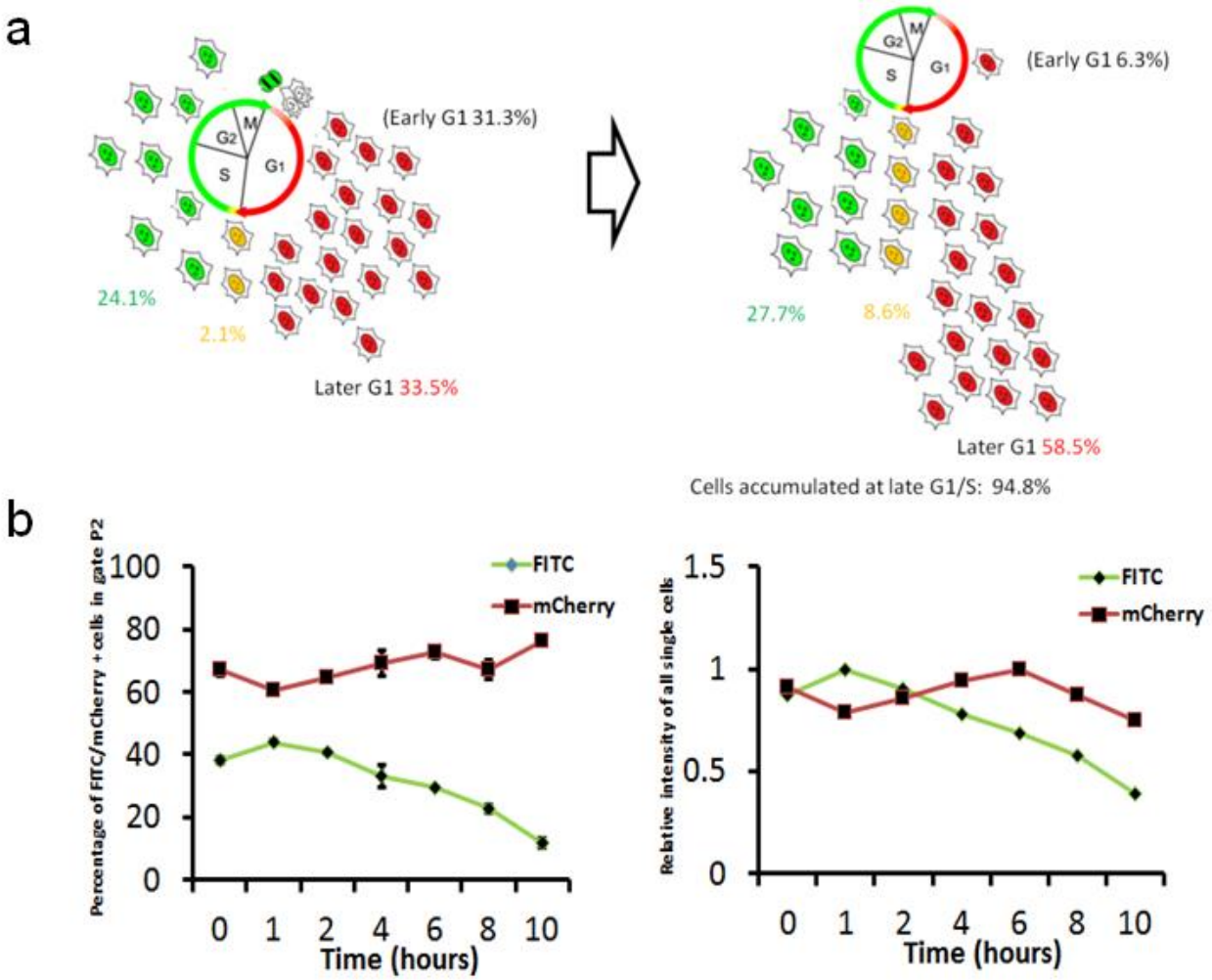

Figure 19. NSCs were synchronized at late G1/early S phase

(a) Schematic picture of cell cycle distribution before and after dTB cell synchronization. (b) Time course release of dTB synchronized Fucci2 NSCs.

3.14 Sox2 is not transcriptionally regulated by mTOR

To further investigate the regulation of mTOR on Sox2 expression, synchronized NSCs were treated with Torin for 1 and 2 hours (Figure 20). Candidate genes such as Sox2, Rpl18, Dusp4 and Actb were analyzed by qPCR. Dusp4 increased on the transcriptional level upon Torin treatment while Sox2, Rpl18 and Actb remained the same, comparable to the vehicle control. Therefore, mTOR inhibition doesn't change Sox2 expression at the transcriptional level.

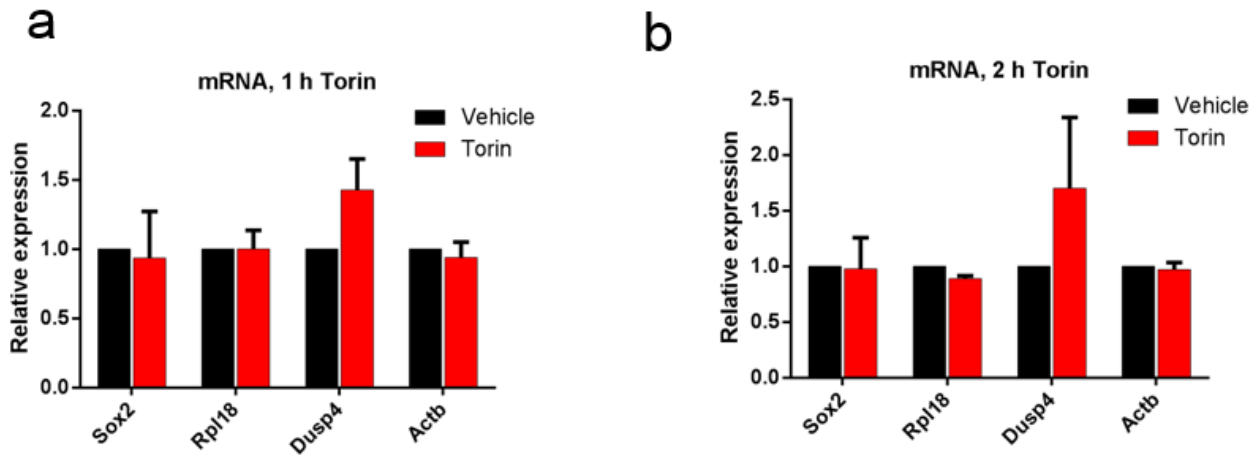

Figure 20. The transcription of Sox2 is not changed upon mTOR inhibition in cell cycle synchronized NSCs

Relative gene expression of Sox2, Rpl18, Dusp4 and Actb in NSCs after 1 or 2 hour Torin treatment was analyzed. DMSO served as a vehicle control.

3.15 Inhibition of mTOR represses Sox2 translation

Next, we focused on the regulation of mTOR on Sox2 mRNA translation. Western blot analysis was performed to assess the effect of mTOR inhibition on Sox2 translation in synchronized NSCs (Figure 21). The synchronized NSCs were treated with Torin for 1h, 2h, and 4h. DMSO treatment served as a vehicle control. Besides, unsynchronized NSCs and synchronized NSCs without any treatment were also set as controls.

Upon Torin treatment, p-p70-S6K as mTOR downstream activity indicator dropped significantly. The same drop was also observed for p-S6, p-AKT and p-4EBP1 though there was no change in their total protein level. SOX2 also exhibited repressed translation 1h, 2h or 4 hours after Torin treatment. This was further confirmed by the shift in polysome profile to lighter fractions for Sox2, indicating the post-transcriptional regulatory role of mTOR on Sox2 at G1 phase.

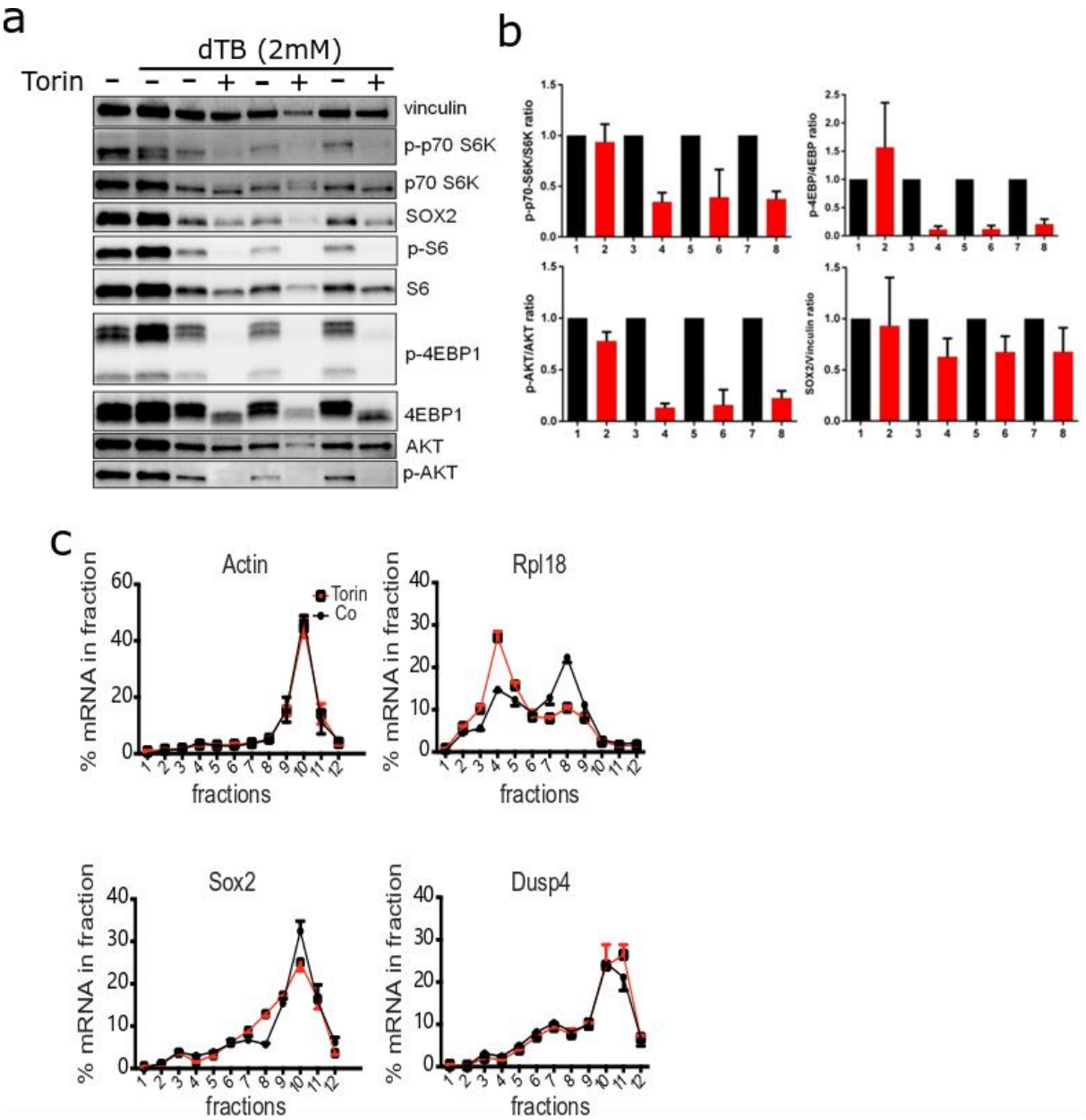

Figure 21. The translation of Sox2 is repressed upon mTOR inhibition in synchronized early passage NSCs

(a) Western blot representative images of different time points of Torin treatment for the effects on the mTOR effectors and SOX2. (b) Quantifications of SOX2, p-S6, p-4EBP1, and p-AKT normalized either to the loading control Vinculin or to the respective total protein (n=3). (c) Polysome profiling using cell cycle synchronized NSCs showed the repressed translation for Sox2 upon Torin treatment.

4 Discussion

4.1 Analyzing the transition from NSCs to ENBs

4.1.1 Global protein synthesis during the NSC-to-ENB transition

Protein synthesis virtually relates to all fundamental cellular processes such as cell growth, proliferation, differentiation. Therefore, protein synthesis is tightly regulated and proper techniques to study the level of protein synthesis are needed to understand the physiological state of the cell. One of those is based on incorporation of a chemical compound O-Propargyl-puromycin (OP-Puro) upon ongoing translation (Liu et al., 2012). OP-Puro is a puromycin analog, bearing a terminal alkyne group. Biosynthetic incorporation of it into the nascent peptide causes protein synthesis termination. The resulting peptides can be fluorescently detected by copper (I)-catalyzed azide-alkyne cycloaddition (CuAAC) (Liu et al., 2012). This method shows improved sensitivity and accuracy in comparison with previous tools (Isaacs and Fulton, 1987; Starck et al., 2004; Smith et al., 2005; Dieterich et al., 2010). It can be used both *in vitro* and in the living organism (Liu et al., 2012). However, OP-Puro could not go through the blood brain barrier, making quantification of protein synthesis in NSCs and ENBs *in vivo* difficult. Therefore, OP-Puro assay was conducted using ex vivo NSCs and ENBs, which were kept in culture for only 2 hours before OP-Puro incoporporation. Whether OP-Puro incorporation in ex vivo NSCs and ENBs reflect faithfully the *in vivo* scenario remains to be further validated with the development of techniques, which could be applied well *in vivo*.

Mis-regulation of global protein synthesis causes malfunction of the cell. In the $Rpl24^{Bst/+}$ mice, the hypomorphic mutation in ribosomal protein gene Rpl24 causes a significant drop for global protein synthesis in multiple cell types, which exhibit impaired functions. For example, $Rpl24^{Bst/+}$ bone marrow cells show significant decreased proliferative potential (Signer et al., 2014). Conditional deletion of Pten in HSCs strongly increased protein synthesis by 30%. An accompanying phenotype is reduced self-renewal, final exhaustion of the HSCs and even leukaemogenesis (Yilmaz et al., 2006; Zhang et al., 2006; Signer et al., 2014).

Improper increase of protein synthesis in the NSCs could cause impaired neurogenesis. Pten deletion in adult mice led to disturbed differentiation of premature neuroblasts by termination of their migration along the RMS to the OB, meaning that presumably the increased protein synthesis accelerated the maturation of neuroblasts (Zhu et al., 2012). During the transition from NSCs to ENBs, which are ready to initiate long distance migration along the RMS, cells experience dramatic changes such as reduction in cell size and lowered proliferative potential, which is mirrored in a significant decreased global protein synthesis. In comparison with such a translational decrease, translation during T cell differentiation is more dynamically controlled (Araki et al., 2017). The translation of mRNAs encoding translation machinery was upregulated during the T cell clonal-expansion phase upon antigen stimulation while inhibited when CD8+ effector T cells stopped dividing before the contraction phase. Besides, there are also examples where global protein synthesis is only increased during the differentiation process, e.g. in the transition from murine ESCs to embryoid body (Sampath et al., 2008), or in muscle stem cells, where the level of protein synthesis is kept low under stemness conditions by the phosphorylation of translation initiation factor eIF2α at serine 51. Differentiation of these cells is induced by dephosphorylation of eIF2α, which results in increased global protein synthesis (Zismanov et al., 2016). So, the trend of global protein synthesis varies a lot across cell types during the process of differentiation, probably directly linked to cell proliferation. The proliferative nature of NSCs, which means their self-renewal potential, is important to maintain the stem cell pool constant and furthermore to provide neuronal resources for brain homeostasis. Neuroblasts are less proliferative and are characterized by their migratory property. The decrease in global protein synthesis exhibits its regulatory role in NSC differentiation and presumably underlies the reduced proliferation capacity of ENBs.

4.1.2 Combined analysis of transcriptome and translatome revealed post-transcriptional regulation during the NSC-to-ENB transition

The high throughput single cell sequencing technique made it possible to investigate cellular heterogeneity of various cell types with high accuracy and resolution. Accumulated data on single cell transcriptomes showed the dynamic of activity of different individual genes in stem cell activation and differentiation. However, study about the translatomes of these cells had slow progress until the invention of the TRAP technique which was development by Heiman and colleagues (Doyle et al., 2008; Heiman et al., 2008). Based on bacterial artificial chromosome (BAC) transgenic technique, they introduced an EGFP tagged large-subunit ribosomal protein L10a (EGFP-L10a) to the genome, which results in tagged ribosomes and thereby purifying ribosome bound mRNAs through immunoprecipitation. In a preliminary in vitro experiment in HEK293T cell transfected with EGFP-L10a, 10% of RPL7 was co-purified from 30% of cells expressed EGFP-L10a, meaning 1/3 of ribosomes are tagged in the vector transfected cells. Analysis based on *in vivo* bacTRAP mouse model revealed that immunoaffinity-purified samples exhibited no bias for mRNA length or abundance.

However, the TRAP is based on random integration of exogenous vector into the genome, which exhibits unstable expression of the tagged protein in a mouse line dependent manner. This problem was improved by the work from Sanz and colleagues, who tagged endogenous ribosomal protein Rpl22 with HA and developed the Ribotag mouse line (Sanz et al., 2009). This line expresses the tagged epitope in a better controllable manner, minimizing the potential of unknown effects coming from the random integration of exogenous vectors. Therefore, our work based on this Ribotag mouse line has greater reliability compared to the TEAP line. However, one accompanying issue is that the proportion of epitope labelled ribosomes for the targeted cells is unknown, which could affect data analysis and interpretation later on. In rat, the estimated half-lives for brain ribosomal RNA and protein were 9 days (Retz and Steele, 1980), which means ribosome turnover in mouse NSCs and ENBs takes around the same time to ensure all ribosomes to be tagged. When immunoprecipitation was performed at 3 or 4 days after TAM administration, both untagged and tagged ribosomes exist in the NSCs or ENBs. To what extent the tagged ribosome bound mRNA

transcripts could recapitulate the intact translatome of the targeted cells remains to be explored. Since the translation of different gene transcripts varies a lot, a clear answer to this question would greatly help to improve the data interpretation, especially when it comes to combined analysis of multiple gene transcripts which differ in their translation efficiency.

An accompanying issue with the Ribotag technique is the “noise”, which comes from the unspecific binding of the antibody during immunoprecipitation. Reduction of the “noise” could be improved by following standardized experimental procedures such as strict control of tissue dissection, timing of treatments of multiple reagents, the use of antibody with improved specificity. We applied mock immunoprecipitation as well as subsequent sequencing to subtract the “noise” from the translatomes, ending up with good quality data, which was further validated through conventional methods such as qRT-PCR and Western blot. The relative expression of gene activity revealed from the RNA-seq data on the transcriptional changes was consistent with what we quantified via qPCR. The high correlation of the fold changes discovered between Western blot and RiboIP-seq data further confirmed the liability of the Ribotag method to investigate the translatome. The combined analysis of the transcriptome and the translatome allowed us to calculate the translational activity of specific transcripts during the NSC-to-ENB transition and to detect considerable changes of the activity indicative of a critical role for post-transcriptional regulation during the transition.

Though our Ribotag mouse model made it possible to co-analyze the transcriptome and the translatome of NSCs and ENBs, care should be taken when analyzing and interpreting the data because ribosome loading does not necessarily mean that proteins are produced. For example, ribosomal stalling is a mechanism to control protein quality normally caused by mRNA degradation and ribosome recycling (Joazeiro, 2017). During the stalling process, no proteins are being produced. But, the stalling ribosome bounded mRNAs can be mistakenly classified as “being translated” while using the Ribotag mouse model, which would be a false positive result. Besides, translation reinitiation upon the use of multiple upstream open reading frames could give rise to totally different proteins, which is again beyond the power of Ribotag. Notably, the above mentioned translation events could be well annotated by ribosome profiling, a technique to identify the location of ribosomes on their bounded mRNAs (Ingolia et al., 2009). As a

complementary method in studying translation, ribosome profiling could be co-applied with Ribotag to investigate the transition from NSCs to ENBs with improved resolution and accuracy.

4.2 Molecular mechanisms of post-transcriptional regulation at the onset of NSC differentiation

4.2.1 mTOR activity during NSC-to-ENB transition

mTOR is the master regulator of various cellular events such as cell growth, proliferation, metabolism. Environmental inputs such as growth factors and nutrients are well orchestrated by mTOR to regulate protein synthesis in the cell. During the transition from NSCs to ENBs, we found that mTORC1 activity decreased significantly, suggesting its tight association with NSC differentiation.

Upstream of mTORC1, multiple pathways or components could be targets of regulatory signals such as growth factors, amino acids, stress, etc. Grow factors could positively regulate multiple pathways to activate mTORC1 (Sengupta et al., 2010). Upon NSC activation, these proliferative cells express grow factor receptors for sensing those positive signals. Accompanying the NSC-to-ENB transition, cells lose expression of growth factor receptors, which contributes to mTOR activity reduction in ENBs. Moreover, the low exposure to nutrients in the compact RMS as well as decreased cell body size to adapt migration could also restrict mTOR activity in ENBs. mTOR activity is actively adjusted by these environmental inputs during NSC-to-ENB transition to guarantee proper protein production and differentiation.

Given the important role of mTOR in almost all types of cells, any deregulation may cause severe consequences such as obesity, diabetes and cancer (Dann et al., 2007; Populo et al., 2012). Accumulated evidence showed that hyperactivation of mTOR activity in NSCs induces premature differentiation (Magri et al., 2011; Feliciano et al., 2012; Costa et al., 2016). On the other hand, improper mTORC1 reduction could also cause impaired neurogenesis. Hartman et al. showed that genetically decreased mTORC1 activity by silencing RHEB in SVZ NSCs leads to decreased neuronal production (Hartman et al., 2013).

The role of mTORC2 is still not very clear. Growing evidence indicated that mTORC2 works upstream of AKT and is part of the PI3K/AKT pathway (Sengupta et al., 2010). This is in line with our finding that Torin inhibition of mTORC2 significantly decreased the level of phospho AKT (Figure 12). However, we could not observe a significant drop in the level of phospho AKT through LY294002 mediated PI3K inhibition though its application in 293 cells exhibited significant mTOR inhibition (Stolovich et al., 2002). This was probably because of its non-selectivity (Maira et al., 2009) or concentration dependent effects in different cell systems. The same reason may also explain why the mTOR inhibitor AZD2014 was not working in the NSC system though it was shown to work better than the clinically approved rapalogs in breast cancer cells (Guichard et al., 2015).

mTOR activity is not consistent throughout the whole cell cycle (Edelmann et al., 1996; Boyer et al., 2008). Recently Romero-Pozuelo and colleagues reported that TORC1 activity is high when cells enter the G1/S transition in Drosophila wing disc (Romero-Pozuelo et al., 2017). This is mediated by CycD/Cdk4 binding and phosphorylating the TOR inhibitor TSC2. Similar result was also observed in the Drosophila eye disc (Kim et al., 2017), where Kim and colleagues reported that the spatial activation of TORC1 is via Hedgehog and this mechanism is conserved in mammals as well. In our synchronized NSC system, mTOR repression exhibited a clear repression for Sox2 translation (Figure 16), highlighting cell cycle regulation on mTOR activity.

mTOR activity depends on the cellular state. We found that the transient chemical activation of mTOR in the early differentiated neuroblasts could alter the fate of the cell and reprogram the ENBs to a more stem cell-like state (Figure 15, 16, 17). Similar results were also reported previously in different cell systems. Zhao and colleagues found that stimulation of the AKT/mTOR pathway leads to retinal pigment epithelial cell dedifferentiation and hypertrophy (Zhao et al., 2011). The dedifferentiation of liposarcomas also is also accompanied by activation of mTOR (Ishii et al., 2016). However, dedifferentiation of NSCs through activation of mTOR should be further validated *in vivo*. Moreover, mTOR driven dedifferentiation *in vivo* could cause pathological consequences (Zhao et al., 2011). Future work could be performed to understand more about the impact of mTOR activation on fate determination of neuroblasts.

4.2.2 Cell cycle progression is involved in NSC fate determination

Pauklin and colleagues showed that the cell cycle stages of human embryonic stem cells respond differently to differentiation signals (Pauklin and Vallier, 2013). Cells staying in the early G1 phase differentiate into endoderm. At the late G1 phase, Cyclin D blocks Smad2/3 mediated endodermal cell fate and drives the cells towards neuroecotodem while the S/G2/M phases don't respond to differentiation signals. Sela and colleagues showed that human ESCs in G1 have higher propensity to differentiate than cells in S and G2 phase (Sela et al., 2012). Differentiation is presumably preceded by checkpoint activation, which is indicated by dephosphorylation of the checkpoint regulator retinoblastoma protein on Ser-795 residue. They reported that ESCs in S/G2 phase are not sensitive to differentiation. Increased cell density also prevents cell differentiation into G1. The same could be observed by co-culture experiments of G1 cells in S/G2 phase. In particular, this underpins the necessity of cell cycle synchronization of NSCs for in vitro studies of mTOR activity and potential effects of its modulation on the expression of stemness and differentiation markers such as Sox2.

After double thymidine treatment to mediating cell cycle synchronization, over 90% of the NSCs are arrested in the late G1/early S phase. According to our data, inhibition of mTOR activity in synchronized NSCs kept them in late G1/early S phase, which enabled the more prominent repression for "PRM" containing mRNA transcripts featured with attenuated translation of Sox2 mRNA. Overall, these results emphasize the significance of mTOR regulation in G1 phase to modulate NSC differentiation.

4.2.3 Molecular regulatory mechanism of neuronal fate determination during NSC differentiation

We identified a biological process during the NSC-to-ENB transition *in vivo* that critically depends on the selective sensitivity of gene transcripts to mTOR-mediated translation. The study conducted in our lab identified about 282 transcripts translationally repressed during this transition (Baser et al., 2019). Among these are the PRM containing mRNAs encoding ribosomal proteins, which significantly decrease ribosome biogenesis and as a result exerts a considerable reduction of global protein synthesis. This could be the reason for decreased cell proliferation and cell size in the ENBs.

Key stemness maintenance factors Pax6 and Sox2 are among the repressed transcripts. The expression level of these master genes usually plays a critical role in regulating differentiation of stem cells. Pax6 is involved in the regulation of many fundamental developmental events including embryonic and adult neurogenesis. Pax6 has three isoforms produced via alternative splicing as well as usage of different promoters or translation start codons (Epstein et al., 1994; Kammandel et al., 1999; Kim and Lauderdale, 2006). The cooperative expression of these isoforms guarantees the normal development of embryonic brain. Pax6 interacts with multiple molecules, which are key components of multiple signaling pathways. These interactions are involved in many fundamental processes such as cell proliferation, differentiation, adhesion and tissue patterning. Given the fact that Pax6 operates upstream of so many regulatory pathways and processes, its translational regulation is essential for the control of cell's fate.

Sox2 is a key transcription factor, whose over-expression in the terminally differentiated cells changes expression of numerous genes and causes cell reprogramming, reverting the cells back to a pluripotent stem state (Takahashi and Yamanaka, 2006; Takahashi et al., 2007; Yu et al., 2007). Similar finding was previously shown that the ectopic expression of transcription factor MyoD in fibroblasts reprogrammed these cells into myoblasts (Davis et al., 1987; Weintraub et al., 1991). We found that increased level of SOX2 in ENBs could dedifferentiate the cells back to stemness, highlighting the importance to control the level of SOX2 during the process of NSC differentiation. As a master regulator of translation, well controlled mTOR activity is indispensible to coordinate the complicated gene networks.

The well-known role of mTOR in translation is the phosphorylation and inactivation of 4EBP proteins, which usually bind to the cap-binding protein eIF4E responsible for PIC recruitment to mRNAs. These cap structure dependent mRNAs are among the most sensitive to mTOR activity, which usually encode abundant proteins in cells, such as the ribosomal proteins. These mRNAs, efficient in translation, form a class of so-called “strong” mRNAs (Pelletier et al., 2015). However, considerable number of mRNAs were also reported to show resistance to mTOR repression and even get stimulated (Hsieh et al., 2012; Thoreen et al., 2012). mTOR activity decreased upon the NSC-to-ENB transition and as a result repressed translation of “strong” mRNAs, such as ribosomal proteins and stem cell markers Sox2 and Pax6. In addition, a subset of previously less competitive “weak” mRNAs such as Sp8 and Dusp4 increased their translation efficiency. Other studies demonstrated that many such mRNAs can apply other mechanisms of 40S recruitment independent on the eIF4E-cap interaction, thereby being less dependent on eIF4E (Shatsky et al., 2014). Translation of these mRNAs is through isoforms of initiation factors eIF4E and eIF4G, which do not bind to 4EBP and could confer less dependence on mTOR to these mRNAs. Furthermore, these mRNAs being less competitive under high mTOR activity get considerable advantages upon mTOR inhibition, taking advantage of the resources due to repressed translation of the “strong” mRNAs.

Sp8 is a zinc finger transcription factor expressed in migrating neuroblasts as well as the olfactory bulb interneurons. Sp8 regulates survival, migration, and molecular specification of the migrating neuroblasts (Waclaw et al., 2006). DUSP4 was shown to be required for neuronal differentiation (Kim et al., 2015). The specific elements of such mRNAs providing mTOR independence remain to be studied. Recently discovered capability of N6-methylated adenines localized in the 5’-UTRs to directly attach 40S in an eIF4E-independent manner might be a potential mechanism to explain the mTOR independence of those genes (Meyer and Jaffrey, 2017). Future studies of N-6-methylated adenines may further our understanding of increased translation efficiency in the frame of low mTORC1 activity for this set of mRNA transcripts.

4.2.4 The role of Sox2 in ENBs

Sox2 is involved in many regulatory events in neural stem cells (Pevny and Nicolis, 2010). During the NSC-to-ENB transition, translational repression of master gene Sox2 dramatically decreased its protein level. However, the RNA level remains comparable in the two cell types, opening a question about the functional meaning for that. Does the Sox2 mRNA specifically stored in ENBs resume translation further in LNBs or neurons after the long distance migration? Or is it finally degraded later during neuronal maturation?

Though we revealed post-transcriptional repression of Sox2 mRNA by reduced mTOR in ENBs, the molecular mechanism responsible for establishing such “silenced” state is still not clear. In ESCs, RNA nuclear export of pluripotency gene transcripts is well controlled to balance self-renewal and differentiation of the cells (Wang et al., 2013). Thoc2 and Thoc5, two members of the THO complex, are involved in RNA export of transcripts from the nucleus. The knockdown of Thoc2 and Thoc5 causes nuclear accumulation of a subset of pluripotency mRNAs, including Sox2. In another study, also using ESCs, it was shown that RNA binding protein Rbm35a binds to the 5'UTR of the Sox2 and Oct4 mRNAs and prevents their ribosomal loading, what could finally drive differentiation (Fagoonee et al., 2013). Future studies should pay attention to the translocation of Sox2 mRNA during the transition from NSCs to ENBs. Regulatory proteins or protein complex like the THO complex in regulating Sox2 mRNA nuclear export, transport, and translation may be critical for leading to the “silenced” state of Sox2 mRNA in ENBs. Besides, numerous mRNA modifications such as N6-methyladenosine (m6A), N1-methyladenosine (m1A), 5-methylcytosine (m5C) and pseudouridine work collectively to form the epitranscriptome to regulate mRNA metabolism via control of their stability, localization and involvement in protein synthesis might be responsible for the modulation of Sox2 mRNA activity as well (Zhao et al., 2017). Further, comprehensive studies of the specific regulation of Sox2 translation in ENBs would provide new insights into our understanding of the molecular mechanisms of neurogenesis and its regulation.

4.3 Concluding remarks

Finally, we proposed a post-transcriptional regulation model, critical for the onset of NSC differentiation.

During NSC maintenance, the activated mTOR activity promotes high protein synthesis to support cell proliferation. Upon the need of differentiation, mTOR activity is repressed at G1 phase and global protein synthesis is significantly inhibited. The translation of PRM motif containing transcripts such as Sox2 is inhibited while the translation of neuronal specification transcripts such as Sp8 is enhanced, both synergistically triggering and driving NSC differentiation.

5 References

Aitken, C. E., and Lorsch, J. R. (2012). A mechanistic overview of translation initiation in eukaryotes. Nature structural & molecular biology *19*, 568.

Altman, J. (1969). Autoradiographic and histological studies of postnatal neurogenesis. IV. Cell proliferation and migration in the anterior forebrain, with special reference to persisting neurogenesis in the olfactory bulb. J Comp Neurol *137*, 433-457.

Altman, J., and Das, G. D. (1965). Autoradiographic and histological evidence of postnatal hippocampal neurogenesis in rats. Journal of Comparative Neurology *124*, 319-335.

Amaldi, F., and Pierandrei-Amaldi, P. (1997). TOP genes: a translationally controlled class of genes including those coding for ribosomal proteins. In Cytoplasmic fate of messenger RNA, (Springer), pp. 1-17.

Araki, K., Morita, M., Bederman, A. G., Konieczny, B. T., Kissick, H. T., Sonenberg, N., and Ahmed, R. (2017). Translation is actively regulated during the differentiation of CD8+ effector T cells. Nature immunology *18*, 1046.

Avni, D., Shama, S., Loreni, F., and Meyuhas, O. (1994). Vertebrate mRNAs with a 5'-terminal pyrimidine tract are candidates for translational repression in quiescent cells: characterization of the translational cis-regulatory element. Molecular and cellular biology *14*, 3822-3833.

Baser, A. (2018) Dynamic Control of Translation During Adult Neurogenesis.

Baser, A., Skabkin, M., Kleber, S., Dang, Y., Gulculer Balta, G. S., Kalamakis, G., Gopferich, M., Ibanez, D. C., Schefzik, R., Lopez, A. S.*, et al.* (2019). Onset of differentiation is post-transcriptionally controlled in adult neural stem cells. Nature *566*, 100-104.

Baser, A., Skabkin, M., and Martin-Villalba, A. (2017). Neural stem cell activation and the role of protein synthesis. Brain plasticity (Amsterdam, Netherlands) *3*, 27-41.

Bellusci, S., Grindley, J., Emoto, H., Itoh, N., and Hogan, B. (1997). Fibroblast growth factor 10 (FGF10) and branching morphogenesis in the embryonic mouse lung. Development *124*, 4867-4878.

Berg, D. A., Su, Y., Jimenez-Cyrus, D., Patel, A., Huang, N., Morizet, D., Lee, S., Shah, R., Ringeling, F. R., Jain, R.*, et al.* (2019). A Common Embryonic Origin of Stem Cells Drives Developmental and Adult Neurogenesis. Cell.

Bond, A. M., Ming, G.-l., and Song, H. (2015). Adult mammalian neural stem cells and neurogenesis: five decades later. Cell stem cell *17*, 385-395.

Boyer, D., Quintanilla, R., and Lee-Fruman, K. K. (2008). Regulation of catalytic activity of S6 kinase 2 during cell cycle. Molecular and cellular biochemistry *307*, 59-64.

Braccioli, L., Vervoort, S. J., Adolfs, Y., Heijnen, C. J., Basak, O., Pasterkamp, R. J., Nijboer, C. H., and Coffer, P. J. (2017). FOXP1 promotes embryonic neural stem cell differentiation by repressing Jagged1 expression. Stem cell reports *9*, 1530-1545.

Brown, E. J., Beal, P. A., Keith, C. T., Chen, J., Shin, T. B., and Schreiber, S. L. (1995). Control of p70 s6 kinase by kinase activity of FRAP in vivo. Nature *377*, 441.

Calegari, F., and Huttner, W. B. (2003). An inhibition of cyclin-dependent kinases that lengthens, but does not arrest, neuroepithelial cell cycle induces premature neurogenesis. Journal of cell science *116*, 4947-4955.

Cao, H., Wu, J., Lam, S., Duan, R., Newnham, C., Molday, R. S., Graziotto, J. J., Pierce, E. A., and Hu, J. (2011). Temporal and tissue specific regulation of RP-associated splicing factor genes PRPF3, PRPF31 and PRPC8-implications in the pathogenesis of RP. PloS One *6*, e15860.

Carey, K. T., and Wickramasinghe, V. O. (2018). Regulatory potential of the RNA processing machinery: implications for human disease. Trends in Genetics *34*, S0168952517302329.

Carroll, M., Warren, O., Fan, X., and Sossin, W. S. (2004). 5-HT stimulates eEF2 dephosphorylation in a rapamycin-sensitive manner in Aplysia neurites. J Neurochemistry *90*, 1464-1476.

Chaker, Z., Codega, P., and Doetsch, F. (2016). A mosaic world: puzzles revealed by adult neural stem cell heterogeneity. Wiley Interdisciplinary Reviews: Developmental Biology *5*, 640-658.

Clarke, D. L., Johansson, C. B., Wilbertz, J., Veress, B., Nilsson, E., Karlstrom, H., Lendahl, U., and Frisen, J. (2000). Generalized potential of adult neural stem cells. Science *288*, 1660-1663.

Colgan, D. F., and Manley, J. L. (1997). Mechanism and regulation of mRNA polyadenylation. Genes & Development *11*, 2755-2766.

Costa, V., Aigner, S., Vukcevic, M., Sauter, E., Behr, K., Ebeling, M., Dunkley, T., Friedlein, A., Zoffmann, S., and Meyer, C. A. (2016). mTORC1 inhibition corrects neurodevelopmental and synaptic alterations in a human stem cell model of tuberous sclerosis. Cell reports *15*, 86-95.

Damgaard, C. K., and Lykke-Andersen, J. (2011). Translational coregulation of 5'TOP mRNAs by TIA-1 and TIAR. Genes Dev *25*, 2057-2068.

Dann, S. G., Selvaraj, A., and Thomas, G. (2007). mTOR Complex1-S6K1 signaling: at the crossroads of obesity, diabetes and cancer. Trends Mol Med *13*, 252-259.

Davis, R. L., Weintraub, H., and Lassar, A. B. (1987). Expression of a single transfected cDNA converts fibroblasts to myoblasts. Cell *51*, 987-1000.

Dieterich, D. C., Hodas, J. J., Gouzer, G., Shadrin, I. Y., Ngo, J. T., Triller, A., Tirrell, D. A., and Schuman, E. M. (2010). In situ visualization and dynamics of newly synthesized proteins in rat hippocampal neurons. Nat Neurosci *13*, 897-905.

Dinkel, C., Moody, M., Traynor- Kaplan, A., and Schultz, C. (2001). Membrane- Permeant 3- OH- Phosphorylated Phosphoinositide Derivatives. Angewandte Chemie International Edition *40*, 3004-3008.

Doetsch, F., Caille, I., Lim, D. A., García-Verdugo, J. M., and Alvarez-Buylla, A. (1999). Subventricular zone astrocytes are neural stem cells in the adult mammalian brain. Cell *97*, 703-716.

Doyle, J. P., Dougherty, J. D., Heiman, M., Schmidt, E. F., Stevens, T. R., Ma, G., Bupp, S., Shrestha, P., Shah, R. D., and Doughty, M. L. (2008). Application of a translational profiling approach for the comparative analysis of CNS cell types. Cell *135*, 749-762.

Edelmann, H. M., Kuhne, C., Petritsch, C., and Ballou, L. M. (1996). Cell cycle regulation of p70 S6 kinase and p42/p44 mitogen-activated protein kinases in Swiss mouse 3T3 fibroblasts. The Journal of biological chemistry *271*, 963-971.

Epstein, J. A., Glaser, T., Cai, J., Jepeal, L., Walton, D. S., and Maas, R. L. (1994). Two independent and interactive DNA-binding subdomains of the Pax6 paired domain are regulated by alternative splicing. Genes Dev *8*, 2022-2034.

Eriksson, P. S., Perfilieva, E., Bjork-Eriksson, T., Alborn, A. M., Nordborg, C., Peterson, D. A., and Gage, F. H. (1998). Neurogenesis in the adult human hippocampus. Nat Med *4*, 1313-1317.

Fagoonee, S., Bearzi, C., Di Cunto, F., Clohessy, J. G., Rizzi, R., Reschke, M., Tolosano, E., Provero, P., Pandolfi, P. P., and Silengo, L. (2013). The RNA binding protein ESRP1 fine-tunes the expression of pluripotency-related factors in mouse embryonic stem cells. PloS one *8*, e72300.

Faye, M. D., Graber, T. E., and Holcik, M. (2014). Assessment of selective mRNA translation in mammalian cells by polysome profiling. Journal of visualized experiments : JoVE, e52295.

Feliciano, D. M., Quon, J. L., Su, T., Taylor, M. M., and Bordey, A. (2012). Postnatal neurogenesis generates heterotopias, olfactory micronodules and cortical infiltration following single-cell Tsc1 deletion. Human molecular genetics *21*, 799-810.

Fonseca, B. D., Zakaria, C., Jia, J. J., Graber, T. E., Svitkin, Y., Tahmasebi, S., Healy, D., Hoang, H. D., Jensen, J. M., Diao, I. T.*, et al.* (2015). La-related protein 1 (LARP1) represses Terminal Oligopyrimidine (TOP) mRNA translation downstream of mTOR complex 1 (mTORC1). The Journal of biological chemistry *290*, 15996-16020.

Franklin, K. B., and Paxinos, G. (2008). The mouse brain in stereotaxic coordinates).

Fraser, C. S. (2015). Quantitative studies of mRNA recruitment to the eukaryotic ribosome. Biochimie *114*, 58-71.

Fuentealba, L. C., Rompani, S. B., Parraguez, J. I., Obernier, K., Romero, R., Cepko, C. L., and Alvarez-Buylla, A. (2015). Embryonic origin of postnatal neural stem cells. Cell *161*, 1644-1655.

Furutachi, S., Miya, H., Watanabe, T., Kawai, H., Yamasaki, N., Harada, Y., Imayoshi, I., Nelson, M., Nakayama, K. I., Hirabayashi, Y., and Gotoh, Y. (2015). Slowly dividing neural progenitors are an embryonic origin of adult neural stem cells. Nat Neurosci *18*, 657-665.

Götz, M., and Huttner, W. B. (2005). Developmental cell biology: The cell biology of neurogenesis. Nature reviews Molecular cell biology *6*, 777.

Gerstberger, S., Hafner, M., Ascano, M., and Tuschl, T. (2014). Evolutionary conservation and expression of human RNA-binding proteins and their role in human genetic disease. In Systems biology of RNA binding proteins, (Springer), pp. 1-55.

Gingras, A. C., Gygi, S. P., Raught, B., Polakiewicz, R. D., Abraham, R. T., Hoekstra, M. F., Aebersold, R., and Sonenberg, N. (1999). Regulation of 4E-BP1 phosphorylation: a novel two-step mechanism. Genes Dev *13*, 1422-1437.

Gingras, A. C., Kennedy, S. G., O'Leary, M. A., Sonenberg, N., and Hay, N. (1998). 4E-BP1, a repressor of mRNA translation, is phosphorylated and inactivated by the Akt(PKB) signaling pathway. Genes Dev *12*, 502-513.

Godet, A. C., David, F., Hantelys, F., Tatin, F., Lacazette, E., Garmy-Susini, B., and Prats, A. C. (2019). IRES trans-acting factors, key actors of the stress response. Int J Mol Sci *20*.

Goldstrohm, A. C., Hall, T. M. T., and McKenney, K. M. (2018). Post-transcriptional regulatory functions of mammalian pumilio proteins. Trends in genetics : TIG *34*, 972-990.

Gould, E., Reeves, A. J., Graziano, M. S., and Gross, C. G. (1999). Neurogenesis in the neocortex of adult primates. Science *286*, 548-552.

Graves, L. M., Bornfeldt, K. E., Argast, G. M., Krebs, E. G., Kong, X., Lin, T. A., and Lawrence, J. C., Jr. (1995). cAMP- and rapamycin-sensitive regulation of the association of eukaryotic initiation factor 4E and the translational regulator PHAS-I in aortic smooth muscle cells. Proc Natl Acad Sci U S A *92*, 7222-7226.

Guichard, S. M., Curwen, J., Bihani, T., D'Cruz, C. M., Yates, J. W., Grondine, M., Howard, Z., Davies, B. R., Bigley, G., Klinowska, T.*, et al.* (2015). AZD2014, an Inhibitor of mTORC1 and mTORC2, is highly effective in ER+ breast cancer when administered using intermittent or continuous schedules. Mol Cancer Ther *14*, 2508-2518.

Haimon, Z., Volaski, A., Orthgiess, J., Boura-Halfon, S., Varol, D., Shemer, A., Yona, S., Zuckerman, B., David, E., Chappell-Maor, L.*, et al.* (2018). Re-evaluating microglia expression profiles using RiboTag and cell isolation strategies. Nat Immunol *19*, 636-644.

Hartman, N. W., Lin, T. V., Zhang, L., Paquelet, G. E., Feliciano, D. M., and Bordey, A. (2013). mTORC1 targets the translational repressor 4E-BP2, but not S6 kinase 1/2, to regulate neural stem cell self-renewal in vivo. Cell reports *5*, 433-444.

Heiman, M., Schaefer, A., Gong, S., Peterson, J. D., Day, M., Ramsey, K. E., Suárez-Fariñas, M., Schwarz, C., Stephan, D. A., and Surmeier, D. J. (2008). A translational profiling approach for the molecular characterization of CNS cell types. Cell *135*, 738-748.

Hershey, J. W. B., Sonenberg, N., and Mathews, M. B. (2018). Principles of Translational Control. Cold Spring Harb Perspect Biol.

Hinnebusch, A. G. (2017). Structural insights into the mechanism of scanning and start codon recognition in eukaryotic translation initiation. Trends Biochem Sci *42*, 589-611.

Hong, S., Freeberg, M. A., Han, T., Kamath, A., Yao, Y., Fukuda, T., Suzuki, T., Kim, J. K., and Inoki, K. (2017). LARP1 functions as a molecular switch for mTORC1-mediated translation of an essential class of mRNAs. Elife *6*, e25237.

Horisawa, K., Imai, T., Okano, H., and Yanagawa, H. (2009). 3'-Untranslated region of doublecortin mRNA is a binding target of the Musashi1 RNA-binding protein. FEBS letters *583*, 2429-2434.

Hsieh, A. C., Liu, Y., Edlind, M. P., Ingolia, N. T., Janes, M. R., Sher, A., Shi, E. Y., Stumpf, C. R., Christensen, C., and Bonham, M. J. (2012). The translational landscape of mTOR signalling steers cancer initiation and metastasis. Nature *485*, 55.

Ihrie, R. A., and Alvarez-Buylla, A. (2011). Lake-front property: a unique germinal niche by the lateral ventricles of the adult brain. Neuron *70*, 674-686.

Imai, T., Tokunaga, A., Yoshida, T., Hashimoto, M., Mikoshiba, K., Weinmaster, G., Nakafuku, M., and Okano, H. (2001). The neural RNA-binding protein Musashi1 translationally regulates mammalian numb gene expression by interacting with its mRNA. Mol Cell Biol *21*, 3888-3900.

Ingolia, N. T., Ghaemmaghami, S., Newman, J. R., and Weissman, J. S. (2009). Genome-wide analysis in vivo of translation with nucleotide resolution using ribosome profiling. Science *324*, 218-223.

Isaacs, W. B., and Fulton, A. B. (1987). Cotranslational assembly of myosin heavy chain in developing cultured skeletal muscle. Proc Natl Acad Sci U S A *84*, 6174-6178.

Ishii, T., Kohashi, K., Iura, K., Maekawa, A., Bekki, H., Yamada, Y., Yamamoto, H., Nabeshima, K., Kawashima, H., Iwamoto, Y., and Oda, Y. (2016). Activation of the Akt-mTOR and MAPK pathways in dedifferentiated liposarcomas. Tumour biology : the

journal of the International Society for Oncodevelopmental Biology and Medicine *37*, 4767-4776.

Jang, S. K., Davies, M., Kaufman, R., and Wimmer, E. (1989). Initiation of protein synthesis by internal entry of ribosomes into the 5'nontranslated region of encephalomyocarditis virus RNA in vivo. Journal of virology *63*, 1651-1660.

Jang, S. K., Kräusslich, H., Nicklin, M., Duke, G., Palmenberg, A., and Wimmer, E. (1988). A segment of the 5'nontranslated region of encephalomyocarditis virus RNA directs internal entry of ribosomes during in vitro translation. Journal of virology *62*, 2636-2643.

Joazeiro, C. A. P. (2017). Ribosomal stalling during translation: providing substrates for ribosome-associated protein quality control. Annu Rev Cell Dev Biol *33*, 343-368.

Jung, H., Yoon, B. C., and Holt, C. E. (2012). Axonal mRNA localization and local protein synthesis in nervous system assembly, maintenance and repair. Nature reviews Neuroscience *13*, 308-324.

Kageyama, R., Ohtsuka, T., Hatakeyama, J., and Ohsawa, R. (2005). Roles of bHLH genes in neural stem cell differentiation. Exp Cell Res *306*, 343-348.

Kalamakis, G., Brune, D., Ravichandran, S., Bolz, J., Fan, W., Ziebell, F., Stiehl, T., Catala-Martinez, F., Kupke, J., Zhao, S*., et al.* (2019). Quiescence modulates stem cell maintenance and regenerative capacity in the aging brain. Cell *176*, 1407-1419 e1414.

Kammandel, B., Chowdhury, K., Stoykova, A., Aparicio, S., Brenner, S., and Gruss, P. (1999). Distinct cis-essential modules direct the time-space pattern of the Pax6 gene activity. Dev Biol *205*, 79-97.

Kaplan, M. S., and Hinds, J. W. (1977). Neurogenesis in the adult rat: electron microscopic analysis of light radioautographs. Science *197*, 1092-1094.

Kawahara, H., Imai, T., Imataka, H., Tsujimoto, M., Matsumoto, K., and Okano, H. (2008). Neural RNA-binding protein Musashi1 inhibits translation initiation by competing with eIF4G for PABP. The Journal of cell biology *181*, 639-653.

Kim, D. Y. (2016). Post-transcriptional regulation of gene expression in neural stem cells. Cell biochemistry and function *34*, 197-208.

Kim, J., and Lauderdale, J. D. (2006). Analysis of Pax6 expression using a BAC transgene reveals the presence of a paired-less isoform of Pax6 in the eye and olfactory bulb. Developmental biology *292*, 486-505.

Kim, S. Y., Han, Y. M., Oh, M., Kim, W. K., Oh, K. J., Lee, S. C., Bae, K. H., and Han, B. S. (2015). DUSP4 regulates neuronal differentiation and calcium homeostasis by modulating ERK1/2 phosphorylation. Stem Cells Dev *24*, 686-700.

Kim, W., Jang, Y. G., Yang, J., and Chung, J. (2017). Spatial activation of TORC1 is regulated by Hedgehog and E2F1 signaling in the Drosophila eye. Developmental cell *42*, 363-375 e364.

Kriegstein, A., and Alvarez-Buylla, A. (2009). The glial nature of embryonic and adult neural stem cells. Annual review of neuroscience *32*, 149-184.

Lahr, R. M., Fonseca, B. D., Ciotti, G. E., Al-Ashtal, H. A., Jia, J.-J., Niklaus, M. R., Blagden, S. P., Alain, T., and Berman, A. J. (2017). La-related protein 1 (LARP1) binds the mRNA cap, blocking eIF4F assembly on TOP mRNAs. Elife *6*, e24146.

Lee, A. S., Kranzusch, P. J., Doudna, J. A., and Cate, J. H. (2016). eIF3d is an mRNA cap-binding protein that is required for specialized translation initiation. Nature *536*, 96.

Levy, S., Avni, D., Hariharan, N., Perry, R. P., and Meyuhas, O. (1991). Oligopyrimidine tract at the 5' end of mammalian ribosomal protein mRNAs is required for their translational control. Proc Natl Acad Sci U S A *88*, 3319-3323.

Lin, T. A., Kong, X., Haystead, T. A., Pause, A., Belsham, G., Sonenberg, N., and Lawrence, J. C., Jr. (1994). PHAS-I as a link between mitogen-activated protein kinase and translation initiation. Science *266*, 653-656.

Lin, T. A., Kong, X., Saltiel, A. R., Blackshear, P. J., and Lawrence, J. C., Jr. (1995). Control of PHAS-I by insulin in 3T3-L1 adipocytes. Synthesis, degradation, and phosphorylation by a rapamycin-sensitive and mitogen-activated protein kinase-independent pathway. The Journal of biological chemistry *270*, 18531-18538.

Liu, J., Xu, Y., Stoleru, D., and Salic, A. (2012). Imaging protein synthesis in cells and tissues with an alkyne analog of puromycin. Proc Natl Acad Sci U S A *109*, 413-418.

Lledo, P. M., Alonso, M., and Grubb, M. S. (2006). Adult neurogenesis and functional plasticity in neuronal circuits. Nature reviews Neuroscience *7*, 179-193.

Llorens-Bobadilla, E., Zhao, S., Baser, A., Saiz-Castro, G., Zwadlo, K., and Martin-Villalba, A. (2015). Single-cell transcriptomics reveals a population of dormant neural stem cells that become activated upon brain injury. Cell stem cell *17*, 329-340.

Lois, C., and Alvarez-Buylla, A. (1993). Proliferating subventricular zone cells in the adult mammalian forebrain can differentiate into neurons and glia. Proc Natl Acad Sci U S A *90*, 2074-2077.

Lois, C., Garcia-Verdugo, J. M., and Alvarez-Buylla, A. (1996). Chain migration of neuronal precursors. Science *271*, 978-981.

Magri, L., Cambiaghi, M., Cominelli, M., Alfaro-Cervello, C., Cursi, M., Pala, M., Bulfone, A., Garcìa-Verdugo, J. M., Leocani, L., and Minicucci, F. (2011). Sustained activation of mTOR pathway in embryonic neural stem cells leads to development of tuberous sclerosis complex-associated lesions. Cell stem cell *9*, 447-462.

Maira, S. M., Stauffer, F., Schnell, C., and Garcia-Echeverria, C. (2009). PI3K inhibitors for cancer treatment: where do we stand? Biochemical Society transactions *37*, 265-272.

Mendivil- Perez, M., Soto- Mercado, V., Guerra- Librero, A., Fernandez- Gil, B. I., Florido, J., Shen, Y. Q., Tejada, M. A., Capilla- Gonzalez, V., Rusanova, I., and Garcia- Verdugo, J. M. (2017). Melatonin enhances neural stem cell differentiation and engraftment by increasing mitochondrial function. Journal of pineal research *63*, e12415.

Meng, D., Frank, A. R., and Jewell, J. L. (2018). mTOR signaling in stem and progenitor cells. Development *145*, dev152595.

Meyer, K. D., and Jaffrey, S. R. (2017). Rethinking m(6)A Readers, Writers, and Erasers. Annu Rev Cell Dev Biol *33*, 319-342.

Meyuhas, O. (2000). Synthesis of the translational apparatus is regulated at the translational level. Eur J Biochem *267*, 6321-6330.

Meyuhas, O., Avni, D., and Shama, S. (1996). Translational control of ribosomal protein mRNAs in eukaryotes. Cold spring harbor monograph series *30*, 363-388.

Meyuhas, O., and Dreazen, A. (2009). Ribosomal protein S6 kinase from TOP mRNAs to cell size. Progress in molecular biology and translational science *90*, 109-153.

Ming, G. L., and Song, H. (2011). Adult neurogenesis in the mammalian brain: significant answers and significant questions. Neuron *70*, 687-702.

Mira, H., Andreu, Z., Suh, H., Lie, D. C., Jessberger, S., Consiglio, A., San Emeterio, J., Hortiguela, R., Marques-Torrejon, M. A., Nakashima, K.*, et al.* (2010). Signaling through BMPR-IA regulates quiescence and long-term activity of neural stem cells in the adult hippocampus. Cell stem cell *7*, 78-89.

Mirzadeh, Z., Doetsch, F., Sawamoto, K., Wichterle, H., and Alvarez-Buylla, A. (2010). The subventricular zone en-face: wholemount staining and ependymal flow. Journal of visualized experiments: JoVE.

Mirzadeh, Z., Merkle, F. T., Soriano-Navarro, M., Garcia-Verdugo, J. M., and Alvarez-Buylla, A. (2008). Neural stem cells confer unique pinwheel architecture to the ventricular surface in neurogenic regions of the adult brain. Cell stem cell *3*, 265-278.

Morshead, C. M., Reynolds, B. A., Craig, C. G., McBurney, M. W., Staines, W. A., Morassutti, D., Weiss, S., and van der Kooy, D. (1994). Neural stem cells in the adult mammalian forebrain: a relatively quiescent subpopulation of subependymal cells. Neuron *13*, 1071-1082.

Ng, C. K., Shboul, M., Taverniti, V., Bonnard, C., Lee, H., Eskin, A., Nelson, S. F., Al-Raqad, M., Altawalbeh, S., Seraphin, B., and Reversade, B. (2015). Loss of the scavenger mRNA decapping enzyme DCPS causes syndromic intellectual disability with neuromuscular defects. Hum Mol Genet *24*, 3163-3171.

Nousiainen, H. O., Kestila, M., Pakkasjarvi, N., Honkala, H., Kuure, S., Tallila, J., Vuopala, K., Ignatius, J., Herva, R., and Peltonen, L. (2008). Mutations in mRNA export mediator GLE1 result in a fetal motoneuron disease. Nat Genet *40*, 155-157.

Obernier, K., Cebrian-Silla, A., Thomson, M., Parraguez, J. I., Anderson, R., Guinto, C., Rodriguez, J. R., Garcia-Verdugo, J.-M., and Alvarez-Buylla, A. (2018). Adult neurogenesis is sustained by symmetric self-renewal and differentiation. Cell stem cell *22*, 221-234. e228.

Palmer, T. D., Takahashi, J., and Gage, F. H. (1997). The adult rat hippocampus contains primordial neural stem cells. Molecular and cellular neurosciences *8*, 389-404.

Pauklin, S., and Vallier, L. (2013). The cell-cycle state of stem cells determines cell fate propensity. Cell *155*, 135-147.

Pelletier, J., Graff, J., Ruggero, D., and Sonenberg, N. (2015). Targeting the eIF4F translation initiation complex: a critical nexus for cancer development. Cancer Res *75*, 250-263.

Pelletier, J., and Sonenberg, N. (1988). Internal initiation of translation of eukaryotic mRNA directed by a sequence derived from poliovirus RNA. Nature *334*, 320.

Pestova, T. V., Lorsch, J. R., and Hellen, C. U. (2007). The mechanism of translation initiation in eukaryotes. Cold Spring Harbor Monograph Series *48*, 87.

Pevny, L. H., and Nicolis, S. K. (2010). Sox2 roles in neural stem cells. The international journal of biochemistry & cell biology *42*, 421-424.

Philippe, L., Vasseur, J. J., Debart, F., and Thoreen, C. C. (2018). La-related protein 1 (LARP1) repression of TOP mRNA translation is mediated through its cap-binding domain and controlled by an adjacent regulatory region. Nucleic acids research *46*, 1457-1469.

Populo, H., Lopes, J. M., and Soares, P. (2012). The mTOR signalling pathway in human cancer. Int J Mol Sci *13*, 1886-1918.

Proud, C. G. (2002). Regulation of mammalian translation factors by nutrients. Eur J Biochem *269*, 5338-5349.

Retz, K. C., and Steele, W. J. (1980). Ribosome turnover in rat brain and liver. Life sciences *27*, 2601-2604.

Reynolds, B. A., and Weiss, S. (1992). Generation of neurons and astrocytes from isolated cells of the adult mammalian central nervous system. Science *255*, 1707-1710.

Richards, L. J., Kilpatrick, T. J., and Bartlett, P. F. (1992). De novo generation of neuronal cells from the adult mouse brain. Proc Natl Acad Sci U S A *89*, 8591-8595.

Robichaud, N., Sonenberg, N., Ruggero, D., and Schneider, R. J. (2018). Translational control in cancer. Cold Spring Harb Perspect Biol.

Romero-Pozuelo, J., Demetriades, C., Schroeder, P., and Teleman, A. A. (2017). CycD/Cdk4 and discontinuities in Dpp signaling activate TORC1 in the Drosophila wing disc. Developmental cell *42*, 376-387 e375.

Rosbash, M., and Ford, P. J. (1974). Polyadenylic acid-containing RNA in Xenopus laevis oocytes. J Mol Biol *85*, 87-101.

Sampath, P., Pritchard, D. K., Pabon, L., Reinecke, H., Schwartz, S. M., Morris, D. R., and Murry, C. E. (2008). A hierarchical network controls protein translation during murine embryonic stem cell self-renewal and differentiation. Cell stem cell *2*, 448-460.

Sanz, E., Yang, L., Su, T., Morris, D. R., McKnight, G. S., and Amieux, P. S. (2009). Cell-type-specific isolation of ribosome-associated mRNA from complex tissues. Proc Natl Acad Sci U S A *106*, 13939-13944.

Saxton, R. A., and Sabatini, D. M. (2017). mTOR signaling in growth, metabolism, and disease. Cell *168*, 960-976.

Sela, Y., Molotski, N., Golan, S., Itskovitz- Eldor, J., and Soen, Y. (2012). Human embryonic stem cells exhibit increased propensity to differentiate during the G1 phase prior to phosphorylation of retinoblastoma protein. Stem Cells *30*, 1097-1108.

Sengupta, S., Peterson, T. R., and Sabatini, D. M. (2010). Regulation of the mTOR complex 1 pathway by nutrients, growth factors, and stress. Mol Cell *40*, 310-322.

Seri, B., Garcia-Verdugo, J. M., McEwen, B. S., and Alvarez-Buylla, A. (2001). Astrocytes give rise to new neurons in the adult mammalian hippocampus. Journal of Neuroscience *21*, 7153-7160.

Shatsky, I. N., Dmitriev, S. E., Andreev, D. E., and Terenin, I. M. (2014). Transcriptome-wide studies uncover the diversity of modes of mRNA recruitment to eukaryotic ribosomes. Crit Rev Biochem Mol Biol *49*, 164-177.

Shi, Z., Fujii, K., Kovary, K. M., Genuth, N. R., Rost, H. L., Teruel, M. N., and Barna, M. (2017). Heterogeneous ribosomes preferentially translate distinct subpools of mRNAs genome-wide. Mol Cell *67*, 71-83 e77.

Shigeoka, T., Jung, H., Jung, J., Turner-Bridger, B., Ohk, J., Lin, J. Q., Amieux, P. S., and Holt, C. E. (2016). Dynamic axonal translation in developing and mature visual circuits. Cell *166*, 181-192.

Signer, R. A., Magee, J. A., Salic, A., and Morrison, S. J. (2014). Haematopoietic stem cells require a highly regulated protein synthesis rate. Nature *509*, 49-54.

Silvera, D., Formenti, S. C., and Schneider, R. J. (2010). Translational control in cancer. Nature Reviews Cancer *10*, 254.

Simsek, D., Tiu, G. C., Flynn, R. A., Byeon, G. W., Leppek, K., Xu, A. F., Chang, H. Y., and Barna, M. (2017). The mammalian Ribo-interactome reveals ribosome functional diversity and heterogeneity. Cell *169*, 1051-1065 e1018.

Smith, W. B., Starck, S. R., Roberts, R. W., and Schuman, E. M. (2005). Dopaminergic stimulation of local protein synthesis enhances surface expression of GluR1 and synaptic transmission in hippocampal neurons. Neuron *45*, 765-779.

Sonenberg, N., and Hinnebusch, A. G. (2009). Regulation of translation initiation in eukaryotes: mechanisms and biological targets. Cell *136*, 731-745.

Starck, S. R., Green, H. M., Alberola-Ila, J., and Roberts, R. W. (2004). A general approach to detect protein expression in vivo using fluorescent puromycin conjugates. Chemistry & biology *11*, 999-1008.

Starck, S. R., and Roberts, R. W. (2002). Puromycin oligonucleotides reveal steric restrictions for ribosome entry and multiple modes of translation inhibition. RNA *8*, 890-903.

Stolovich, M., Tang, H., Hornstein, E., Levy, G., Cohen, R., Bae, S. S., Birnbaum, M. J., and Meyuhas, O. (2002). Transduction of growth or mitogenic signals into translational activation of TOP mRNAs is fully reliant on the phosphatidylinositol 3-kinase-mediated pathway but requires neither S6K1 nor rpS6 phosphorylation. Mol Cell Biol *22*, 8101-8113.

Takahashi, K., Tanabe, K., Ohnuki, M., Narita, M., Ichisaka, T., Tomoda, K., and Yamanaka, S. (2007). Induction of pluripotent stem cells from adult human fibroblasts by defined factors. Cell *131*, 861-872.

Takahashi, K., and Yamanaka, S. (2006). Induction of pluripotent stem cells from mouse embryonic and adult fibroblast cultures by defined factors. Cell *126*, 663-676.

Tanackovic, G., Ransijn, A., Thibault, P., Abou Elela, S., Klinck, R., Berson, E. L., Chabot, B., and Rivolta, C. (2011). PRPF mutations are associated with generalized defects in spliceosome formation and pre-mRNA splicing in patients with retinitis pigmentosa. Hum Mol Genet *20*, 2116-2130.

Thoreen, C. C., Chantranupong, L., Keys, H. R., Wang, T., Gray, N. S., and Sabatini, D. M. (2012). A unifying model for mTORC1-mediated regulation of mRNA translation. Nature *485*, 109.

Waclaw, R. R., Allen II, Z. J., Bell, S. M., Erdélyi, F., Szabó, G., Potter, S. S., and Campbell, K. (2006). The zinc finger transcription factor Sp8 regulates the generation and diversity of olfactory bulb interneurons. Neuron *49*, 503-516.

Wang, L., Miao, Y.-L., Zheng, X., Lackford, B., Zhou, B., Han, L., Yao, C., Ward, J. M., Burkholder, A., and Lipchina, I. (2013). The THO complex regulates pluripotency gene mRNA export and controls embryonic stem cell self-renewal and somatic cell reprogramming. Cell stem cell *13*, 676-690.

Weintraub, H., Davis, R., Tapscott, S., Thayer, M., Krause, M., Benezra, R., Blackwell, T. K., Turner, D., Rupp, R., and Hollenberg, S. (1991). The MyoD gene family: nodal point during specification of the muscle cell lineage. Science *251*, 761-766.

Yilmaz, O. H., Valdez, R., Theisen, B. K., Guo, W., Ferguson, D. O., Wu, H., and Morrison, S. J. (2006). Pten dependence distinguishes haematopoietic stem cells from leukaemia-initiating cells. Nature *441*, 475-482.

Yu, J., Vodyanik, M. A., Smuga-Otto, K., Antosiewicz-Bourget, J., Frane, J. L., Tian, S., Nie, J., Jonsdottir, G. A., Ruotti, V., and Stewart, R. (2007). Induced pluripotent stem cell lines derived from human somatic cells. Science *318*, 1917-1920.

Zappulo, A., van den Bruck, D., Ciolli Mattioli, C., Franke, V., Imami, K., McShane, E., Moreno-Estelles, M., Calviello, L., Filipchyk, A., Peguero-Sanchez, E*., et al.* (2017). RNA localization is a key determinant of neurite-enriched proteome. Nature communications *8*, 583.

Zhang, J., Grindley, J. C., Yin, T., Jayasinghe, S., He, X. C., Ross, J. T., Haug, J. S., Rupp, D., Porter-Westpfahl, K. S., and Wiedemann, L. M. (2006). PTEN maintains haematopoietic stem cells and acts in lineage choice and leukaemia prevention. Nature *441*, 518.

Zhang, M., Chen, D., Xia, J., Han, W., Cui, X., Neuenkirchen, N., Hermes, G., Sestan, N., and Lin, H. (2017). Post-transcriptional regulation of mouse neurogenesis by Pumilio proteins. Genes Dev *31*, 1354-1369.

Zhao, B. S., Roundtree, I. A., and He, C. (2017). Post-transcriptional gene regulation by mRNA modifications. Nature reviews Molecular cell biology *18*, 31-42.

Zhao, C., Yasumura, D., Li, X., Matthes, M., Lloyd, M., Nielsen, G., Ahern, K., Snyder, M., Bok, D., Dunaief, J. L*., et al.* (2011). mTOR-mediated dedifferentiation of the retinal pigment epithelium initiates photoreceptor degeneration in mice. The Journal of clinical investigation *121*, 369-383.

Zhu, B., Carmichael, R. E., Solabre Valois, L., Wilkinson, K. A., and Henley, J. M. (2018). The transcription factor MEF2A plays a key role in the differentiation/maturation of rat neural stem cells into neurons. Biochem Biophys Res Commun *500*, 645-649.

Zhu, G., Chow, L. M., Bayazitov, I. T., Tong, Y., Gilbertson, R. J., Zakharenko, S. S., Solecki, D. J., and Baker, S. J. (2012). Pten deletion causes mTORC1-dependent ectopic neuroblast differentiation without causing uniform migration defects. Development *139*, 3422-3431.

Zismanov, V., Chichkov, V., Colangelo, V., Jamet, S., Wang, S., Syme, A., Koromilas, A. E., and Crist, C. (2016). Phosphorylation of eIF2alpha is a translational control mechanism regulating muscle stem cell quiescence and self-renewal. Cell stem cell *18*, 79-90.